

26705



National Library of Canada

Bibliothèque nationale du Canada

CANADIAN THESES ON MICROFICHE

THÈSES CANADIENNES SUR MICROFICHE

NAME OF AUTHOR / NOM DE L'AUTEUR PARVEEN NIHAL SINGH BAWA

TITLE OF THESIS / TITRE DE LA THÈSE LINEAR ANALYSIS of MYOTATIC REFLEXES
IN CAT & MAN

UNIVERSITY / UNIVERSITÉ UNIV. of ALBERTA, EDMONTON

DEGREE FOR WHICH THESIS WAS PRESENTED / GRADE POUR LEQUEL CETTE THÈSE FUT PRÉSENTÉE Ph.D

YEAR THIS DEGREE CONFERRED / ANNÉE D'OBTENTION DE CE GRADE 1975

NAME OF SUPERVISOR / NOM DU DIRECTEUR DE THÈSE PROF. R. B. STEIN

Permission is hereby granted to the NATIONAL LIBRARY OF CANADA to microfilm this thesis and to lend or sell copies of the film.

L'autorisation est, par la présente, accordée à la BIBLIOTHÈQUE NATIONALE DU CANADA de microfilmer cette thèse et de prêter ou de vendre des exemplaires du film.

The author reserves other publication rights, and neither the thesis nor extensive extracts from it may be printed or otherwise reproduced without the author's written permission.

L'auteur se réserve les autres droits de publication; ni la thèse ni de longs extraits de celle-ci ne doivent être imprimés ou autrement reproduits sans l'autorisation écrite de l'auteur.

DATED / DATE Oct 17, 1975 SIGNED / SIGNÉ Parveen N. S. Bawa

PERMANENT ADDRESS / RÉSIDENCE FIXE Dept. of Physiology, Univ. of Alberta,
Edmonton, Alberta

THE UNIVERSITY OF ALBERTA
LINEAR ANALYSIS OF MYOTATIC REFLEXES IN CAT AND MAN

BY
PARVEEN NIHAL SINGH BAWA

A THESIS
SUBMITTED TO THE FACULTY OF GRADUATE STUDIES AND RESEARCH
IN PARTIAL FULFILMENT OF THE REQUIREMENTS FOR THE DEGREE
OF DOCTOR OF PHILOSOPHY

IN
BIOPHYSICS

DEPARTMENT OF PHYSIOLOGY

EDMONTON, ALBERTA

FALL, 1975

THE UNIVERSITY OF ALBERTA
FACULTY OF GRADUATE STUDIES AND RESEARCH

The undersigned certify that they have read, and recommend to the Faculty of Graduate Studies and Research, for acceptance, a thesis entitled "Linear Analysis of Myotatic Reflexes in Cat and Man" submitted by Parveen Nihal Singh Bawa in partial fulfilment of the requirements for the degree of Doctor of Philosophy.

R. Borten

.....
Supervisor

W. H. ...

.....
R. ...

.....
M. Pearson

Peter ...

.....
External Examiner

Date *Oct 7, 1975*

IN MEMORY OF MY BROTHER

AMRIT

ABSTRACT

The dynamic properties of the hindlimb muscles, the muscle afferents and the associated reflex loops were studied by linear analysis. Coherence values from spectral analysis data gave an estimate of the linearity of each system.

The soleus and plantaris muscles in the cat and the human soleus muscle all behave like low pass filters of the second order. A second-order system is described by three parameters, the low frequency gain, the natural frequency and the damping ratio. The variation of these parameters was examined with systematic changes in (a) length of the muscle, (b) mean rate of stimulation of the motor nerve and (c) the stiffness of the external elastic loads against which the muscle was allowed to shorten. From these observations, a linear visco-elastic model of second-order was proposed. To test the validity of the model, the muscle was allowed to shorten against various inertial loads. The experimental frequency response curves and the theoretical predictions from the model agreed well.

The frequency response curves of the muscle afferents were computed both for anaesthetized and decerebrate cats. The experimental data from the primary fibres agreed well with the empirical transfer function of the primary afferents given by Poppele and Bowman (1970). The transfer characteristics of the secondary endings and Golgi tendon organs fitted with the empirical expression of the secondaries given by the same authors. Various non-linearities have been discussed.

The dynamics of the feedback pathway for the human soleus

muscle were studied under voluntary force conditions. The gain curve-fitted with the gain curve of the primary spindle afferents (Poppele & Bowman, 1970). The delay involved in the pathway, calculated from the phase data, was long enough to involve higher centres. In decerebrate cats there was evidence of short and long latency reflex pathways. The short latency pathway could be spinal while the long latency pathway may involve the cerebellum.

ACKNOWLEDGEMENT

Good life means having a good supervisor for one's graduate studies. Professor Richard B. Stein undoubtedly fulfils this requirement. He is not only an excellent biophysicist, but a tremendous person as well. I am highly indebted to him for all he has done for me. I hope I have the opportunity to work with him again.

I thank Professor M. Schachter, the Chairman of the Department, who gave me all the necessary working facilities.

Doctor T. Richard Nichols has been a great academic help and an equally good friend. I am most grateful to him for everything he has done for me.

Doctor Allan Mannard deserves my many thanks for both helping me academically and being a good friend throughout the course of this work.

I thank Doctor Andrew French for his availability to help with the computer work.

Mr. Dean Charles deserves my thanks for his technical help in the laboratory. It is good to have a person like him, with a super sense of humour, in the laboratory.

Work with a smile, that is how Mrs. Ortella White works. I am grateful to her for her efficient and excellent typing throughout the last three years for me, especially for this thesis.

I thank Mr. Fred Loeffler and Mr. Ken Burt for very nice drafting and photography.

My many close friends, who did not contribute much towards this thesis directly, have provided good company and support during the course of this work. I thank them all.

This work was supported by the Medical Research Council of Canada.

TABLE OF CONTENTS

Chapter		Page
1	INTRODUCTION	1
	Muscle	2
	Alpha-Motor Neurons	6
	Muscle Afferents	7
	'Servo-Assisted' Hypothesis and Reflex Control	12
2	ANALYSIS AND SIMULATIONS	18
	Analysis	18
	Recording	18
	Spectral Analysis	19
	Second Order Curve Fitting	23
	Confidence Intervals	24
	Averaging	25
	Simulations	26
3	EFFECTS OF ELASTIC LOADS ON THE CONTRACTIONS OF CAT MUSCLES	39
	Introduction	39
	Methods	42
	Results	44
	Effects of Elastic Loads on the Twitch	44
	The Frequency Response with Elastic Loads	49
	Discussion	58
4	PREDICTIONS AND EXPERIMENTAL TESTS OF A VISCO-ELASTIC MUSCLE MODEL USING ELASTIC AND INERTIAL LOADS	62
	Introduction	62

Chapter	Page
Theoretical Predictions	64
Equations of Motion	66
Elastic Loading	67
Inertial Loads	70
Results	72
Elastic Loads	72
Inertial Loads	77
Effect of k_e	80
Effect of k_i	82
Effect of k_p	82
Effect of B	82
Effect of β	86
Discussion	86
5. PROPERTIES OF HUMAN SOLEUS MUSCLE AND THE ASSOCIATED FEEDBACK LOOP	90
Introduction	90
Methods	92
Stimulation	92
Force Measurement	95
EMG	95
Analysis	96
Random Stimulation	96
Twitches	97
Results	99
Properties of Human Soleus Muscle Under Rest Conditions	99

Chapter	Page
Twitch Contractions at Rest	105
Effects of Voluntary Contractions	105
Feedback Transfer Function	108
Discussion	112
Muscle Properties	112
Sensory Feedback	115
Appendix	118
 6	
DYNAMICS OF THE MUSCLE AFFERENTS AND THE FEEDBACK PATHWAY	120
Introduction	120
Methods	124
Empirical Relations	125
Results	126
Afferent Transfer Functions	126
Compensation of Muscle Properties by Afferents ..	132
Low Frequency Behaviour Using Various Loads	135
Reflex Studies	140
Discussion	141
BIBLIOGRAPHY	148

LIST OF TABLES

Table

Page

1	Values of experimentally determined parameters for a visco-elastic model of plantaris muscle in the cat	76
---	---	----

LIST OF FIGURES

Figure		Page
1.1	Voluntary and reflex control of muscle	16
2.1	Block diagram of simulated stretch reflex	28
2.2	Frequency response curves of a simulated muscle	29
2.3	Gain curves for simulated muscle spindle afferent, with reflex loop open	31
2.4	Gain curves for simulated muscle spindle afferent, showing the effect of a pause in the firing	33
2.5	Gain curves for simulated muscle spindle, showing the effect of changing coefficient of variation in the mean firing rate	35
2.6	Gain curves for simulated muscle spindle, with reflex loop closed	36
2.7	Time domain response of simulated muscle with varying delays in the feedback pathway	38
3.1	Schematic diagram of the system used to apply varying elastic and inertial loads to the muscle	43
3.2	Effect on twitch tension of adding springs in series with plantaris and soleus muscles	45
3.3	Changes in parameters of twitches in plantaris muscle measured with spring loads of different stiffnesses	47
3.4	Frequency response curves of a plantaris nerve-muscle preparation under isometric and with various loading conditions	50
3.5	The gain and phase data for plantaris muscle under isometric conditions	52
3.6	Effect of elastic stiffness on the gain, natural frequency and damping ratio for plantaris and soleus muscles	54
3.7	Effects on the two rate constants of changing (a) the stiffness of the spring load, (b) length of the muscle, and (c) rate of stimulation	56

Figure	Page
4.1	Schematic representation of a muscle model with various types of external loads 65
4.2	The effect of varying the stiffness of the spring load on the visco-elastic rate constant of plantaris muscle 73
4.3	Effect of varying the compliance of the spring load on the inverse of the product of low frequency gain and active state rate constant 75
4.4	Comparison of experimental data with predictions for the effect of adding inertial loads for plantaris muscle 78
4.5	Effect of inertial load on the twitch of plantaris muscle 79
4.6	Variation of frequency response gain curve with the variation of external spring stiffness 81
4.7	Effect of varying internal series elasticity on the gain curve 83
4.8	Effect of varying internal parallel elasticity on the gain curve 84
4.9	Effect of changing the internal coefficient of viscosity on the frequency response gain curve 85
4.10	Effect of changing the active state decay constant on the frequency response gain curve 87
5.1	Schematic diagram of the experimental arrangement for human work 93
5.2	A block diagram of the functional stretch reflex 98
5.3	The gain and phase data for human soleus muscle with angle of the ankle fixed at 88° 101
5.4	Gain data for human soleus muscle at different angles of the ankle under rest conditions 103
5.5	Variation of low frequency gain, natural frequency and damping ratio with angle of the ankle 104
5.6	Variation of twitch tension, contraction time and half-relaxation time of the twitch with angle of the ankle 106

Figure	Page
5.7	Frequency response curves of human soleus muscle under voluntary force conditions 107
5.8	Oscillations in EMG with corresponding oscillations in twitch tension under voluntary force conditions 109
5.9	The gain and phase data of the feedback transfer function under voluntary force conditions 111
5.10	Phase differences between the observed responses due to sensory feedback and those expected for the primary muscle spindle afferents 113
6.1	Gain data of a primary afferent transfer function for soleus muscle in a decerebrate preparation 128
6.2	Gain data of a secondary afferent transfer function for soleus muscle in a decerebrate cat 130
6.3	Gain data for (a) efferent-muscle, (b) efferent-Ia afferent, and (c) muscle-Ia afferent transfer functions for soleus muscle in a decerebrate cat 133
6.4	Gain curves for (a) efferent-muscle, (b) efferent-II afferent, and (c) muscle-II afferent transfer functions for plantaris muscle in an anaesthetized cat 134
6.5	Gain curves for (a) efferent-muscle, (b) efferent-Ib afferent, and (c) muscle-Ib afferent transfer functions for soleus muscle of a decerebrate cat 136
6.6	Post-stimulus time histogram for a primary ending and a Golgi tendon/organ 137
6.7	Low frequency gains for muscle afferents for various spring loads 139
6.8	Oscillations in reflex EMG with corresponding twitch tension in a decerebrate cat 142
6.9	Phase difference between observed experimental data and primary transfer function plotted versus frequency 143

CHAPTER I

INTRODUCTION

The mammalian skeletal muscle, by active contraction, generates force. This force is utilized to support the weight of the body and perform linear and angular motions against various external loads. The performance of the muscle is controlled by the central nervous system via the motoneurons. However, the muscle with its motor innervation does not work as an open loop system. If a muscle in an intact or decerebrate animal is stretched, it contracts quickly towards its original length. This property was first demonstrated by Liddell and Sherrington (1924) and they called it a myotatic reflex. Since then it has been shown that the muscle afferents are constantly feeding back information about the state of the muscles to different levels of the central nervous system. The control signal (Houk & Henneman, 1974) and the afferent feedback are compared, the resulting error signal is carried by the efferent fibres to the muscle. Afferent fibres from the skin and joint receptors also affect the muscle but their action will not be discussed in this work.

The muscle with its afferent and efferent innervation forms a closed loop control system. In the following work linear analysis techniques have been applied to study the dynamics of the muscle, muscle afferents and associated reflex pathways. The INTRODUCTION reviews the general structural and physiological properties of the above mentioned systems. Chapter 2 discusses briefly the theory of

linear analysis used in this work. Later in the chapter the analysis has been applied to a simulated muscle and its reflex loop. Examples are given where the analysis may and may not be applied successfully. Each of the following chapters is complete in itself with a detailed INTRODUCTION followed by METHODS, RESULTS and DISCUSSION.

MUSCLE

A striated skeletal muscle is made up of muscle fibres, each muscle fibre being a long multinucleated cell. In addition, each muscle has extra fibrous and tendonous tissue, its own nerve and blood supply. Each fibre is composed of longitudinal subunits called myofibrils. Spaces between myofibrils are filled with glycogen, mitochondria, a tubular network called the sarcoplasmic reticulum and other plasma components. Each myofibril is divided into transverse sections called sarcomeres. A sarcomere is bounded at each end by a disc called the Z line. The Z lines of different myofibrils are in register with each other which gives the muscle its striated appearance. The contractile material of each sarcomere is made up of interdigitating thick (myosin) and thin (actin) filaments. The distance between the axes of thick and thin filaments is $\approx 260\text{\AA}$. Cross-bridges, are the globular heads of myosin molecules, project out of the thick filaments (Hanson & Huxley, 1953; Huxley & Hanson, 1954; Huxley, H.E., 1969, 1971). The thin filaments, in addition to actin, have troponin and tropomyosin molecules; the latter two are the regulatory proteins for actin-myosin interaction (Weber & Murray, 1973; Murray & Weber, 1974).

The sarcolemma is invaginated by the T-tubule system. Each T-tubule forms rings around the myofibrils and also communicates freely with the extracellular space at both ends. The terminal cisternae of the sarcoplasmic reticulum make contact with the T-tubules (reviews by Fuchs, 1974 and Huxley, 1974).

When a muscle is stimulated, the action potential travels along the sarcolemma and down into the T-tubules. This activity results in the release of calcium ions from the sarcoplasmic reticulum (Ashley & Moiescu, 1973; Fuchs, 1974). Troponin combines with Ca^{++} , removing inhibition for the actin-myosin interaction. Cross-bridges from the thick filament combine with the available sites on the actin molecules, and a conformational change takes place in the myosin heads. The cross-bridges pull on the actin filament, bringing it towards the centre of the sarcomere and the cross-bridges detach themselves from the thin filament (Huxley & Niedergerke, 1954; Huxley, 1957, 1971, 1974; Huxley & Simmons, 1971). The conformational change and the cross-bridge detachment are accompanied by adenosine triphosphate (ATP) hydrolysis into adenosine diphosphate (ADP) and inorganic phosphate. As long as calcium ions are available, the cross-bridges detach cyclically to allow sliding of the filaments. This results in shortening of the muscle and development of smooth tension. Calcium ions are pumped back into the sarcoplasmic reticulum by an active process and the muscle relaxes. If, on the other hand, a second stimulus is given to the muscle before it relaxes completely, the effect of the second response adds on to the first one. Tetanus results if the rate of stimulation is such that no relaxation occurs

during stimulation.

In mammalian skeletal muscles, muscle fibres have been found to be mainly of three types both histochemically (Close, 1972) and functionally (Burke *et al.*, 1973). Different authors have used different terminology for the fibre classification (Close, 1972); here they will be referred to as the pale, red and intermediate types. Pale fibres have short contraction times (fast fibres), fatigue quickly, have high glycolytic, high ATPase activities, low mitochondrial content and low oxidative activity. The red fibres have short contraction times (fast fibres), fatigue slowly, have intermediate glycolytic and high myofibrillar ATPase activities; they have many mitochondria and high oxidative activity. The intermediate fibres have long contraction times (slow fibres) and fatigue slowly, have low glycolytic and low myofibrillar ATPase activities; they possess high mitochondrial content and high oxidative enzyme activities. The cat soleus muscle has 95-100% intermediate fibres and the gastrocnemius has approximately 51% pale, 28% red and 21% intermediate (Close, 1972).

For a particular muscle, the amount of tension developed and the speed of shortening depends on the load attached to the tendon of the muscle (Hill, 1938, 1964; Huxley, 1974). The greater the load, the smaller is the velocity and the higher is the tension developed.

When the amplitude of stretch (or release) of an actively contracting muscle is plotted versus tension, a linear relationship between length and tension can be seen over a small range of lengths. The slope of the plot in a linear region is a measure of the stiffness of the muscle. The skeletal muscle seems to have two regions of

response, a high stiffness region for very small fast stretches (or releases) and a low stiffness region for larger stretches (Huxley & Simmons, 1971; Huxley, 1974; Rack & Westbury, 1974; Nichols, 1975). Huxley and Simmons have attributed the short range stiffness mainly to the cross-bridges. In their view the range of short range stiffness depends on the extent to which a cross-bridge can extend and exert tension before breaking. These authors have shown it to be at least 13 nm. Beyond the high stiffness region the cross-bridges start to break and make connections at random for the muscle to shorten. This is the region of lower stiffness. The high stiffness region may be involved in the regulation of posture and low stiffness region in locomotion.

The stiffness of the muscle also depends on the rate of stimulation. The higher the rate of stimulation, the higher is the amount of Ca^{++} available and consequently, the higher is the number of cross-bridges connected to the actin filament contributing to tension. The curve of tension versus rate of stimulation is a sigmoid function which is characteristic of a given muscle (Rack & Westbury, 1969). The region of greatest slope of this curve is usually where a muscle naturally operates (Stein, 1974).

The active tension developed under isometric conditions is also a function of the length of the muscle or the sarcomere length. The peak of tetanic tension versus length curve is around a sarcomere length of 2.8 μ , which is short of the maximum physiological length (Rack & Westbury, 1969).

The exact role of ATP during a cross-bridge cycle and other

biochemical reactions leading to muscle contraction have not been completely studied (Weber & Murray, 1973). However, from the present available knowledge, the overall mechanical response of a muscle, namely the shape of a twitch, work done during contraction, heat of shortening, has been related to the internal mechanisms (Julian, 1969; Stein & Wong, 1974).

In Chapters 3 and 4 we have proposed a linear visco-elastic model of the muscle which accounts for the observed physiological properties. The validity of this model was tested by letting the muscle contract against elastic and inertial loads. Chapters 3 and 4 were initially drafted by Dr. R.B. Stein for publication. Dynamics of the human soleus muscle have been shown in Chapter 5.

ALPHA MOTOR NEURONS

The active contraction of a muscle is directly controlled by the alpha motor neurons which take their origin from the ventral horn, of the spinal cord. The muscle fibres are functionally arranged as units called motor units. All muscle fibres in one unit are of the same type (Burke *et al.*, 1973). One motor neuron innervates all fibres of one and only one motor unit. Slow conducting axons usually innervate slowly contracting motor units and fast conducting axons innervate fast contracting motor units. In an intact animal all motor units of a muscle are rarely recruited. The level of force generated by the muscle is either increased by recruiting more motor units or increasing the firing rate of motoneurons which are already firing (Milner-Brown *et al.*, 1973a, b).

MUSCLE AFFERENTS

The feedback signals from the muscle to the central nervous system are carried by the spindle afferents and Golgi tendon organ afferents. Spindles are fusiform organs which lie between the extrafusal muscle fibres and are connected to them at both ends. Each spindle contains about 2-12 intrafusal muscle fibres which are surrounded by a connective tissue sheath. The intrafusal muscle fibres are of two types, the nuclear bag and the nuclear chain fibres (Matthews, 1972). Nuclear bag fibres are longer than the nuclear chain fibres; also the former are thicker at the centre containing numerous nuclei as opposed to the latter which have only one row of nuclei. A primary spindle afferent (Ia) (12-20 μ in diameter) divides into fine endings inside a spindle; each ending coils around the centre of each intrafusal fibre. Only one primary ending supplies one spindle. There are often more than one secondary endings (4-12 μ in diameter) for one spindle. A secondary ending (II) coils around the juxtaequatorial region of the chain fibre; it may occasionally give out a branch to nuclear bag fibre which ends in a spray ending.

The intrafusal fibres have their own motor innervation by the static and the dynamic gamma fibres (3-9 μ in diameter). A single dynamic gamma fibre innervates one bag fibre while one static gamma axon can terminate on several chain and bag fibres (Laporte & Monod-Dérand, 1973).

The spindle afferent endings are length detectors. When the intrafusal fibres contract more than the extrafusal fibres, the afferent endings are stretched. This stretch generates a rate of nerve impulses

In the axon. However, the spindle endings unload and stop firing if the extrafusal fibres contract more than the intrafusal fibres. A stretch of the muscle stretches the nerve endings, resulting in the firing of the afferent fibres.

Primary spindle endings are sensitive to the rate of change of length (velocity) and also to acceleration (Matthews & Stein, 1969a; Poppele & Bowman, 1970; Matthews, 1972). The response to steady stretch has been termed the static response and the response to the rate of change of the length the dynamic response. If a ramp stretch is applied to an active muscle, the firing of a secondary afferent follows the ramp quite closely while the primary afferent shows increased firing during ramp stretch and an abrupt decrease in firing rate at the end of the ramp stretch, i.e. when the dynamic change in length is reduced to zero. This decrease in firing rate with maintained stretch continues for some time before a steady firing rate is assumed. This phenomenon of sensory adaptation is another expression of the dynamic response. The secondary endings do show a dynamic response but much less than that shown by the primaries. 'Dynamic Index' (Matthews, 1972) measures the decrease in firing rate from the completion of the ramp stretch to 0.5 sec after that. For a particular velocity, the dynamic index of primary endings is much higher than that of the secondaries.

Dynamic index is affected differently by the two types of gamma fibres. Stimulation of the dynamic gamma fibres does not change the dynamic response of the secondaries much but increases the dynamic index of the primary afferents (Matthews, 1972). Stimulation of the

static gamma fibres decreases the dynamic response of both the primary and secondary endings to a small extent. The detailed effects are more complex and will be discussed in Chap. 6 (Goodwin & Matthews, 1971; Chen & Poppele, 1973).

In terms of systems analysis, spindle endings are highly non-linear elements. To get linear approximations of their behaviour in the frequency domain, one has to restrict the analysis to very small amplitude stretches and releases of the muscle. 'Sensitivity' of an ending has been defined by Matthews and Stein (1969a) as the change in firing rate per unit change in amplitude of sinusoidal stretch, the dimensions of sensitivity being impulses/sec/mm. In the frequency domain, when sensitivity of an ending is plotted versus the frequency of stretch, the sensitivity increases very little at low frequencies, but above about 1.7 Hz it starts to increase very rapidly. The frequency where sharp increase in the sensitivity takes place is called the corner frequency. The corner frequency has the same value for both the primary and secondary endings (except under static gamma fibre stimulation). Although the sensitivity curves look very similar (below 7 Hz) for both spindle endings, the absolute values are very much higher for the primary endings. Moreover, above about 7 Hz, the primary ending shows a faster increase in sensitivity than the secondary ending does; this is attributed to the acceleration sensitivity of the primary endings.

Various models of transduction of length and velocity into afferent signals have been proposed by different workers (Houk *et al.*, 1966; Rudjord, 1970a, b; Matthews, 1972; Poppele, 1973). Since we have

used Poppele's (1973) empirical expressions to compare with our data, his block diagram will be discussed in a little detail. The receptor organ is thought to consist of (1) a mechanical filter, (2) a transducer, and (3) an encoder. The mechanical filtering, which is supposed to be due to the visco-elastic properties of the intrafusal fibres, accounts for the slow adaptation of the afferents. In the frequency domain, the response of the endings below 0.5 Hz is attributed to this component. The mechanoelectric transducer, converting mechanical deformation of the endings into generator potential, has been suggested to account for the velocity and acceleration responses. This implies that the transducers are different for the two endings because the secondaries do not show an acceleration response. In the frequency domain, this component accounts for the behaviour of the spindle organs above 1 Hz. Both of the above components are considered linear over a small range of stretches. The encoder is a non-linear component which produces spikes from the generator potential and also shows the phase locking behaviour.

The Golgi tendon organs, afferents which feed back tension, lie at the musculo-tendinous junctions and thus lie in series with the contractile machinery of the muscle. Each tendon organ is connected to many motor units but it may sample only two or three fibres of one motor unit (Houk & Henneman, 1966). The afferent fibres (Ib) from the tendon organs have diameters in the range 6-16 μ . During an active twitch contraction, the receptor firing at a steady rate increases its firing rate during the contraction phase. The threshold for increased firing of the tendon organ receptors is much lower for active contraction

than for the passive stretches (Houk & Henneman, 1966). If a tendon organ is given a step force input, the response shows an overshoot at the end of the step which falls back slowly to a steady level. Thus the tendon organ responds to force and rate of change of force, the former is the static response and the latter the dynamic response. Very little work has been done on modelling of these receptors. Houk and Henneman (1967) have attributed the very slow adaptation to the visco-elastic properties of the connective tissue surrounding the receptor and the faster adaptation due to the visco-elastic properties of the contractile material or may lie within the receptor itself at the transduction level. In the frequency domain, the transfer characteristics of Ib fibres have been shown to be similar to those of primary afferent fibres (Rosenthal *et al.*, 1970; Anderson, 1974).

For spinal feedback pathways, the primary afferent fibres make monosynaptic excitatory connections with motoneurons of agonistic muscles, while the Ib fibres make diynaptic inhibitory connections with the same motoneurons. The contribution of the secondary afferents has been very controversial (Matthews, 1972, 1973). These muscle receptors had been lumped with group II cutaneous afferents as being inhibitory to the extensors and excitatory to the flexors. However, now it has been shown that the group II muscle afferents have an excitatory contribution to the tonic stretch reflex (Westbury, 1972; Rymer, 1973; Kirkwood & Sears, 1975).

Chap. 6 shows the frequency response results of muscle afferents with muscle length (tension) or motor spikes as input. The extent to which spindle endings and tendon organ receptors can compensate for muscle properties has been discussed.

'SERVO-ASSISTED' HYPOTHESIS AND REFLEX CONTROL

Having discussed the basic structure of the muscle and its motor and sensory innervations, we can discuss how its response is controlled by this innervation. The most accepted hypothesis is the 'servo-assisted' method of producing a movement (Matthews, 1972; Stein, 1974). These authors have also reviewed the other hypotheses. According to the 'servo-assisted' control of movement, the alpha and gamma motoneurons are activated simultaneously by the central nervous system. If the extrafusal and intrafusal muscle fibres contract by the same amount, the spindle receptors are unaffected. However, if the extrafusal fibres do not contract as much as the intrafusal fibres (due to fatigue or extra heavy load), the afferent endings are activated more. This leads to higher activation of the homonymous motoneurons leading to more contraction of the muscle. The coactivation of alpha and gamma fibres was first demonstrated by Granit and Kaada (1952). It has been shown in humans by Vallbo (1971) and walking mesencephalic cats (Severin *et al.*, 1967). This feedback is controlled at the level of the spinal cord by various descending pathways which can have excitatory or inhibitory effects (Feldman & Orlovsky, 1972).

How does a muscle carry on its normal tasks when the internal properties of the muscle change (e.g. fatigue) or there are external perturbations? When a muscle is stretched, the spindle afferents are activated which excite the homonymous motoneurons leading to shortening of the muscle. If the muscle is fatigued and does not produce enough tension, tendon organ afferents feed back less inhibition, leading to

tension (Houk *et al.*, 1970).

In addition to reflex control, the stiffness of the muscle accounts for many of its properties (Grillner, 1972, 1973; Grillner & Ude *et al.*, 1971). If a contracting muscle is stretched, the tension increases with extension even if there is no increase in the firing rate or the number of motor units. Muscle stiffness has been suggested to account for this property. The muscle properties also account for non-reflex load compensation (Partridge, 1966, 1967) which will be elaborated on in Chap. 4.

In addition to the short latency spinal feedback, longer latency muscle responses have been demonstrated (Melvill Jones & Watt, 1971; Evarts, 1973; Marsden *et al.*, 1973; Milner-Brown *et al.*, 1975; Tattom & Lee, 1975; Angel & Lemon, 1975). The electromyogram (EMG) of a muscle, after stretch, shows three peaks, the M_1 wave with spinal latency, the later M_2 and M_3 responses have longer latencies for which transcortical and transcerebellar pathways, respectively, have been suggested. These results indicate that in an intact animal there are three dominant reflex pathways, but anatomically these have not been traced.

There are a number of pathways known to exist for the motor system which could be involved in the long loop reflexes. There are four main tracts known to project to the cerebellum carrying information from muscle afferents. The dorsal spinocerebellar tract (DSCT) carries information from Ia, Ib and II muscle afferents, ascends the cerebellum at the medullary level and terminates ipsilaterally in the cerebellar vermal cortex (Oscarsson, 1965). The ventral spinocerebellar tract

(VSCT) crosses at the spinal level, enters the cerebellum at the pontine level. Both the DSCT and the VSCT carry information from the hindlimbs of the animal. Muscle afferents from the upper cervical regions terminate in the accessory cuneate nucleus of the medulla which gives rise to the cuneocerebellar tract (CCT). The CCT is the upper limb equivalent of DSCT. In the cat Oscarsson and Uddenberg (1964) have shown the presence of rostral spino-cerebellar tract which is the ipsilateral forelimb equivalent of VSCT.

The descending pathways known from the cerebellum to the spinal cord are the cerebello-vestibulo-spinal pathway, cerebello-fastigial-reticulo-spinal pathway and cerebello-rubrospinal pathway (Eccles, 1975a, b; Allen & Tsukahara, 1974).

The most obvious descending pathway from the cerebral cortex which can be involved in transcortical reflexes is the pyramidal tract. Short latency activation of the pyramidal tract by peripheral stimulation has been shown by various workers (Brooks & Stoney, 1971; Phillips, 1973; Asanuma, 1975). Both in primates and in cats the muscle afferents project to the motor cortex. For the forelimb the possible pathways are (Murphy *et al.*, 1974, 1975) (1) the spino-reticular pathway ascending through the central intralaminar nuclei of the thalamus, (2) the lemniscal pathway, ascending through the main cuneate nucleus and ventral posterolateral nucleus of the thalamus, (3) the transcerebellar pathway involving external cuneate nucleus, pars intermedia, interpositus and ventrolateral (VL) nucleus of the thalamus, and (4) the transcerebellar pathway involving RSCT, interpositus and VL nucleus. The pyramidal tract (PT) fibres converge

mainly on the interneurons in the spinal cord. However, Landgren *et al.* (1962) have shown that some PT fibres in primates terminate directly onto motoneurons.

In addition to the PT system, other descending pathways, collectively known as extrapyramidal system, are known. Fibres from the motor cortex project to the basal ganglia, red nucleus and the reticular formation. The rubrospinal and reticulospinal tracts are a part of the extrapyramidal system.

There are multiple small loops known to affect the ascending and descending cerebellar and cerebral cortical pathways (Allen & Tsukahara, 1974). These may control the inhibition or excitation levels of the main pathway and also affect their dynamics.

Chap. 5 discusses the dynamics of the long loop reflex pathway for human soleus muscle; Chap. 6 contains similar studies in decerebrate cats.

A block diagram for the voluntary and reflex control of the muscle is shown in Fig. 1.1. Dotted lines do not represent true feedback, but merely the load compensation and length-dependent response of the muscle due to its visco-elastic properties. The feedback from Golgi tendon organs, represented by F and \dot{F} (force and rate of change of force) goes to the alpha motoneurons, the cerebellum and the motor cortex. The length and velocity feedback from the spindles, represented by X and \dot{X} respectively, also goes to the same levels of the central nervous system. The tendon organ afferents feed inhibition (-) and spindles excitation (+) to the α -motoneurons for spinal reflexes, but their effect at the higher levels are not very well specified in

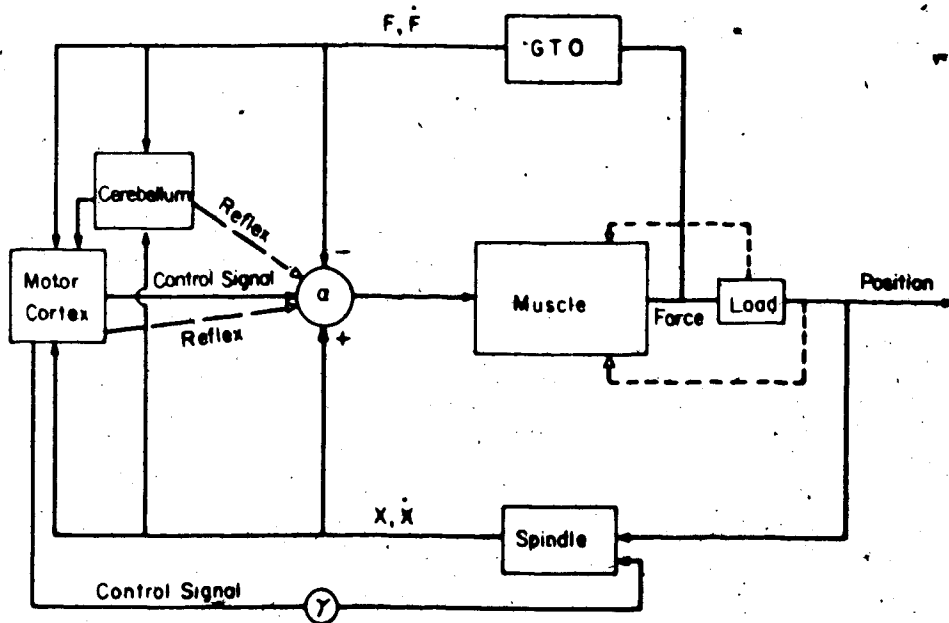


Fig. 1.1. The voluntary and reflex pathways for the control of muscle are shown in the above block diagram. Control signals represent the voluntary input to alpha and gamma motoneurons. Feedback from the spindles and the Golgi tendon organs is shown to go to alpha motoneurons, the cerebellum and the motor cortex. The broken lines show the possible long loop reflex feedbacks. The dotted lines do not represent a true feedback but merely the dependence of muscle output on its length and load.

the literature. The long loop reflex shown from the motor cortex could involve only the motor cortex (for M_2 wave) or the cerebellum and motor cortex (for M_3 wave). The reflex shown from the cerebellum does not involve the motor cortex, but only the cerebellum and brain stem structures.

CHAPTER 2

ANALYSIS AND SIMULATIONS

The whole stretch reflex loop is comprised of the following elements: (i) muscle, (ii) muscle afferents, (iii) motoneurons, and (iv) neurons between the afferents and the motoneurons. Biological systems are known to be highly nonlinear. However, for a system to be studied mathematically, the first step is to determine its linear properties. For this project the properties of the various elements have been evaluated to a linear approximation. From coherence estimates we have been able to know how linear each component is and over what range of frequencies. The data were analyzed on a LAB-8 computer (Digital Equipment Corporation). The major portion of the analysis was done in the frequency domain, but some time domain analysis was also done. When the input stimulus pulses were regularly spaced, the averaging technique (French, 1973b) was used, and when a random train of impulses was used then spectral analysis was applied (French, 1973a). A general idea of the two methods will be discussed below. The success of these techniques applied to simulated components is shown in the latter part of the chapter. Some examples are shown where the analysis did not work.

ANALYSIS

Recording

Tension from the cat experiments was recorded using a Grass FT-100 transducer and a Tektronix 3C66 carrier amplifier. For human

experiments the transducer was replaced by a Micro-Measurements EA-13-250MQ-350 strain gauge set-up (Chap. 5). The stimulus pulses, afferent spikes, tension and e.m.g. were recorded during the experiment on four channels of a Hewlett-Packart 7700 recorder and stored on magnetic tape for analysis. Checks for the stationarity of the mean and standard deviation of the tension fluctuations were introduced through use of a hot-stylus recorder during the cat experiments and a short computer program during analysis. In addition, a number of twitches were recorded once every 2 seconds (cat experiments) or once every 3 seconds (human experiments) before and after a period of random stimulation to check for stationarity. Records were analyzed only if the mean level showed drifts of less than 20% from the initial values.

Spectral Analysis

Frequency response function: The spectral analysis package was used to compute the input spectra, output spectra, cross spectra and the frequency response functions for any pair of inputs and outputs, i.e., either one could be a digital or an analog signal. These signals were prerecorded on an FM tape recorder. The analysis was done using the Fast-Fourier transform (FFT) technique as described by French and Holden (1971a, b). In order to apply FFT, both input and output signals were prepared as follows. The user assigns a sampling interval, t_s , at which the time series is sampled. The number of samples to be used was fixed at $N = 512$. The Nyquist frequency, f_N , is given by $\frac{1}{2t_s}$ and the frequency resolution by $\frac{1}{512t_s}$. The interval t_s is chosen such that there are no frequency components expected in the data above f_N . If this choice

interferes with the choice of frequency resolution, the data should be filtered so that no frequency components are left above f_n before the signal is fed into the computer. The time record is sampled 512 times every t_g milliseconds. For the digital data to be sampled this way, the time of incoming spikes is recorded. If T is the time of occurrence of a spike, it is convolved with the function $\frac{\sin(2\pi f_n t)}{2\pi f_n t}$, where t is the time centred around T . The convolved spike is sampled every t_g msec just as the analog signal is. This way the analog and digital data are transformed into equispaced series of amplitude values for the use of FFT:

The Fourier transform of a discrete time series is a discrete spectral component series in the frequency domain. If there are N sample values, the FFT algorithm reduces the number of calculations from N^2 to $N \log_2 N$ (Bendat & Piersol, 1971; French & Holden, 1971c). To compute the discrete Fourier transforms, the two time series are written as

$$x(n) = x(n t_g), y(n) = y(n t_g), n = 0, 1, \dots, N - 1.$$

If \bar{x} and \bar{y} are means of the input and output series, the zero mean series are given by

$$x(n) = x(n) - \bar{x}$$

$$y(n) = y(n) - \bar{y}$$

where

$$\bar{x} = \frac{1}{N} \sum_{n=1}^N x(n) ,$$

$$\bar{y} = \frac{1}{N} \sum_{n=1}^N y(n) .$$

The discrete Fourier transforms are given by

$$X(m) = \frac{1}{N} \sum_{n=0}^{N-1} x(n) e^{-2\pi j \frac{mn}{N}}$$

$$Y(m) = \frac{1}{N} \sum_{n=0}^{N-1} y(n) e^{-2\pi j \frac{mn}{N}} , m = 0, 1, \dots, N-1,$$

with the frequencies given by

$$f = \frac{m}{N t_s}$$

$$\text{or } \omega = \frac{2\pi m}{N t_s}$$

The power spectral densities can be written as

$$S_{xx}(\omega) = X(m) X^*(m) ,$$

$$S_{yy}(\omega) = Y(m) Y^*(m) ,$$

$$S_{xy}(\omega) = X(m) Y^*(m) ,$$

$$S_{yx}(\omega) = Y(m) X^*(m) .$$

where S_{xx} and S_{yy} are input and output power spectral densities, respectively, and S_{xy} and S_{yx} are forward and backward cross power spectral densities, respectively. The superscript * is for complex conjugation. The frequency response function is given by

$$G(\omega) = \frac{S_{xy}(\omega)}{S_{xx}(\omega)}$$

if additive noise appears in the output and

$$G(\omega) = \frac{S_{yy}(\omega)}{S_{yx}(\omega)}$$

if noise appears in the input.

From the transfer function one can compute the gain and phase for the output/input series. The coherence function which is the measure of linearity of the system is written as

$$\gamma^2(\omega) = \frac{|S_{xy}|^2}{S_{xx} S_{yy}}$$

where $|S_{xy}|$ is the absolute value of the forward cross power spectral density. In this work, empirical expressions were used for the linear transfer functions of the muscle and spindle afferents. The coherence values indicate how justified we were to use a linear model to fit the data.

All the above analysis is for the record length 512 t, which gives one spectrum. The total run for one observation, L, was usually 1 minute long so that we had $q = \frac{L}{512 t}$ spectra. The results were

averaged over q spectra.

While computing the gain, phase and coherence values, frequency smoothing was carried on at higher frequencies. The frequency resolution at lower frequencies is given by $\frac{1}{512 t_s}$. At higher frequencies l neighbouring components were averaged in such a way that successive samples were approximately evenly spaced on a logarithmic frequency scale; the resolution frequency increased to $\frac{l}{512 t_s}$ (Bendat & Piersol, 1971, Chap. 6 and 9).

Second-order curve fitting: In Chapters 3 and 5 the gain and phase data of the nerve-muscle transfer function have been fitted with a second-order curve by the least mean square error method. A second-order system is characterized by three parameters: G_0 , the low frequency gain, f_n , the natural frequency, and ζ , the damping ratio; we wanted to get the best estimates of these parameters. A short computer program was used for this purpose. Initial values of the parameters were chosen from the experimental gain data, and each parameter was varied in turn by a preset percentage. The change which produced the greatest reduction in the least mean square error of the gain data points from the predicted gain curve was accepted. The process was repeated until no further reduction in error could be obtained with that percentage of variation. The percentage was then reduced until the best-fitting parameters were obtained to the nearest 1%. When the damping ratio $\zeta \geq 1$, the two time constants were calculated. Using the values of parameters derived from the gain curve, the predictions for the phase as a function of frequency were examined. The phase is affected by

the pure time delays involved in nervous conduction, neuromuscular transmission and excitation-contraction coupling. The best-fitting value of the total time delay could be calculated so as to minimize the mean square error.

Altogether three criteria were available for checking the adequacy of a second-order model: (1) the decline in gain at high frequencies according to the second power of frequency, (2) no phase lags greater than approximately 180° after accounting for the pure time delays, (3) the goodness of fit of the second-order curve. Standard deviations of the points from the fitted curve were typically less than $\pm 10\%$.

Confidence intervals: The confidence intervals were calculated for some of the gain and phase data in Chapters 3, 5 and 6. The detailed derivation of the expressions for confidence intervals of the frequency response is discussed by Bendat and Piersol (1971). In the confidence intervals the F distribution is involved; therefore, to know the degrees of freedom of a particular estimate discussed above, a spectral estimate with independent real and imaginary parts has 2 degrees of freedom. If we average q number of estimates, the degrees of freedom are $2q$. Further, if frequency averaging is done, considering l frequency components at a time, the total number of degrees of freedom increases to $n = 2ql$. The approximate $(1 - \alpha)$ confidence intervals for the gain $|G(f)|$ and phase factor $\phi(f)$ are given at each frequency, f , by

$$|\hat{G}(f)| - \hat{r}(f) \leq |G(f)| \leq |\hat{G}(f)| + \hat{r}(f)$$

$$\hat{\phi}(f) - \Delta\hat{\phi}(f) \leq \phi(f) \leq \hat{\phi}(f) + \Delta\hat{\phi}(f)$$

where

$$\hat{r}^2(f) = \frac{2}{n-2} F_{2, n-2; \alpha} [1 - \hat{\gamma}_{xy}^2(f)] \frac{\hat{S}_{yy}(f)}{\hat{S}_{xx}(f)},$$

$$\Delta\hat{\phi}(f) = \sin^{-1} \left[\frac{\hat{r}(f)}{|\hat{G}(f)|} \right],$$

$n = 2ql \equiv$ number of degrees of freedom of each spectral estimate,

$F_{2, n-2; \alpha} = 100 \alpha$ percent point of an F distribution

with $n_1 = 2$, and $n_2 = n-2$ degrees of freedom,

$\hat{S}_{xx}(f)$ = estimate for the power spectrum of input $x(t)$,

$\hat{S}_{yy}(f)$ = estimate for the power spectrum of output $y(t)$,

$\hat{\gamma}_{xy}$ = sample estimate of the coherence function between input $x(t)$ and output $y(t)$.

The hats (^) indicate that the quantities are experimental estimates.

Averaging

The averaging technique was used either where random stimulation could not be applied or where time domain properties were studied. Both input and output had to be in analog form. The analog time record was either twitch tension or rectified and filtered EMG or modified and filtered sensory afferent impulses.

To determine contraction time, half-relaxation time, peak

tension and area under the twitch, a certain number of twitches were averaged depending on the experiment (Chap. 3 and 5). Another program computed and typed out the above parameters.

To determine the frequency response function between (i) tension as input, afferent impulses as output, (ii) afferent impulses as input, EMG as output, (iii) tension as input and EMG as output, the following procedure was used. Before feeding EMG into the computer, the EMG was rectified and passed through a Paynter filter (Gottlieb & Agarwal, 1970) which had a cut-off frequency of ~100 Hz. The Paynter filter introduced phase lags which were corrected for in the final data. To make the afferent data into analog signals comparable to the EMG, each spike triggered a pulse generator to produce a standard pulse of 5 msec duration, which was passed through a Paynter filter. This did not introduce any dynamics into the system over the range of frequencies of interest, but introduced phase lags which were corrected for in the final results. About 100 responses for the required input and output were averaged and plotted. The next program took the Fourier transform of the input and output averaged data. Finally, the gains and the phases at various frequencies were computed.

SIMULATIONS

The biological systems, i.e., the muscles and the sensory muscle receptors, are known for their nonlinearities (Nichols & Houk, 1973; Houk *et al.*, 1973). To test the effect of some nonlinearities on the accuracy of the linear analysis, the analysis was done on the response

of simulated elements. A block diagram of a complete simulated feedback loop for the myotatic reflex is shown in Fig. 2.1. The muscle was simulated by a critically damped, second-order, low pass RC filter, stage I. The input to the RC circuit was either a random train of short duration impulses to apply spectral analysis technique or regularly spaced impulses for the averaging technique. Fig. 2.2 shows the gain curves for theoretically calculated values, spectral analysis and averaging technique results. The three are very similar. The coherence values are available only for the spectral analysis.

The output of the simulated muscle was fed into an RC circuit (stage II) which responded to position and velocity. The frequency response function of this element with input from the simulated muscle was exactly the same as that of secondary spindle afferents given by Poppele and Bowman (1970) up to 30 Hz (Fig. 2.3a). This output was fed to the model neuron (French & Stein, 1970), whose firing rate could be varied (stage IV). Also, different levels of noise could be added. The output of the model neuron was passed through a pulse generator to increase the duration of the spikes and then through a Paynter filter before feeding it into the computer as an analog signal. Stages II and IV together simulate the muscle spindle afferent or muscle spindle afferent plus motoneuron assuming that the motoneurons do not add any dynamics to the feedback system (Chap. 5 and 6; also Poppele & Terzuolo, 1968). Between stages II and IV different pulse time delays (stage III) were added. Fig. 2.3a shows the gain of the transfer function for RC circuit of stage II with an analog signal as input and an analog signal as output. The corresponding phases of this stage are purely due to the

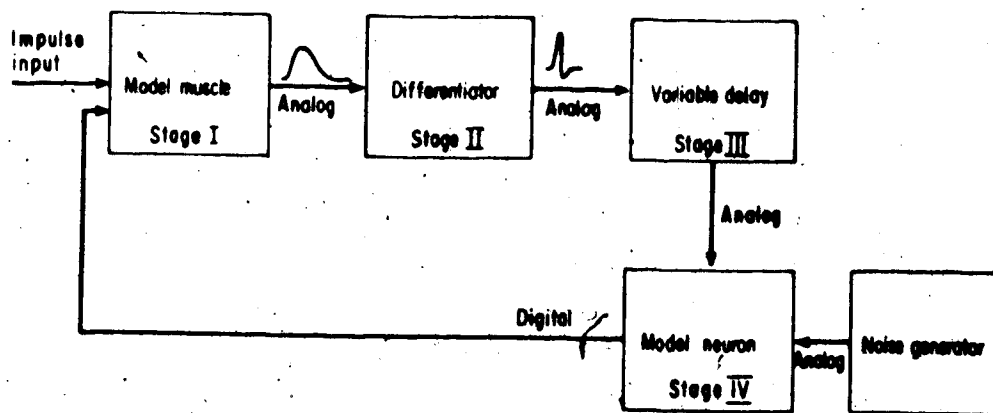


Fig. 2.1. Block diagram of simulated stretch reflex loops with adjustable noise input at the model neuron stage. Stages II, III and IV form the feedback part of the loop.

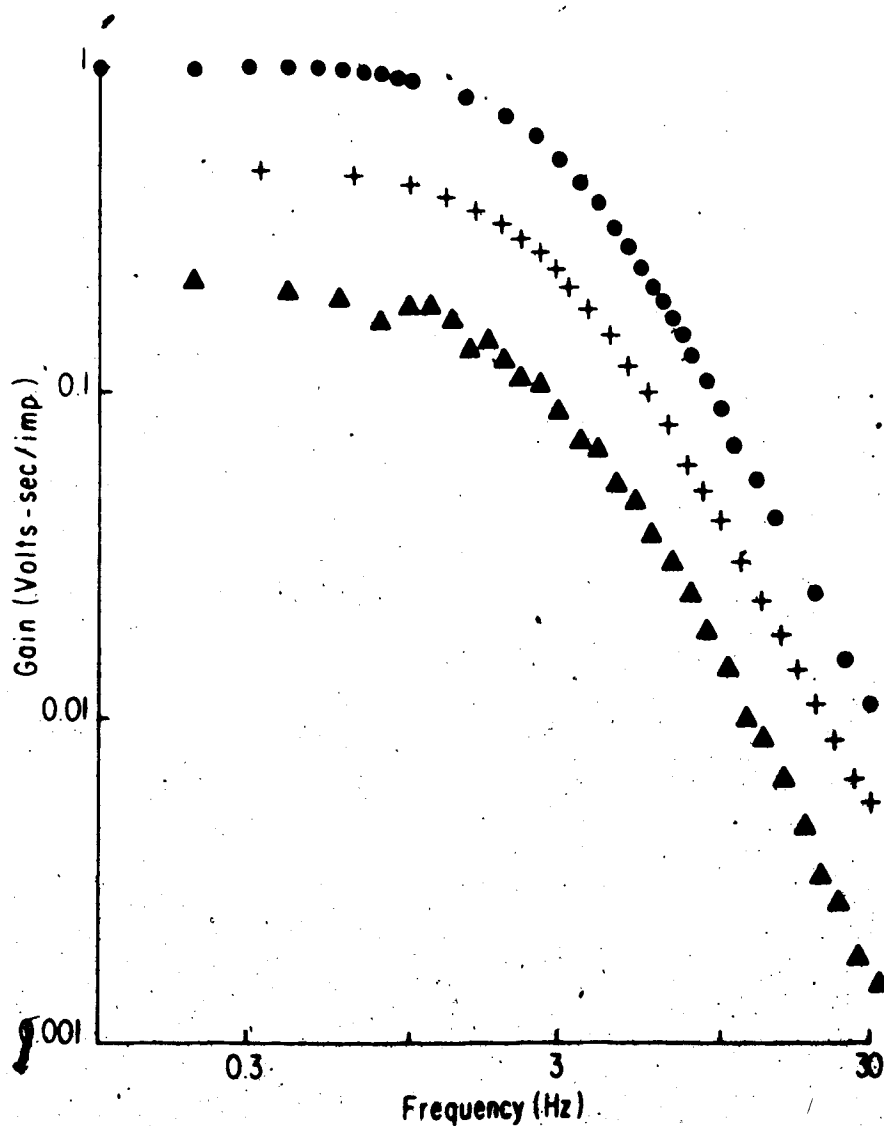


Fig. 2.2. Gain curves of the frequency response function of critically damped, second-order RC filter simulating the muscle. (•) give the calculated values from circuit analysis. (+) show the gain values computed by the averaging technique and (Δ) show the gain values computed by spectral analysis when input random impulses were applied at a mean rate of 5/sec. The absolute values of gain are different in three cases.

dynamics with no pure time delay contribution. Fig. 2.3b shows the gain for stages II, III and IV with a delay of 20 msec. The model neuron firing rate ($\sim 100/\text{sec}$) was only modulated by the input. Curve 2.3b is similar to curve 2.3a. Thus adding the delay and the non-linear element (model neuron) does not affect the dynamics; the analysis is still accurate.

The difference between phases of 2.3b and 2.3a was due to the pure time delay (Chap. 5). There was a linear relationship between these phase differences and frequency. The slope of this straight line gave the time delay in the pathway; the computed delay agreed with the delay introduced. This was repeated for different delays; the gain curves were not affected, only the phases were. If the delay is t msec, the modulation of the model neuron begins after t msec. One can eliminate this part of the model neuron output in the computer averaging. This elimination introduces a phase advance $\phi = 0.36 f t$ degrees. If this was taken into account, then the transfer function was not affected by elimination of the first t msec of model neuron output (this application was used in the elimination of M and H waves from ECG records in Chap. 5 and 6).

When the input to the model neuron was large enough, instead of modulating the firing rate the model neuron stopped firing altogether for a period equal to several interspike intervals at the mean rate of firing. This can be considered as a saturation nonlinearity. Fig. 2.3c shows the gain when the model neuron was missing about 5-6 spikes, giving a pause of ~ 80 msec. From different pause lengths of t_p sec, it seems that a dip in the gain curve occurs at a frequency of $\frac{1}{t_p}$ Hz. The

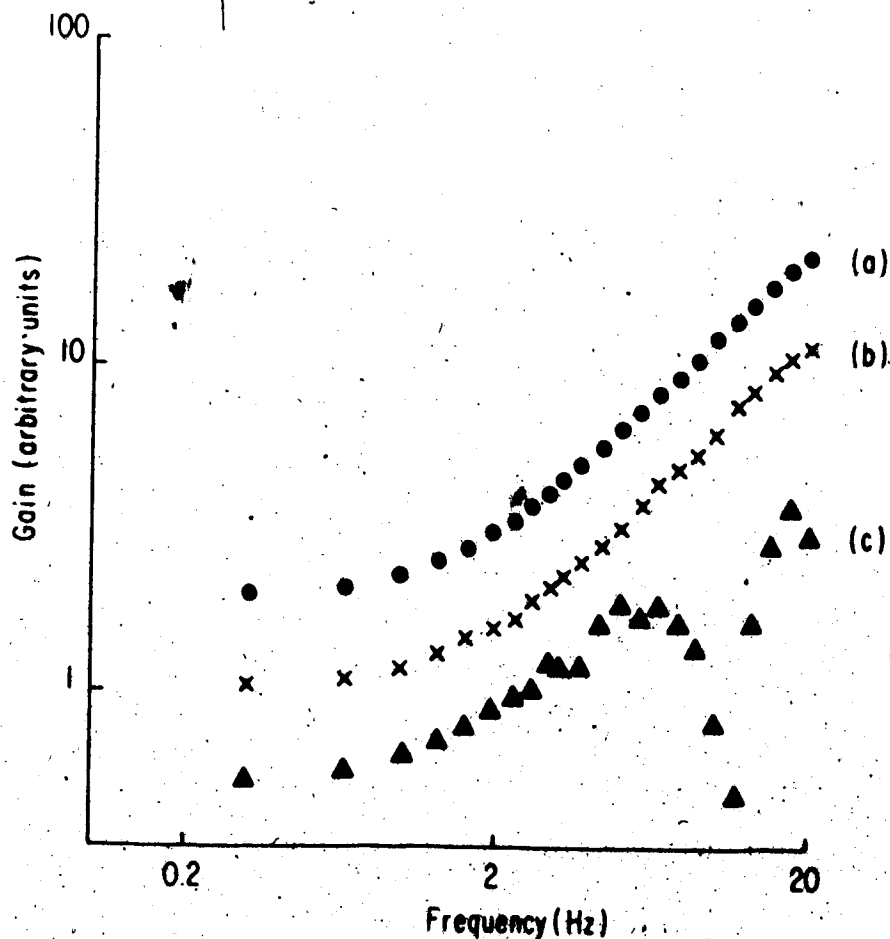


Fig. 2.3. Gain curves of the frequency response functions for simulated muscle spindle afferents. (a) shows the gain of position and velocity sensitive RC circuit only. (b) shows the gain of stages II, III and IV when the delay added was 20 msec, and (c) shows the gain for the same stages when the delay added was -80 msec and there was an initial pause of 80 msec in the firing of the model neuron. The model neuron firing rate in (b) and (c) was around 100/sec. Low frequency gain in (b) has been normalized to unity. Gain of (a) and (c) have been shifted by $\times 2$ up or down for clarity.

corresponding phases were also affected. Delay introduced for Fig. 2.3c was about 80 msec but the computed delay from the phases (up to 10 Hz) is 110 msec. The delays calculated were always much higher when a pause was introduced. Thus the results were not reliable when there were saturation nonlinearities introduced. Effects of this kind on our analysis of the afferent data will be discussed in Chapter 6.

If, in addition to the saturation nonlinearity, the firing rate of the neurons was low, this also made the results unreliable. Peaks in the gain curves occurred at the firing frequency and its higher harmonics. Correspondingly, there were large, non-monotonic variations in the phases. One could not calculate the pure time delays from these phase lags. Analysis was done for various firing rates, introducing different durations of the pause. Fig. 2.4 shows the gain curves up to 40 Hz for a firing rate of 28/sec with two different pauses. In Fig. 2.4a the pause was around 50 msec (missing one spike) with a slight trough in the gain curve ~20 Hz. There is a peak ~30 Hz (firing rate). It was seen around 60 and 90 Hz too. The delay of 87 msec calculated from the corresponding phase data was close to the introduced delay of ~80 msec. Fig. 2.4b had a pause ~120 msec (missing three spikes); the trough is around 9 Hz with a peak at the firing rate ~30 Hz. The computed delay of 117 msec was much longer than the introduced delay. So the analysis again breaks down.

Transfer function of stages II, III and IV was computed for different rates (15, 20, 28 and 63/sec) adding separate amounts of noise in the firing rate of the nodal neuron. The firing rate of the nodal neuron was only modulated and no clear pause was introduced. The higher

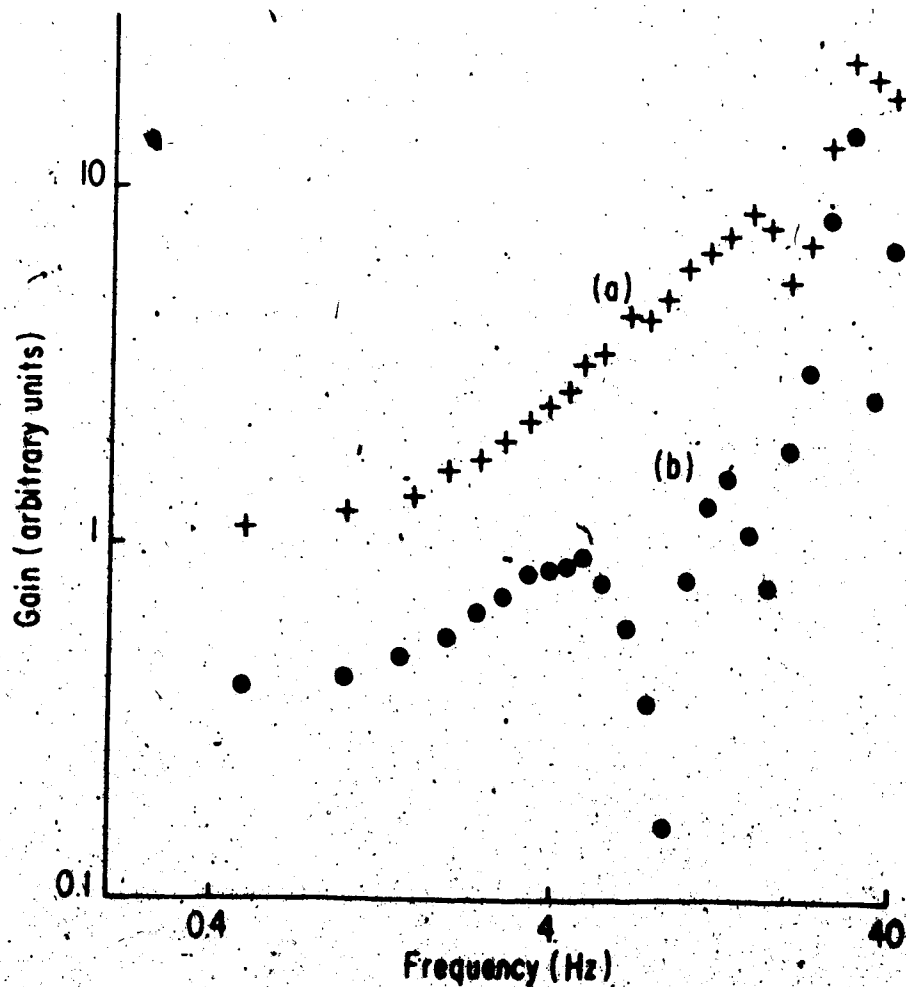


Fig. 2.4. Gain curves shown for stages II, III and IV with the model neuron firing at 28/sec. The initial pause in the firing of the model neuron was -50 msec in (a) and -120 in (b). There is a peak around 30 Hz in both cases which is the firing rate of the model neuron. Low frequency gains have been normalized to unity. Gains in (b) have been halved for clarity.

the firing rate, the more reliable were the data at higher frequencies. With firing rates of 28/sec and 63/sec, the data with and without noise were good up to 20 Hz and the delays calculated were correct. At lower rates (e.g., 15 and 20/sec) the scatter in the data increased as the noise level was increased. The scatter made the sharp trough and peaks disappear. Fig. 2.5 shows the gain curves with and without noise when the firing rate was 16/sec. Fig. 2.5a has no noise added to the model neuron; the peak at the firing frequency is sharp and the phase data are reliable only up to 10 Hz. The computed delay (93 msec) is a little longer than the added delay. The same is true of Fig. 2.5b where the standard deviation of the mean interval is 4.3 (mean interval 62.5). However, when the S.D. increased to 19.5, the scatter increased, the phase data were usable up to 20 Hz and the calculated delay was 86 msec, very close to the added delay. The same results were true for higher firing rates; only the usable frequency range increased.

The next step was to close the loop and check if the transfer function for stages II, III and IV was still the same and correct time delay values could be computed. Different delays were added. When the feedback oscillation was heavily damped, there was no clear pause in the firing of the model neuron and the firing rate was only modulated; the computed delays were correct and the gain curves were not affected. As soon as a pause of length t_p sec was introduced, a dip in the gain curve occurred at $\frac{1}{t_p}$ Hz and the difficulties were the same as for the open loop.

Another difficulty is encountered when the loop is closed. If the loop gain is very high to keep the oscillation going, power at the frequency of oscillation is very high relative to the power at other

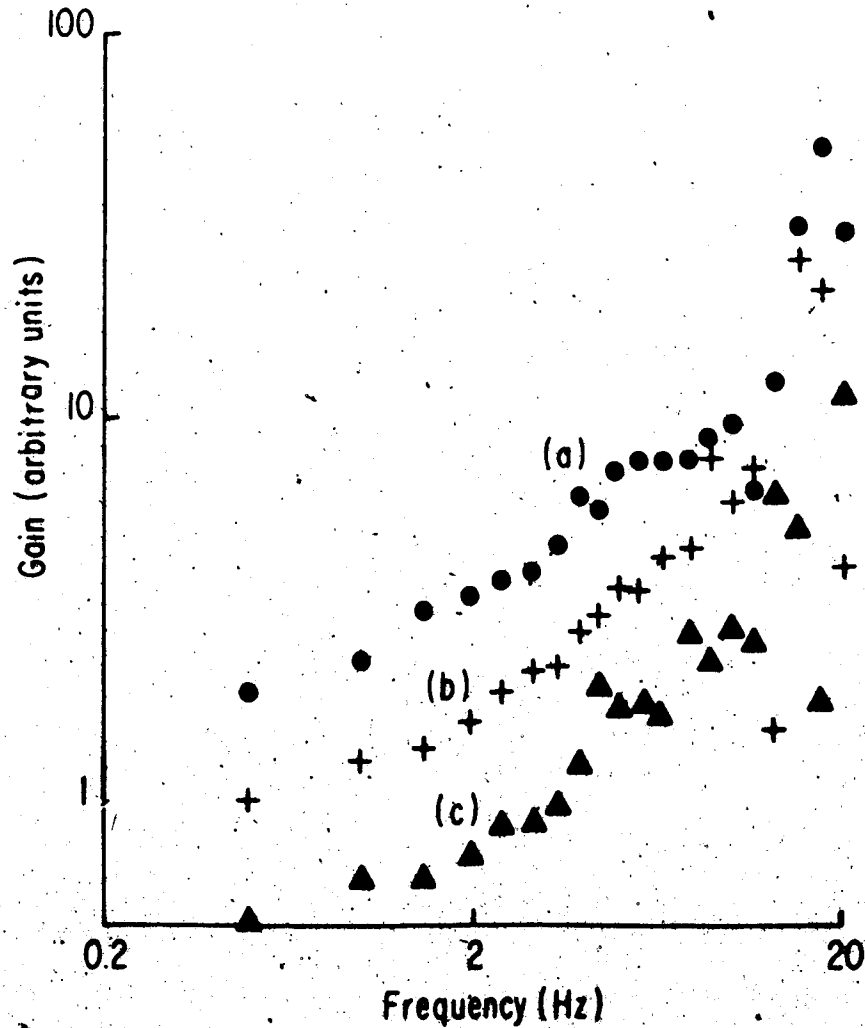


Fig. 2.5. Gain values are shown for stages II, III and IV when the coefficient of variation of the mean interval of the model neuron firing was (a) 0.00, (b) 0.07, and (c) 0.3. The mean firing rate was around 16/sec. Low frequency gain in (b) has been normalized to unity. Gain of (a) and (c) have been shifted by x2 up or down for clarity.

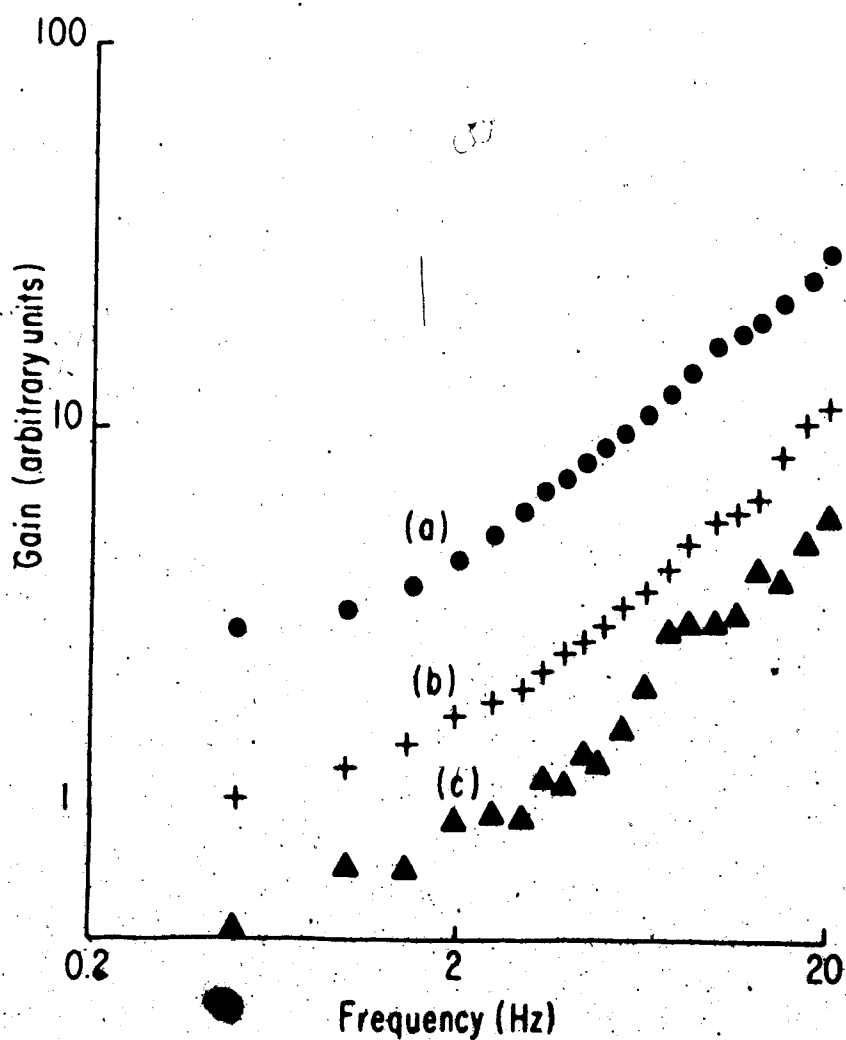


Fig. 2.6. Gain curves shown for stages II, III and IV when the loop was closed. The delays added in the feedback pathway were (a) 20 msec, (b) 40 msec, and (c) 80 msec. In (c) noise was added to the model neuron firing. Low frequency gain in (b) has been normalized to unity. Gains of (a) and (c) have been shifted by $\times 2$ up or down for clarity.

frequencies. One cannot compute any reliable results under such conditions except getting the correct frequency of oscillation. Fig. 2.6 shows the gain curves for stages II, III and IV when the delays added in the feedback were 20, 40 and 80 msec, respectively, for the curves a, b and c with no large oscillations. The computed delays agreed with the delays introduced. For Fig. 2.6c noise was added to the model neuron. Fig. 2.7 shows the inverted oscillatory output in the time domain for the model muscle in three cases. The inverted output corresponds to the length change to which the model neuron (or the spindle afferents) respond. As the feedback delay was increased, the frequency of oscillation decreased. For 20 msec delay, no clear oscillation is shown; only a hump on the falling phase is visible. This small amount of feedback response is enough to calculate the feedback transfer function accurately. This is the form of some closed loop muscle responses observed in human as well as in the cat work (Chap. 5 and 6).

It is clear from the simulation work that the analysis was unreliable under certain well-defined conditions. Difficulties arose only when (i) there was a pause in EMG or afferent firing, (ii) afferent firing rate was low, or regularly firing single motor units were recorded in the EMG, or (iii) when there were large undamped oscillations.

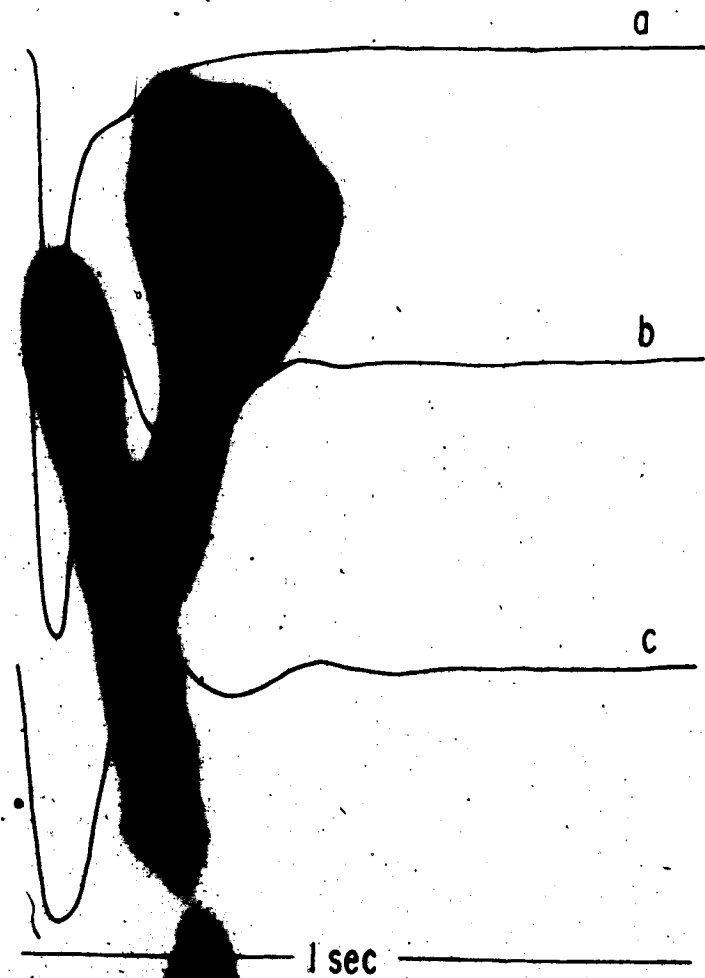


Fig. 2.7. Time domain input-output of the simulated muscle is shown when the loop was closed. The feedback latencies introduced were (a) 20 msec, (b) 40 msec, and (c) 80 msec. The frequency of oscillation decreased with an increase in time delay.

CHAPTER 3

EFFECTS OF ELASTIC LOADS ON THE CONTRACTIONS OF CAT MUSCLES

INTRODUCTION

The partially fused contractile responses resulting from random nerve stimulation resemble the natural activity of muscle more closely than do isolated twitches or fused tetani. We have been interested in describing the tension fluctuations of muscles under conditions of random activation and in drawing inferences from such a description about the underlying contractile mechanism.

Mannard and Stein (1973) showed that in response to random stimulation the partly fused responses of an isometric muscle of the cat were similar to those of a simple, linear, second-order system, i.e., the relationship between nerve stimuli and tension fluctuations, under various conditions of mean stimulation rate and muscle length, conformed to a family of second-order frequency response curves. A frequency response curve measures the ability of a system to respond to inputs of various frequencies. In the case of muscle this curve measures both the gain and phase changes muscles will contribute to cyclic activity found in natural movements such as walking, running and tremor. A second-order frequency response curve is conveniently described by the values of three parameters. Two of these parameters are, under specified conditions, the *time constants* or the *rate constants* of the system (Milsum, 1966). Since normally functioning muscles are often free to shorten appreciably, we extended these experiments to muscles which were free to contract against elastic loads. As will be described, the second-order model still holds for muscles contracting against springs

with widely different stiffnesses.

Models of force generation in muscle generally contain a contractile element which has kinetic properties that determine the generation of force internally. This force is then modified by the dynamics of the muscle and external loads, considered as a visco-elastic system. One might expect that several variables would be needed to describe the behaviour of such a system, but the fact that a second-order model holds for both isometric and elastic loading implies that *only two variables are rate-limiting*.

Theoretical studies (Stein & Wong, 1974) were undertaken using a model for contraction based on the sliding filament theory (Huxley, 1957) as expanded by Julian (1969) to include the kinetics of activation produced by Ca ions. These studies suggested that one of the rate-limiting processes was the reuptake of Ca by the sarcoplasmic reticulum. This process determined the relaxation phase of an isometric twitch. However, it was not clear whether the second process which determined the contractile phase of a twitch involved the rate of making and breaking cross-bridges between actin and myosin molecules, or depended on the visco-elastic properties of muscle. Earlier models of muscle (Hill, 1938; Houk, Cornew & Stark, 1966) tended to assume that the increase in tension during a twitch was mainly limited by visco-elastic properties. However, in isolated single fibers of the frog in which tendon compliance had largely been eliminated, Huxley & Simmons (1971) showed that the formation of cross-bridges limited the rate of rise of an isometric twitch. Other possible rate-limiting steps include the breaking of cross-bridges (Podolsky, Nolan & Zaveler, 1969),

the movement of cross-bridges (Weber & Murray, 1973) or the binding of Ca ions (Ashley & Moïşescu, 1973). Although studies on the dynamic properties of whole muscles are unlikely to distinguish conclusively between these various possibilities, we felt we could test the visco-elastic hypothesis by varying the loading conditions.

We studied the plantaris and soleus muscles in the cat, both under isometric conditions and with elastic loads. Under isometric conditions both muscles behaved according to the predictions of the second-order model, although the natural frequency of soleus muscle (a mainly slow twitch muscle; Henneman & Olson, 1965) was much lower than for plantaris muscle (a mainly fast twitch muscle; Binkhorst, 1969). For plantaris muscle with elastic loads one rate constant did increase systematically when increasingly stiff springs were added in series with the muscle, as expected if the visco-elastic properties of the muscle limited the rate of contraction. Chapter 4 compares the experimental results with a quantitative model of muscle based on this possibility. This model can predict the results of experiments when a muscle contracts, not only against elastic loads, but also against various inertial loads. However, when elastic loads were applied to soleus muscle, some properties were observed which would not be expected for a linear, second-order system. These are described qualitatively in the RESULTS and discussed further with respect to other recent work on this muscle (Joyce, Rack & Westbury, 1969; Burke, Rudomin & Zajac, 1970; Nichols & Houk, 1973).

METHODS

The experimental arrangements for this and Chapters 4 and 6 are shown schematically in Fig. 3.1. Random trains of supramaximal stimuli at a mean rate of between 5/sec and 10/sec were applied for 1 minute to the nerve to either plantaris or soleus muscles (details in Mannard & Stein, 1973). The two heads of gastrocnemius were divided and either plantaris or soleus muscle was freed. The Achilles tendon was divided so that only the muscle to be studied was left attached to the calcaneum. The tendon would then be attached either to

- (1) a stiff tension transducer (stiffness = 10 kg/mm) - *isometric loading*;
- (2) an external spring of varying stiffness (8 g/mm to 570 g/mm) - *elastic loading*;
- (3) an external spring after going around a pulley to which varying inertial loads could be added - *inertial loading*.

Under conditions (2) and (3) the tension transducer was connected to the other end of the external spring. Except when the effect of length was being studied, the muscle was kept at the length which produced the largest *isometric* twitch tension. The passive tension corresponding to this optimal length was noted and when elastic loads were changed, each spring was stretched to produce the same level of passive tension. Different flywheels coaxial with the pulley constituted inertial loads in the range 4-1500 g. After each experiment the system was calibrated by replacing the muscle with a spring, and observing the damped oscillations that resulted from brief displacements of the

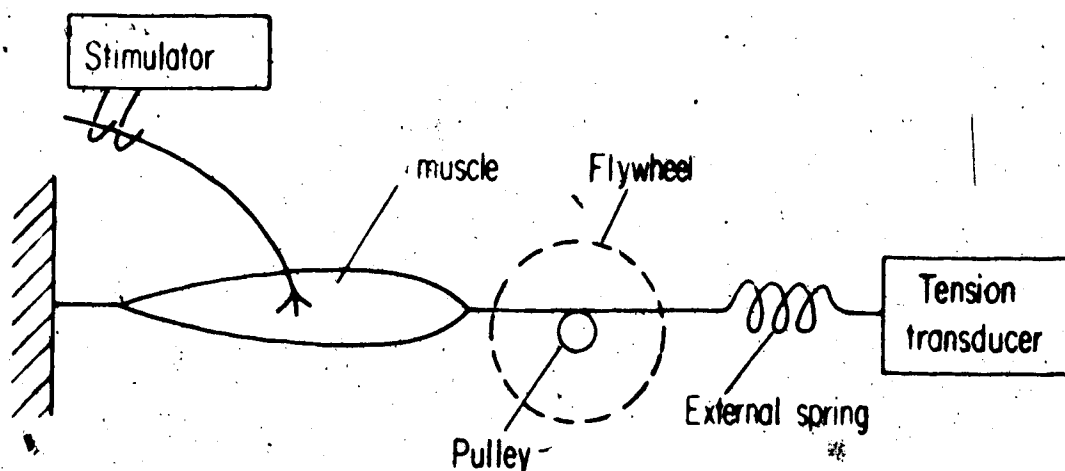


Fig. 3.1. Schematic diagram of the system used to apply varying elastic and inertial loads to a muscle. The pulley and flywheels for inertial loading (interrupted lines) were not connected except for experiments described in Chaps. 4 and 6. They were included, when required, by passing the thread from the muscle around the pulley. The thread was knotted and attached tightly at one point so that no slippage could occur. The pulley had a sufficiently large diameter (6 cm) that only a fraction of a rotation occurred even with maximal contractions.

various inertial loads. The damping of the pulley system was small compared to the probable damping introduced by the normal antagonistic muscles, but the range of elastic and inertial loads probably included most of the physiological range (A. Mannard & R.B. Stein, unpublished observations).

Values of tension are given in grams weight in this work because these are easily comprehended and are consistent with much of the previous literature. These values can be easily converted to the more widely accepted MKS units of force, Newtons, by dividing by 1000 (to convert grams to kilograms) and multiplying the results by the acceleration of gravity, 9.8 m/sec^2 . Similarly, the values of stiffness can be easily converted to N/m .

RESULTS

Effect of Elastic Loads on the Twitch

Plantaris muscle: Fig. 3.2 shows a typical isometric twitch of plantaris muscle in response to supramaximal stimulation at its optimal length, together with the effects of putting increasingly compliant springs in series with the muscle. Note that the twitch tension is markedly reduced when more compliant springs are used, and the contraction time is lengthened somewhat. Similar results have been observed for sartorius muscle of the frog (Hill, 1951).

However, it is not obvious from Fig. 3.2 whether the relaxation phase of the twitch is similarly affected. To study this several twitches were averaged and various parameters were calculated from the average

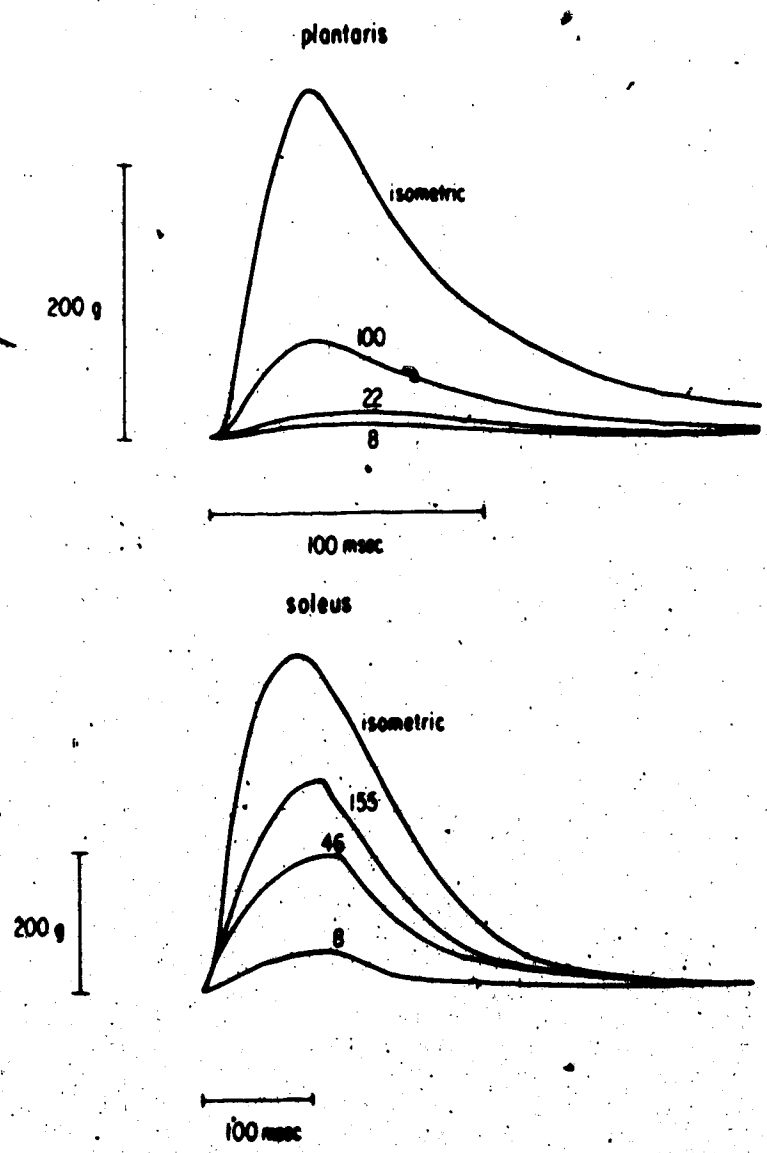


Fig. 3.2. Effect on twitch tension of adding springs in series with plantaris and soleus muscles. The values indicated give the stiffness of the added springs in g/mm. The superposition was carried out by tracing the twitches from the original photographs.

twitch. Twitches were applied before and after each period of random stimulation so the effect of random stimulation at 10 stimuli/sec for 60 sec could also be determined. These results are summarized in Fig. 3.3 for the same muscle as used in Fig. 3.2. The left half of Fig. 3.3 indicates that the half-relaxation time, as well as the contraction time, decreased when increasingly stiff springs were used. It was more difficult to measure changes in the final exponential decay of the twitch below the half-relaxation point (see also Jewell & Wilkie, 1960). Small increases or decreases were observed in different experiments after increasing the stiffness of external springs.

Much more dramatic than the changes in time course are the changes in twitch tension and the area under the twitch shown on the right side of Fig. 3.3. The best-fitting straight lines have been computed for the data in each part of Fig. 3.3 to indicate the trends more clearly. The lines do not necessarily imply that these variables are all linearly related to series stiffness. The expected relations between some of these variables will be considered in Chapter 4.

By comparing the data points in Fig. 3.3 measured before (-) and after (+) a period of random stimulation, we see that a period of random stimulation slightly potentiated the twitch and shortened its time course. These two effects of stimulation cancelled in this experiment so that the area under a twitch (measured in g-sec) was little affected.

Soleus muscle: The time course of the twitch in soleus was much longer than plantaris under isometric conditions and with all

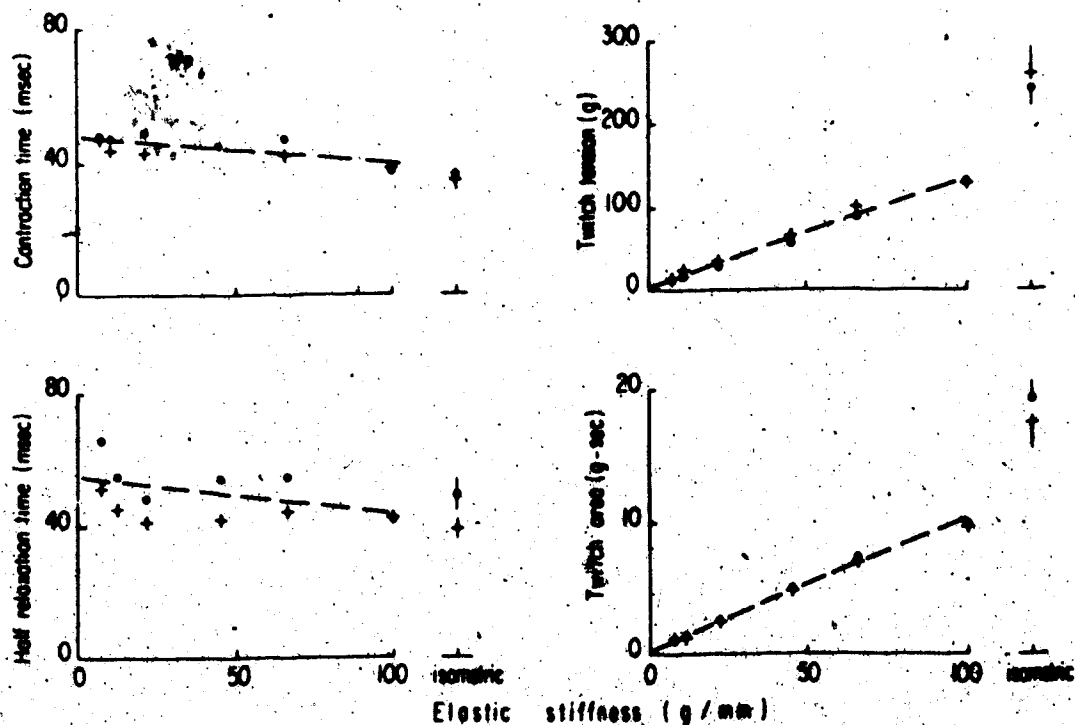


Fig. 3.3. Changes in parameters of twitches in plantaris muscle measured with series springs of different stiffnesses. The \cdot 's were values obtained before and the $+$'s were values obtained after a period of random stimulation. The fitted straight lines were calculated using all the data for elastic loads. Several isometric runs were interposed between the trials using elastic loads and the vertical extent of the symbols for the isometric conditions gives the standard deviation of the values for each parameter. Same muscle as in Fig. 3.2.

elastic loads. We also consistently observed that the duration of the twitch contractions of soleus muscle against weak springs increased toward a steady level and then declined abruptly (Fig. 3.2). The contraction times were therefore longer with weak springs, as for plantaris, but the half-relaxation times were less. The unusual form of the twitch was presumably due to the formation of stable bonds during the contraction of this slow twitch muscle, the effects of which have been described previously (Joyce *et al.*, 1969; see also the DISCUSSION).

Another effect of these stable bonds was that during the occasional long pauses in the random stimulation the mean level of tension would drop dramatically and only return to its previous level with a time course of a second or more (see also Burke *et al.*, 1970). These nonlinear effects were much more prominent in the slow soleus muscle than in the faster plantaris, so that most of the subsequent linear analysis will deal with plantaris. However, comparisons with soleus will be included at several points in the RESULTS and in the DISCUSSION.

A final difference between the two muscles was that the twitch tensions in soleus were generally somewhat depressed immediately after a period of random stimulation at a mean rate of 5 or 10/sec, when these periods were separated by a minute or so. Potentiation of the twitch was occasionally observed, particularly when higher, near-tetanic rates of stimulation were used.

Fatigue: Each period of random stimulation contained several hundred stimuli and during a long experiment 10 - 20,000 stimuli might be

applied. Soleus muscle proved more stationary in that it fatigued less during a long experiment than did plantaris, presumably because of the higher percentage of slow twitch, slowly fatiguing fibers in soleus (Henneman & Olson, 1965). The twitch of plantaris muscle inevitably declined with time, and isometric runs were therefore interposed between every few conditions with elastic loads. The vertical extent of the symbols for isometric loading in Fig. 3.3 gives the standard deviation of four runs over the period of this series. Thus, the vertical extent includes any systematic changes as well as random fluctuations. Long-term changes were minimized by randomizing the order of elastic loads and repeating the first couple of elastic loads at the end of the series. The values for 8 and 66 g/mm in Fig. 3.3 represent the average of two runs.

Results similar to those illustrated in Fig. 3.3 were observed consistently. They indicate that the interaction of an external elastic element with the internal contractile visco-elastic elements of muscle markedly alters the twitch tension and affects the time course of a twitch to some extent. However, these results do not lend themselves easily to a quantitative analysis which could determine if the visco-elastic properties of muscle directly limit the rate of contraction. This is more easily done by analysis in the frequency domain rather than in the time domain.

The Frequency Response with Elastic Loads

Plantaris muscle: Fig. 3.4 shows the gain curves for the frequency response obtained by spectral analysis of the tension

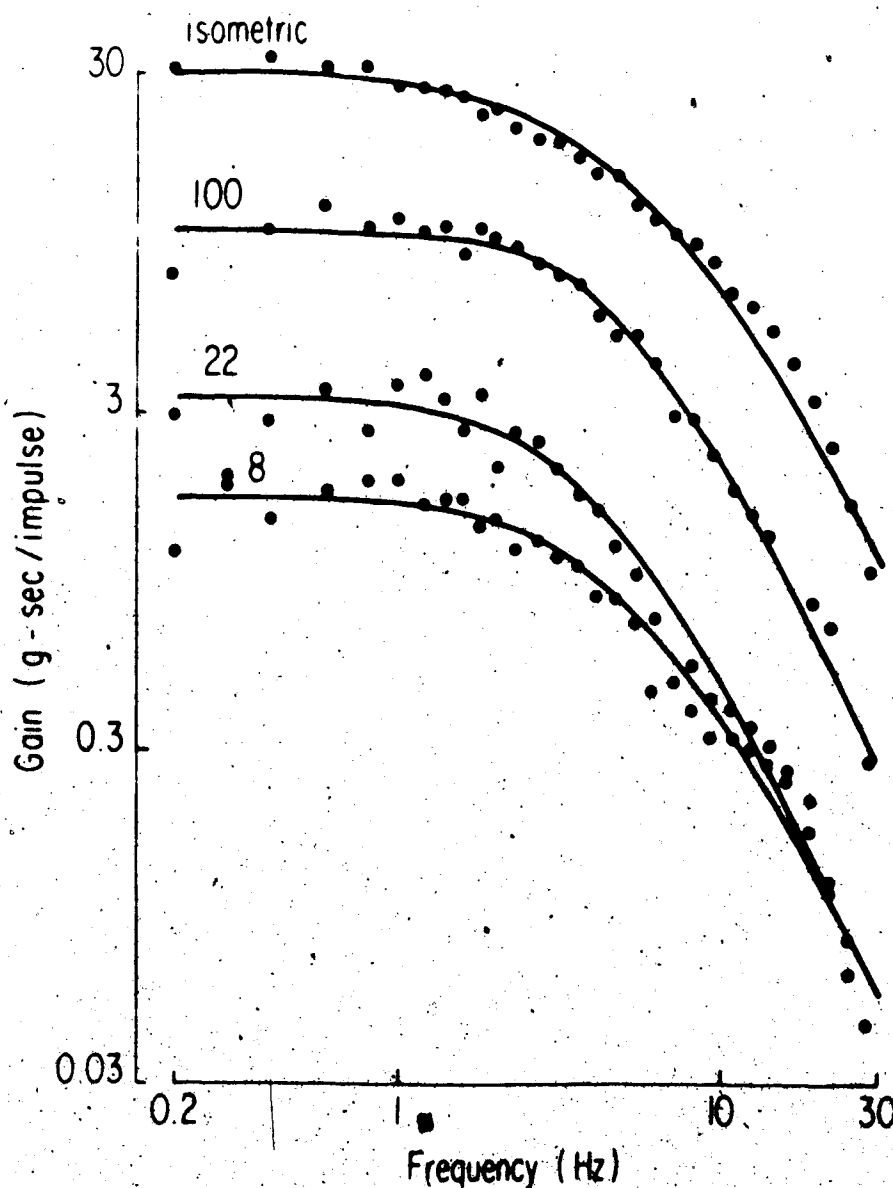


Fig. 3.4. Gain of a plantaris nerve-muscle preparation measured during random stimulation as a function of frequency under isometric conditions and with various elastic loads. The values on the Fig. indicate the stiffness of the springs in g/ms. The fitted curves for a second-order linear system were computed as described in the methods. Both ordinate and abscissa are logarithmic scales. Different muscle from that used for Fig. 3.2 and Fig. 3.3.

fluctuations using random stimulation and the same elastic loads as in Fig. 3.2. The gain curves have the same dimensions as the area under a twitch (g-sec/impulse), and in a linear system (Milsum, 1966) the gain at low frequencies would be identical to the area under the twitches. Note that the low frequency gain, like the twitch area (Fig. 3.3) is much greater with stiffer springs.

Fig. 3.4 also indicates that the responses decline as the second power of the frequency at high frequencies (a slope of -2 on these log-log plots). The transitions between the low frequency portions of these curves and the high frequency portions occur at about the same frequency, although the shapes of the curves vary somewhat with different elastic loads. This suggests that the plantaris muscle still behaves like a linear second-order system with about the same natural frequency but with a damping ratio which may vary with the elastic load. The phase data for the responses as a function of frequency (not shown in Fig. 3.4) were consistent with the gain data. The coherence functions (a normalized measure of the linearity of the response; Bendat & Piersol, 1971) were uniformly high, typically between 0.6 and 0.9 for all springs over most of the frequency range shown. A coherence value of 1.0 would indicate a completely linear system.

Fig. 3.5 shows an example of the computed 95% confidence intervals for an isometric run of the plantaris muscle. The thick lines show the fitted second-order curves for the gain and the phase data. The nonlinearity of the muscle and the bias errors not considered in analysis could account for the fitted curve not lying completely within the confidence intervals. Moreover, the second-order model may not be

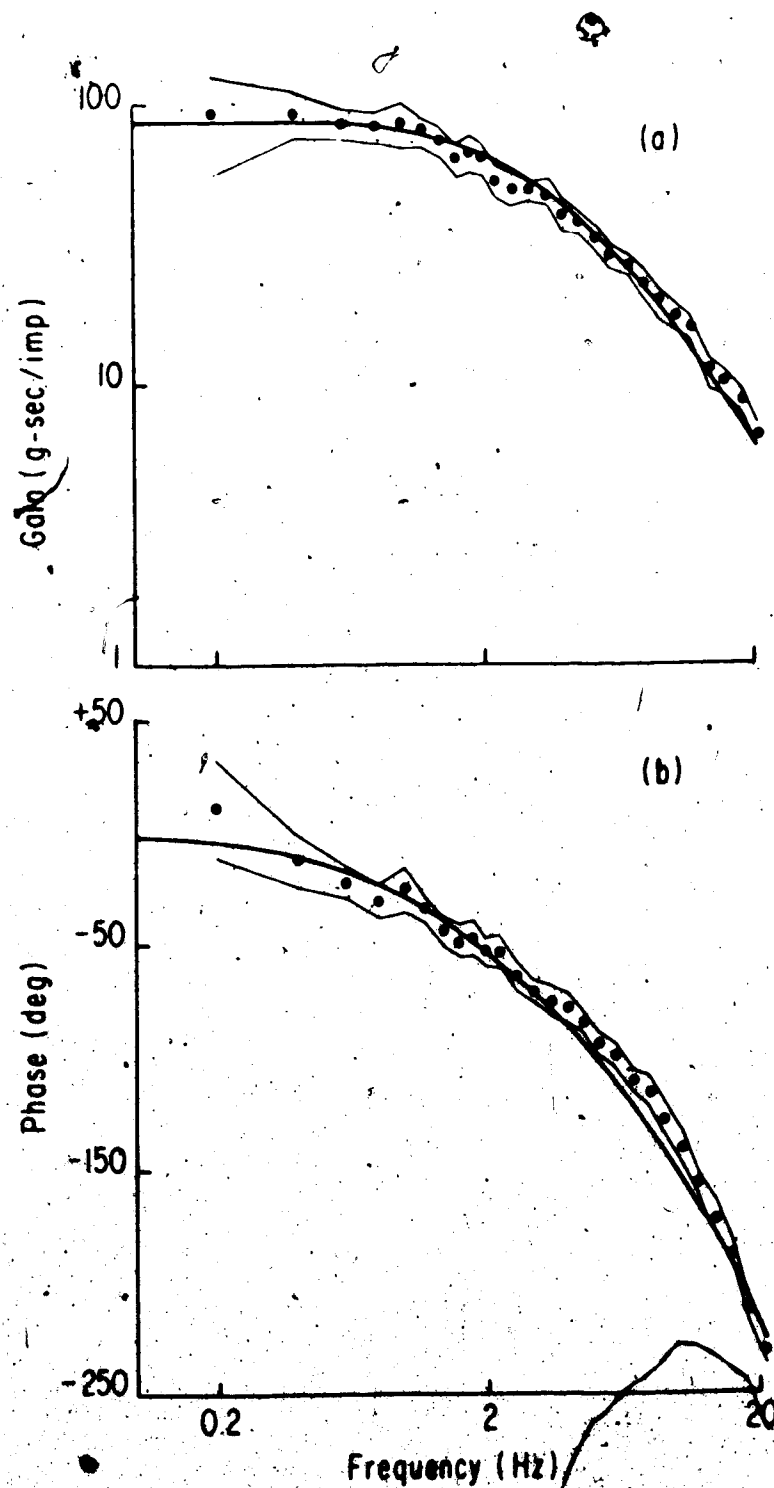


Fig. 3.5. The dots show gain (a) and phase (b) data points for an isometric condition for the plantaris muscle. The fine lines show the 95% confidence intervals for the data points, and the thick lines are the fitted second-order curves.

completely adequate (Chap. 5). Although the coherence values fall at higher frequencies, the confidence intervals are still narrow because of the frequency averaging (Chap. 2).

The left-hand side of Fig. 3.6 shows the best-fitting values of gain, natural frequency and damping ratio (see methods) as a function of elastic stiffness for the same muscle as in Fig. 3.4 (\cdot), and another plantaris muscle ($+$). The gain increases steadily with stiffness, while the natural frequency showed no marked change. No consistent trends in natural frequency were observed in ten experiments. The relative constancy of the natural frequency implies that muscles should be able to follow oscillatory signals from the central nervous system of roughly the same bandwidth whether contracting isometrically or under quite light loads.

The damping ratio followed a U-shaped curve with a minimum at intermediate values of stiffness. This shape was observed in every experiment with plantaris muscle. The minimum value was always close to one (critical damping; Milsum, 1966) although slightly underdamped or overdamped values were obtained in some experiments.

The three parameters: low frequency gain (G_0), natural frequency (f_n) and damping ratio (ζ) are sufficient to completely describe a linear second-order system. When the damping ratio is greater than or equal to one, an equivalent set of parameters is the low frequency gain and two rate constants or time constants (Milsum, 1966).

The relation between the two rate constants, r_1 and r_2 , and the other parameters is given by

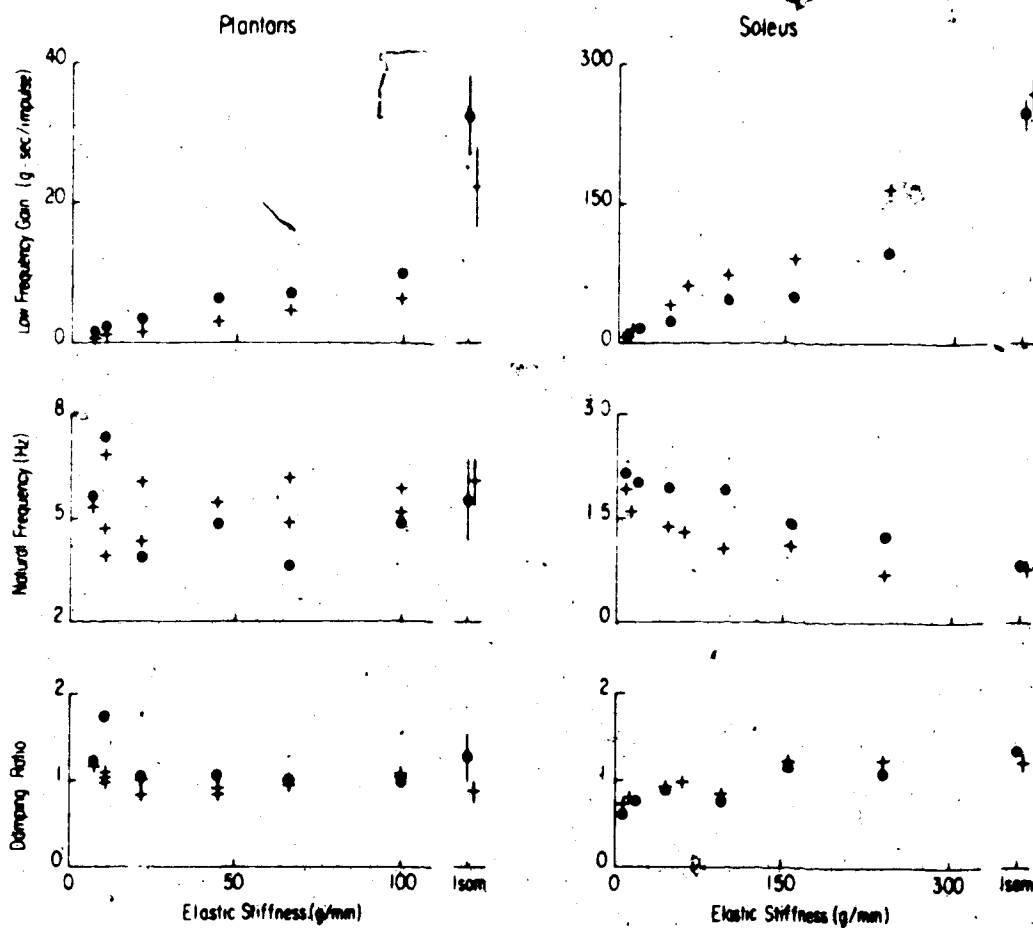


Fig. 3.6. Effect of elastic stiffness on the gain, natural frequency and damping ratio measured from the frequency response curves for plantaris and soleus muscles. Gain increases steadily with increasing stiffness in both muscles, but the natural frequency and the damping ratio are affected differently. The implications of these results are discussed in the text. The two types of symbols give data from different experiments with each muscle. The vertical extent of the symbols for isometric conditions with plantaris muscle indicate the S.D. of the values obtained from four runs. Note the different scales for the two muscles.

$$r_1, r_2 = 2\pi f_n (\zeta \pm \sqrt{\zeta^2 - 1}), \zeta \geq 1 \quad (3.1).$$

Note that when $\zeta = 1$, $r_1 = r_2$. For $\zeta < 1$ the response is oscillatory but the envelope of the oscillation will decay exponentially with a rate constant r , where

$$r = 2\pi f_n \zeta \quad (3.2).$$

Time constants can also be defined which are the inverse of the rate constants. The faster rate constant (shorter time constant) will determine the rising phase of a twitch while the slower rate constant will determine the relaxation phase.

Fig. 3.7A shows the values of these rate constants (left ordinate) or time constants (right ordinate) as a function of the stiffness of the external springs. A wide range of springs is shown and most values were repeated more than once. The two rate constants computed from Eq. (3.1) vary in opposite directions, and in this experiment appear to cross at a stiffness of 30-40 g/mm. In some other experiments the crossing over occurred at somewhat higher stiffnesses (50-100 g/mm).

As pointed out above, a damping ratio of 1 occurs when both rate constants have the same value. Whenever the rate constants differ the damping ratio will be greater than 1 which explains the U-shaped damping curve seen in Fig. 3.6. Under several conditions in this experiment the best-fitting damping ratio was slightly less than 1. This occurred because the relaxation phase was relatively faster than

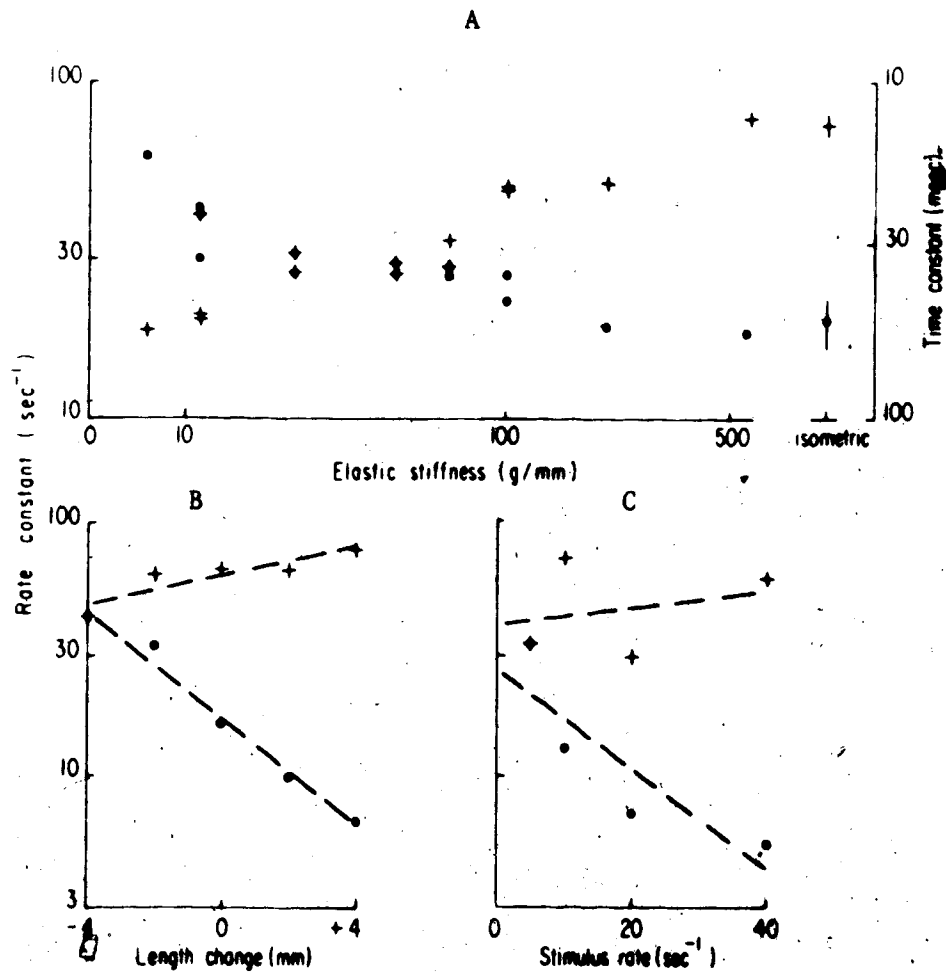


Fig. 3.7. Changing either (A) the stiffness of springs in series with a muscle, (B) the length of the muscle from that which produces the largest twitch, or (C) the mean rate of stimulation affects the two rate constants. Isometric conditions were used for (B) and (C). The computed best-fitting straight lines on the semi-log plots in (B) and (C) have been drawn to indicate the trend of the data. Note that the two rate constants in (A) appear to cross. The corresponding values of time constants can be determined from the right-hand scale in (A). All three graphs give data from different plantaris muscles.

expected for a critically damped, second-order system. The rate constants for these conditions were set equal to the value given in Eq. (3.2).

This finding of two rate constants varying in the opposite directions with increasing stiffness would explain the relative constancy of the natural frequency (which depends on the product of the rate constants). Similar changes in the rate constants were observed when the length of the muscle was varied about the length which gave the largest twitch tension (Fig. 3.7B) or when the mean rate of stimulation was varied (Fig. 3.7C). The trains of pulses used were prerecorded on a tape recorder so that the rate could be changed over an eight-fold range without altering the form of the distribution of pulses (see also Mannard & Stein, 1973).

Soleus muscle: Because the twitches of soleus were much longer (see Fig. 3.2), lower mean rates of stimulation (5 or 7/sec) were used so that the responses remained relatively unfused. The time course of the twitch was shorter at shorter lengths (Rack & Westbury, 1969) so some experiments were carried out at 10 mm below physiological maximum length. As shown in Fig. 3.6 the low frequency gain of soleus muscle changed with elastic load in much the same way as for plantaris muscle. However, the damping ratio increased and the natural frequency decreased monotonically with the stiffness of the external springs. A U-shaped curve for the damping ratio was never observed. Note that for very compliant springs the best-fitting values of the damping ratio were near 0.6. With such low values the twitches should have been frankly oscillatory, but they were not. The reason stems from the shapes of the twitches (Fig.

3.2) which were not of the expected form for a linear second-order system. The computer program found that the resultant frequency response curve was best fitted by a curve having a damping ratio less than 1. However, the fit was not as good and the values of coherence (a measure of linearity; Bendat & Piersol, 1971) were somewhat lower for soleus muscle. In other words, the nonlinearities in soleus muscle were significant enough that a purely linear analysis begins to break down. The implications of these results will now be discussed.

DISCUSSION

The magnitude of the response, whether measured as gain in the frequency domain or twitch tension in the time domain, increased systematically with the stiffness of elastic load. This result is expected from the classical force-velocity curve of Hill (1938). Hill's curve can be modelled by a nonlinear viscous element although it has been reinterpreted by Huxley (1957). He suggested that at the higher velocities, which are reached with weak springs, the fraction of bonds that could be formed would be less. An additional factor is that the muscle will shorten against weak springs to lengths where it is able to develop rather less tension (Gordon, Huxley & Julian, 1966).

The shapes of the frequency response curves for plantaris muscle with elastic loads were well fitted by the responses expected for a simple second-order system, and are therefore consistent with there being two rate-limiting processes. The first and slower rate constant under isometric conditions appears to be equivalent to Hill's

rate constant for the decay of the active state (see also Jewell & Wilkie, 1960). This is now thought to involve the rate at which the sarcoplasmic reticulum can take up Ca^{++} ions (Julian, 1969; Connolly, Gough & Winegrad, 1971; Stein & Wong, 1974). Because of its dependence on external series elasticity, the second is presumably a visco-elastic rate constant involving the muscle's apparent viscosity, series elasticity and parallel elasticity.

In any simple mechanical model (see Chap. 4), a visco-elastic rate constant should increase when stiffer springs are added. Therefore, the rate constant which increases with stiffer springs and becomes the larger one under isometric conditions (Fig. 3.7A) can tentatively be assumed to be visco-elastic in nature. Why the other one, which presumably depends on the active state, should decrease when stiffer springs were used initially seemed obscure. Then we realized that, although the initial length of the muscle was held constant, the muscle will shorten by greater amounts during the contractions when weaker springs are added externally.

Muscle length is known to affect markedly the time course, as well as the magnitude, of a twitch (Rack & Westbury, 1969) and the parameters of the frequency response (Mannard & Stein, 1973). The effect of changing muscle length alone is shown for comparison in Fig. 3.7B. Increasing length decreases the value of one time constant sharply while producing a smaller increase in the other time constant. Increasing the lengths shifts the muscle to a region of higher stiffness (Joyce & Rack, 1969; Grillner, 1972). Therefore, a visco-elastic rate constant would tend to increase with increasing length so the decreasing rate

constant is presumably due to a slowing in the decay rate of the active state.

This hypothesis involving the behaviour of the two rate constants is also consistent with the results obtained by varying the mean rate of stimulation (Fig. 3.7C). Increasing the rate of stimulation would be expected to load the pump responsible for the reuptake of Ca^{++} ions. This will slow the decay of the active state and decrease its apparent rate constant. On the other hand, increasing the rate of stimulation and the tension produced isometrically will lead to further internal shortening against the muscle's series elasticity. Stretching the series elasticity increases its stiffness (Joyce & Rack, 1969), which should increase the other rate constant.

Although the data are consistent with one rate constant depending on the muscle's visco-elasticity, they do not completely rule out the other possible rate-limiting steps mentioned in the Introduction. However, models involving simple contractile and visco-elastic elements have the advantage that predictions can be readily derived and checked experimentally. This is done in Chapter 4. Not only is the behaviour qualitatively consistent with the model, as indicated here, but quantitative predictions are also accurately fulfilled. This provides further evidence that one of the rate constants is visco-elastic in nature.

The generality of these conclusions is weakened by the differences observed between soleus and plantaris muscle. With elastic loads weaker than about 100 g/mm, the frequency response curves of soleus muscle were not well-fitted by a second-order model with two real

time constants. When a second-order model was fitted, the damping ratios observed were less than 1, even though the twitches were not oscillatory. Rather, the twitches approached a steady level, and then declined rapidly. This form is consistent with the stable bonds observed by others in this slow twitch muscle (Joyce *et al.*, 1969). Then there were no longer a sufficient number of bonds to maintain the tension, and the muscle began to relax and be lengthened by the spring, the bonds would be quickly broken and the tension would fall rapidly, as observed. This "catch property" (Burke *et al.*, 1970) is an essential nonlinearity which might warrant a fuller analysis.

The method of random stimulation can be used to determine nonlinear as well as linear terms in a system (Marmarelis & Naka, 1972; French & Butz, 1973). However, it is not certain whether the much greater amount of computation required for nonlinear analysis would add much insight into the nature of these nonlinearities or in the functional role of these muscles for posture and movement. Therefore, the later chapters are restricted to linear models of muscle.

CHAPTER 4

PREDICTIONS AND EXPERIMENTAL TESTS OF A VISCO-ELASTIC MUSCLE

MODEL USING ELASTIC AND INERTIAL LOADS

INTRODUCTION

In the preceding chapter we showed that when a cat plantaris muscle is contracting against elastic loads, as well as under isometric conditions, the forces generated are well described by those expected for a simple, second-order system. By varying the elastic load, the length of the muscle, and the stimulation rate, one of the two rate constants of the second-order system appeared to be visco-elastic in nature, whereas the second corresponded in classical terms (Hill, 1938) to the decay of the active state. As a result we thought it worthwhile to develop the predictions of a muscle model in sufficient detail that the experimental results could be tested quantitatively against the model. Once the parameters are determined, the model can also be used to predict the responses to other types of loads, e.g., inertial loads.

The effects of inertial loads on a muscle's performance are of interest for two reasons. Firstly, in normal contractions muscles work, not only against the elasticity of antagonistic muscles, but must also move inertial loads which vary widely during normal movements. For example, during the swing phase of locomotion the calf muscles extend the ankle before the foot strikes the ground. The foot represents a relatively small inertial load. However, during the stance phase, the muscles again extend the ankle after initially giving under the weight

of the body, but now the inertial load consists of a substantial fraction of the animal's weight, rather than the foot alone. Thus, to understand normal movements it is important to analyze how muscles respond to changes in inertial load.

Secondly, Partridge (1966, 1967) has suggested that muscles have remarkable abilities to compensate for variations in inertial loads. When he varied the inertial load of the triceps surae muscles (soleus + gastrocnemius muscles) by a factor of 28, he found that the movements of the muscles during low frequency sinusoidal inputs were hardly affected. Partridge (1967) argued that 'from basic Newtonian considerations, it is obvious that for the movement amplitude to remain constant, the force amplitude at the test frequency must have increased in proportion to the load inertia. The implication of this basic mechanical relationship is the rather dramatic conclusion that the force delivered by the muscle to the load, at the signal frequency, must have varied by almost $10,000$ times depending on the load impedance'. Partridge then went on to suggest that to explain these results 'the length-tension relationship in muscle forms a functional non-neural servo-feedback. These signal handling characteristics of muscle make it more nearly a "position servo" than a "force motor".'

Our experimental results with inertial loads are consistent with those of Partridge, but our analysis shows that his assumption of a non-neural feedback is unnecessary. From our muscle model, which does not include any internal feedback pathways, we are able to predict that the movements in response to low frequencies of stimulation should be nearly independent of inertial load, as observed experimentally.

Furthermore, our model is able to predict the responses to higher frequencies, including the damped oscillations which result with larger inertial loads. Irrespective of their interpretation, these results do add support to the idea demonstrated by Partridge (1966) that muscles are well designed to produce a given pattern of movement, despite the wide variations in inertial load that they normally encounter.

THEORETICAL PREDICTIONS

Fig. 4.1 shows a simple visco-elastic model of muscle such as proposed by Houk, Cornew and Stark (1966) based on Hill's (1938) model of muscle. This model contains an internal series elastic element of stiffness k_i , and a parallel elastic element of stiffness k_p . It also contains an active state element which produces a contractile force C each time a stimulus is received. The force decays exponentially with a rate constant β . This model is actually simpler than Hill's original model in that the nonlinear force velocity relation he found has been represented by a linear dashpot with viscosity B . A linear dashpot will not be adequate to describe very high shortening velocities. However, our results (Chap. 3) indicate that the linear aspects of muscle can be described by three parameters. This muscle model already contains five parameters so it is worthwhile to consider its properties carefully before adding further complexity. Also included in Fig. 4.1 are an external elastic element of stiffness k_e , a mass M and a dashpot of viscosity D . element k_e simulates

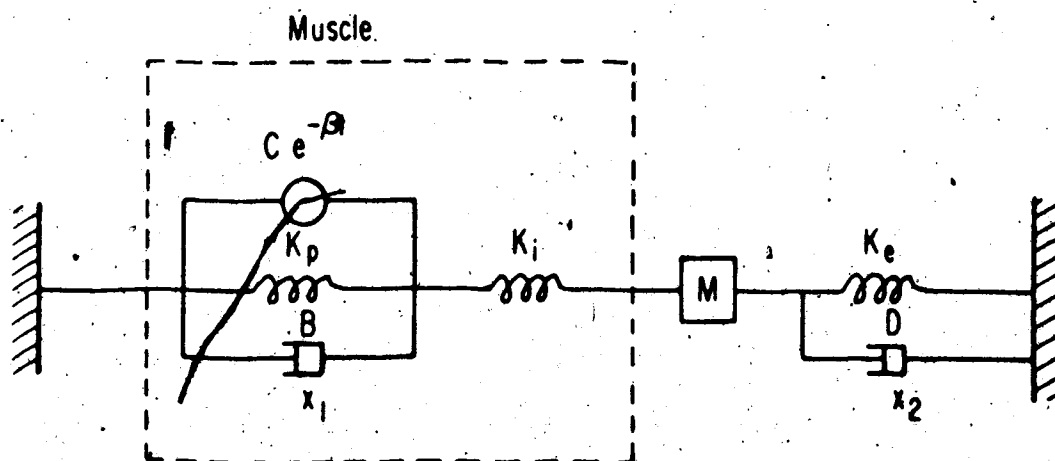


Fig. 4.1. Schematic representation of a muscle model with various types of external loads. The meaning of the parameters is discussed in the text.

the stiffness of antagonist muscles against which contraction always takes place, and the mass M corresponds to both gravitational and inertial masses against which the muscle contracts. There will always be some damping in the external system which is specified by the parameter D .

Equations of Motion.

If x_1 and x_2 represent stretches applied to the parallel and series elastic elements, respectively, two equations of motion can be written for the forces which must balance at the two central nodes of Fig. 4.1

$$k_p x_1 + B\dot{x}_1 + Ce^{-Bt} = k_i x_2; \quad (4.1)$$

$$k_i x_2 + k_e x + D\dot{x} + M\ddot{x} = 0. \quad (4.2)$$

where $x = x_1 + x_2$ is the total displacement of the muscle and derivatives are represented by dots over the appropriate symbols. Substituting in

Eq. (4.1) for

$$x_1 = x - x_2 = x + \frac{1}{k_i} (k_e x + D\dot{x} + M\ddot{x}) \quad (4.3)$$

and rearranging gives an equation for the displacement of the muscle

$$\begin{aligned} \ddot{x}[MB] + \dot{x}[M(k_i + k_p) + DB] + x[k_p k_i + k_p k_e + k_i k_e] \\ = -k_i C e^{-Bt} \end{aligned} \quad (4.4)$$

Taking Laplace transforms we have

$$X(s) = \frac{-k_i C}{(s+\beta) \{ M B s^3 + [M(k_i + k_p) + DB] s^2 + [D(k_i + k_p) + B(k_i + k_e)] s + k_p k_i + k_p k_e + k_i k_e \}} \quad (4.5)$$

where transformed variables are functions of s ; e.g., $X(s) = \int_0^{\infty} x e^{-st} dt$.

The force measured by a transducer in series with the external spring (see Methods, Chap. 3) will simply be the force g generated in the spring

$$g = -k_e x \quad (4.6)$$

Taking Laplace transforms of Eq. (4.6) and substituting from Eq. (4.5) gives

$$G(s) = \frac{k_e k_i C}{(s+\beta) \{ M B s^3 + [M(k_i + k_p) + DB] s^2 + [D(k_i + k_p) + B(k_i + k_e)] s + k_p k_i + k_p k_e + k_i k_e \}} \quad (4.7)$$

Eq. (4.7) is a formidable expression, and before considering the whole expression we will discuss some simplifications. The most important simplification occurs when the mass M and external damping D are negligible. This corresponds to the situation of a pure elastic load studied experimentally in the previous chapter.

Elastic Loading.

When $M = 0$ and $D = 0$ Eq. (4.7) reduces to a simple second-order equation which represents the transfer function of the muscle with elastic loads

$$G(s) = \frac{k_i k_e C}{(s + \beta) \{B(k_i + k_e)s + k_p(k_i + k_e) + k_i k_e\}} \quad (4.8).$$

One rate constant which we will denote by α depends on the external spring. From Eq. (4.8)

$$\alpha = \frac{1}{B} \left(k_p + \frac{k_i k_e}{k_i + k_e} \right) \quad (4.9).$$

If k_e is varied α should reach simple lower and upper limits

$$\lim_{k_e \rightarrow 0} \alpha = \frac{k_p + k_e}{B} \quad (4.10)$$

$$\lim_{k_e \rightarrow \infty} \alpha = \frac{k_p + k_i}{B} \quad (4.11).$$

By plotting α vs. k_e , the slope for weak springs will give the value of $1/B$, according to Eq. (4.10) and from the intercept one can obtain the value of k_p . The value of k_i can then be determined from Eq. (4.11). Thus, using Eqs. (4.10) and (4.11) the parameters k_i , k_p and B can be determined. One further point that can be noted from Eq. (4.9) is that as $k_e \rightarrow k_i$

$$\lim_{k_e \rightarrow k_i} \alpha = \frac{k_p + \frac{1}{2}k_i}{B} \quad (4.12)$$

which is the midway point in the transition from the lower to the upper limits.

The second rate constant is the parameter β for the decay of the active state. The final parameter C can be determined from the limit

of $G(s)$ as $s \rightarrow 0$

$$\lim_{s \rightarrow 0} G(s) = \frac{k_i k_e C}{\beta (k_p k_i + k_e (k_p + k_i))} \quad (4.13).$$

We will call this quantity G_0 in line with previous work (Mannard & Stein, 1973). From it C can be determined using any value of k_e . For example, under isometric conditions

$$\lim_{k_e \rightarrow \infty} G_0 = \frac{k_i C}{(k_p + k_i) \beta_\infty} \quad (4.14)$$

where β_∞ indicates the high stiffness limit of the rate constant β . This notation is used because β changes systematically with the stiffness of springs placed in series with muscle (Chap. 3).

Eq. (4.13) can also be used to obtain an independent estimate of the effective stiffness of the muscle. This is done by plotting $1/(G_0 \beta)$ vs. $1/k_e$. After rearranging Eq. (4.13) one obtains

$$\frac{1}{G_0 \beta} = \frac{1}{C} \left(\frac{k_p + k_i}{k_i} + \frac{k_p}{k_e} \right) \quad (4.15).$$

The ratio of the slope to the intercept of such a plot is $k_p k_i / (k_p + k_i)$. This ratio gives the effective stiffness k of the muscle model since the model contains two springs in series, and

$$\frac{1}{k} = \frac{1}{k_i} + \frac{1}{k_p}$$

or

$$k = \frac{k_p k_i}{k_p + k_i} \quad (4.16).$$

The value of k obtained experimentally from Eq. (4.15) will be compared with that obtained from the values of k_i and k_p from Eqs. (4.10) and (4.1f).

The high frequency limit of Eq. (4.8) is also readily derived. Indeed, one can show that in terms of the quantities already considered

$$\lim_{s \rightarrow \infty} G(s) = G_0 \alpha \beta / s^2 \quad (4.17).$$

Since the quantities G_0 , α , and β have been considered separately, the high frequency limit does not provide new data for evaluating parameters of the model.

Inertial Loads.

Having considered the reduced system of Eq. (4.8) in some detail, we now turn to the more complex system with inertial and viscous loading. The low and high frequency limits are readily derived. In fact, the low frequency limit is identical to Eq. (4.13). *The presence of inertial or viscous loads should not change the steady-state response or the response to sufficiently slowly-changing inputs.* Hence, non-neural feedback is not required for compensation of these loads in contrast to the suggestion by Partridge (1967) which was quoted in the Introduction. In Partridge's (1966) experimental study k_i was small and the amplitude of movement was measured. Under these conditions according to Eq. (4.5)

$$\lim_{k \rightarrow 0} X(0) = \frac{+C}{\beta k_p} \quad (4.18)$$

which shows that the low frequency amplitude is also independent of the mass. The high frequency limit of either Eqs. (4.5) or (4.7) does depend on mass M . For example,

$$\lim_{s \rightarrow \infty} G(s) = \frac{k_e k_i C}{MBs^4} \quad (4.19)$$

It is very difficult to move the mass at high frequencies and the response declines as the fourth power of frequency. The force actually generated by the muscle (as opposed to the signal measured by a length transducer or a force transducer in series with the external spring) declines as the square of frequency at high frequencies. This force f is, using Eq. (4.12)

$$f = k_i x_2 = -(k_e x + D\dot{x} + M\ddot{x}) \quad (4.20)$$

Taking Laplace transforms and substituting from Eq. (4.5) gives

$$F(s) = \frac{k_i C (Ms^2 + Ds + k_e)}{(s+B)(MBs^3 + [M(k_i + k_p) + DB]s^2 + [D(k_i + k_p) + B(k_i + k_e)]s + k_p k_i + k_p k_e + k_i k_e)} \quad (4.21)$$

The limit of Eq. (4.21) as $s \rightarrow \infty$ is simply

$$\lim_{s \rightarrow \infty} F(s) = \frac{k_i C}{Bs^2} \quad (4.22)$$

Eq. (4.22) is identical to the limit of Eq. (4.8) as $s \rightarrow \infty$ and $k_e \rightarrow \infty$, i.e., the isometric condition at high frequencies. Since the mass cannot readily be moved at high frequencies, the force generated by the muscle

approaches its isometric value. At low frequencies much less force is required to move a mass. If under Partridge's experimental conditions the external damping D and elasticity k_e were negligible even at low frequencies, then the force produced by the muscle at low frequencies would be proportional to the mass and to the square of the frequency according to Eq. (4.21), as he suggested.

The higher order and the increased number of parameters in Eqs. (4.5), (4.7) and (4.21) makes it difficult to describe all possible types of behaviour at intermediate frequencies. However, certain general properties can be determined.

We will now turn to comparisons with experimental data. The parameters of the muscle can be determined using elastic loads as indicated above. Then, the effects of varying the inertial or other types of load can be computed for example from Eq. (4.7) and compared with experiment. The effects of varying internal parameters on the frequency response function are shown at the end of the RESULTS section. A further extension of these results when applied to closed loop reflex systems is discussed by Oguztoreli and Stein (1975).

RESULTS

Elastic Loads.

Eq. (4.10) predicts that for weak springs the rate constant α should be proportional to k_e . This prediction is tested in Fig. 4.2. The linear correlation coefficient is 0.77 and no obvious deviation from linearity is observed. The best-fitting straight line has a slope of

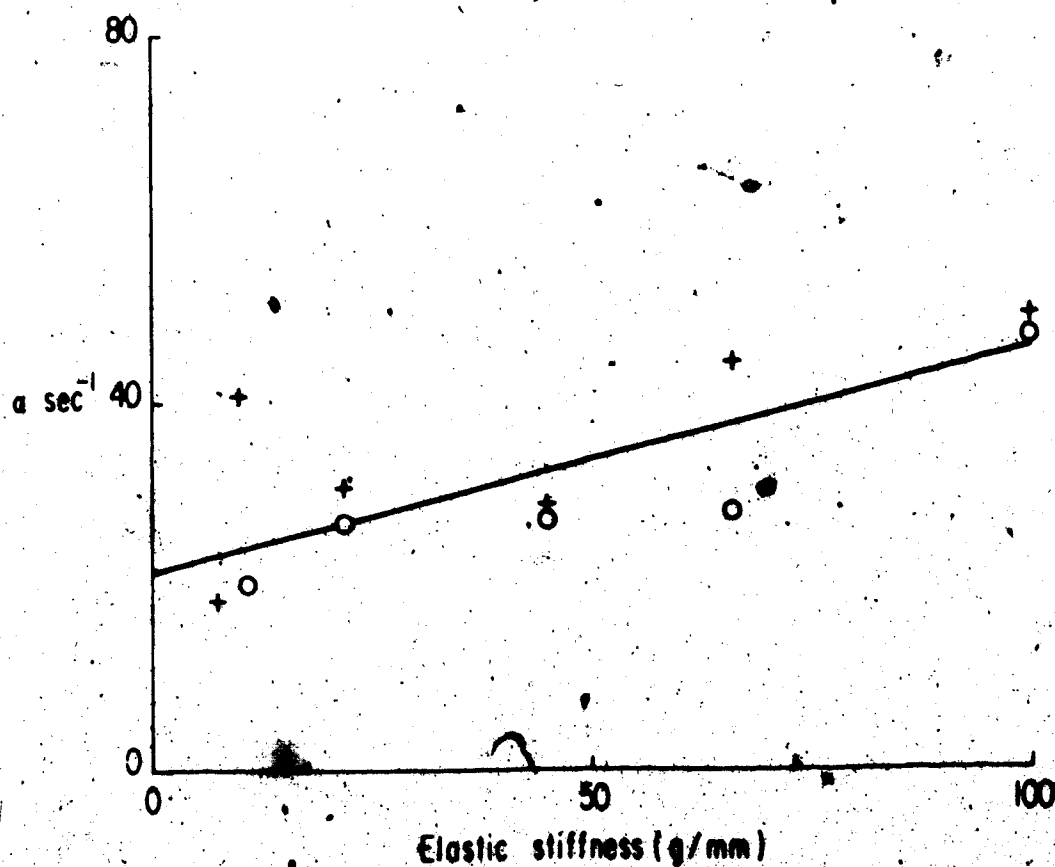


Fig. 4.2. The effect of varying the stiffness of springs in series with a plantaris muscle on the visco-elastic rate constant (a). Values were obtained before (+) and after (o) studying the effects of inertial loads. The rate constants were somewhat smaller in the later series, but the best-fitting straight line has been computed using all the data.

0.24 ± 0.06 (mean \pm S.E.); which indicates that the parameter B for the viscosity of the muscle has a value of 4.1 g-sec/mm. The intercept has a value of 21.5 ± 2.0 (mean \pm S.E.) which would give a value for the parallel elasticity, $k_p \rightarrow 90$ g/mm (see Eq. (4.10)). The isometric value of α was 74.4 ± 2.4 (mean \pm S.E.) which from Eq. (4.11) indicates a series elasticity $k_i = 220$ g/mm.

The effective stiffness of the muscle can also be determined once k_i and k_p are known, and is 63 g/mm (see Eq. (4.16)). As indicated in the theoretical section an independent measure of muscular stiffness can be obtained from the low frequency gain G and the rate constant β . A plot of $1/(G_0\beta)$ vs. $1/k_e$ should give a straight line, and the ratio of the slope to the intercept of that line should give the muscular stiffness. Fig. 4.3 shows such a plot from two series of experimental runs on one plantaris muscle. In between the two sets of runs inertial loads were tested (see below). Because of the large number of stimuli applied and the time elapsed the twitch tensions were smaller for the second set of data (O) compared to the first set (+). However, a straight line has been fitted to all the data and the ratio of the slope to the intercept is 66 g/mm, which is very close to the value of 63 g/mm obtained independently from the rate constant α (see above).

From the low frequency gain the value of the peak active state tension C can also be obtained from Eq. (4.10). The value obtained was 300 g which was somewhat higher than the previous isometric twitch tension, as one would expect. Higher values of C were obtained in other experiments in which larger animals and larger stimuli were used. In Table 1 the values of the parameters determined from a number of experiments are listed.

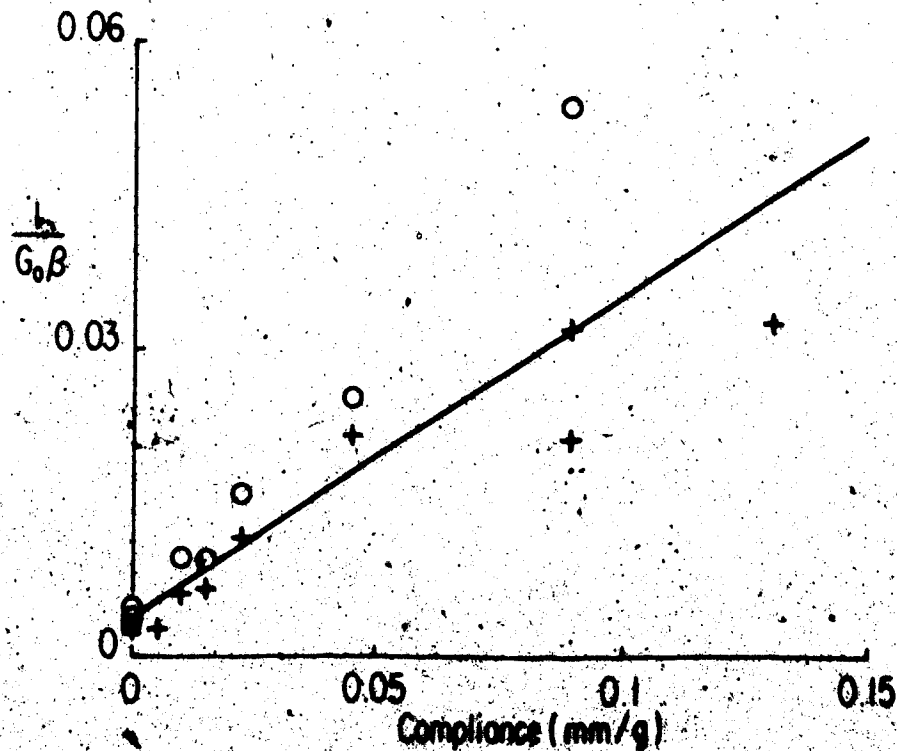


Fig. 4.3. Effect of varying the compliance ($1/k_s$) of a series spring on the inverse of the product of the low frequency gain (G_0) and active state rate constant (β). Same muscle as in Fig. 4.1. The gain declined somewhat between the earlier (+) and later (O) series, but again a single line-fitting straight line has been computed for all data.

Parameter	Mean	S.E. of Mean	Units	Corresponding MKS Values	Units
k (from α)	79	19	g/mm	774	N/m
k (from $G_0\beta$)	47	11	g/mm	461	N/m
k_i	380	84	g/mm	3724	N/m
k_p	103	26	g/mm	1010	N/m
B	6.4	1.0	g-sec/mm	63	N-sec/m
C	999	362	g	9.8	N

Table 1. Values of experimentally determined parameters for a visco-elastic model of plantaris muscle in the cat. The values give the means and S.E. of the mean for at least eight experiments. The effective stiffness k of the muscle could be determined in two ways as indicated in the THEORETICAL section. Values are given in conventional units of grams weight, and after conversion to standard MKS units (see Methods, Chap. 3).

Inertial Loads.

Having determined the parameters of the model, predictions for the responses with inertial loading can be made from Eq. (4.7) with no undetermined constants. Comparison of experimental results with predictions are shown in Fig. 4.4 for the gain of the frequency response using an elastic load of 66 g/mm and three different inertial loads. The shapes of the experimental and theoretical curves are in excellent agreement. Small peaks are observed between 10 and 15 Hz for an inertial mass of 300 g and at about 5 Hz for the inertial mass of 1500 g. The predicted peak for the inertial mass of 40 g is above 30 Hz, and would be very small in amplitude compared to the low frequency gain.

For comparison the twitch contractions are shown in Fig. 4.5 under the same loading conditions. Note the damped oscillations with periods of 70 msec (14 Hz) and 180 msec (5.6 Hz) with inertial masses of 300 and 1500 g, respectively. These oscillations result from the interaction of the inertial mass with the elasticity of the muscle and the external spring. The oscillations are damped by the viscosity of the muscle and the external pulley.

The low frequency gains in Fig. 4.4 differ somewhat from their predicted values. With small inertial masses the data tended to lie below the predicted line whereas with the largest inertial mass, the data tended to lie above the predicted values, when deviations were seen. The reasons for these discrepancies, which were observed consistently, are uncertain. They might arise from the static friction of the pulley which was not included in the model. This friction would be most important with the larger forces that are generated against the spring.

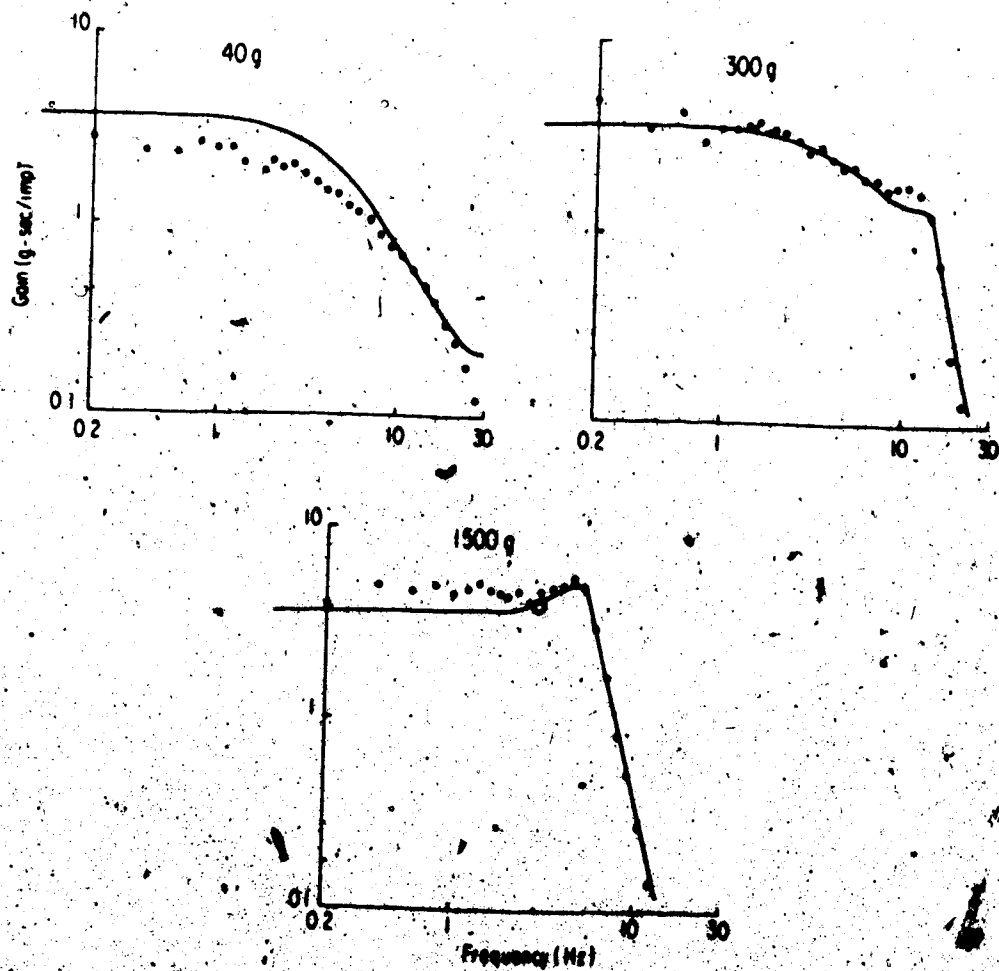


Fig. 4.4. Comparison of experimental data (·) with predictions (continuous lines) for the effect of adding inertial loads corresponding to the masses indicated. An elastic load of 65 g/mm was also present in each part of this test. Further explanation in text.

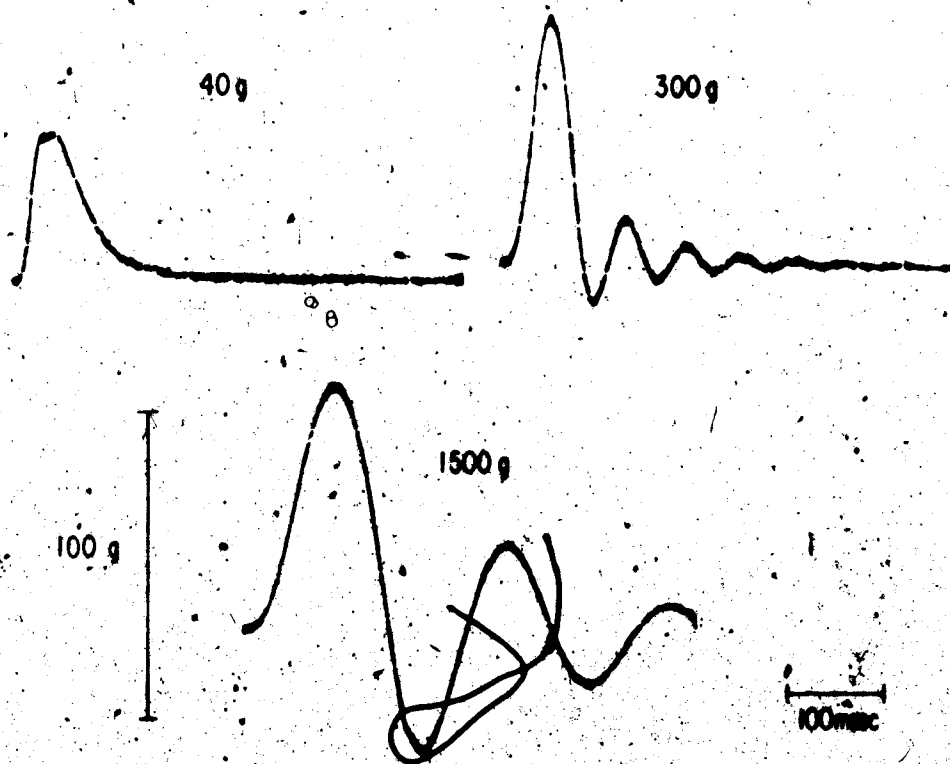


Fig. 4.5. Effect of inertial load on the twitch of plantaris muscle. Note the damped oscillations which occur with the larger inertial masses indicated on the Fig. An elastic load of 66 g/cm was also present in each part of this Fig.

inertial masses. Alternatively, the discrepancies could arise from some nonlinearity in muscle which has been ignored by this linear analysis. This remains a topic for future investigation.

In addition to changing M , one can also change external stiffness k_e and study the effects experimentally on the frequency response of the system. However, we cannot change the internal parameters, each by a predetermined amount and study the effects. It would be nice to know how the frequency response function changes with the change in a particular parameter. These parameters do change with the state of the muscle, e.g., fatigue, number of motor units activated, rate of stimulation, stretch; potentiation, etc. These effects as computed from Eq. (4.7) are discussed below. All results are for $M = 1500$ g; the value of the parameters used in Fig. 4.4 are taken as standard and the variation is expressed as a factor of the value for the muscle in Fig. 4.4.

Effect of k_e

If the muscle is replaced by a spring of equivalent stiffness k then for the system shown in Fig. 4.1 the frequency of oscillation is given by

$$\omega = \left(\frac{k + k_e}{M} \right)^{1/2}$$

i.e., the frequency of oscillation increases with increase in k_e as shown in Fig. 4.6, the peaks at the frequency of oscillation become more prominent with increase in k_e . For $k_e = 300$, peaks are completely damped

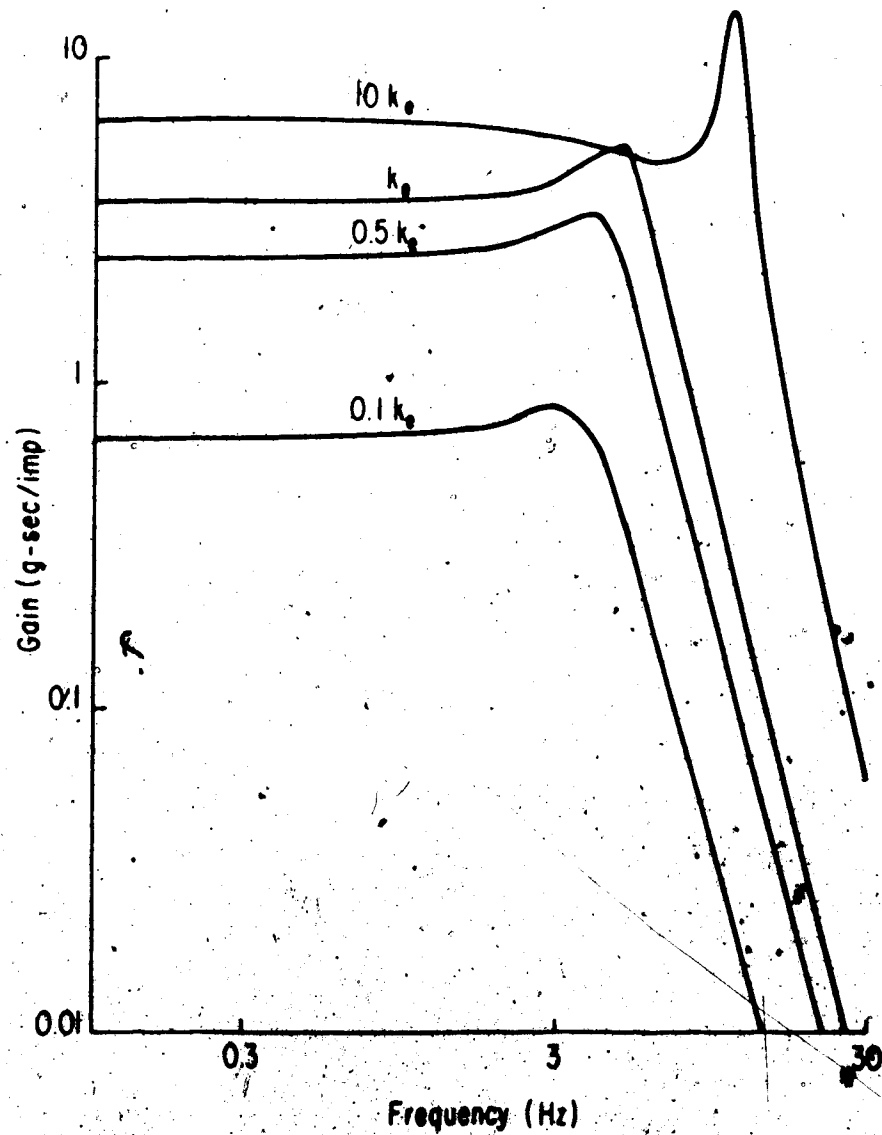


Fig. 4.6. Variation of the frequency response gain curve with the variation of external spring stiffness. Variation is expressed as a factor of k_e , the value used in Fig. 4.4 for $M = 1500$.

out for $0.1 k_e$ and $0.2 k_e$. As M decreases, for the same range of variation in k_e , the range of frequencies of oscillation increases.

Effect of k_i .

The effects of variation in internal series elasticity are quite similar to that of k_e . The overall gain increases and frequency of oscillation increases with increase in k_i (Fig. 4.7). However, the peaks get more damped as k_i increases; this effect was opposite for k_e . It is seen from Eqs. (4.7) and (4.19) that at very low and high frequencies, effects of k_i and k_e are similar.

Effect of k_p .

The effects on frequency response gain curve with the variation of internal parallel elasticity are shown in Fig. 4.8. The frequency of oscillation increases as k_p increases, but the gain decreases. The factor k_p occurs in the denominator of Eq. (4.7) and explains the decrease of gain.

Effect of B .

Since B occurs in the denominator of Eq. (4.7), the gain decreases as B increases, as shown in Fig. 4.9. For $s \rightarrow 0$, Eq. (4.13) is independent of B and hence the very low frequency gains are unaffected. The frequency of oscillation first decreases with increase in B and then increases. Also, the peaks are more prominent at low and very high values of B .

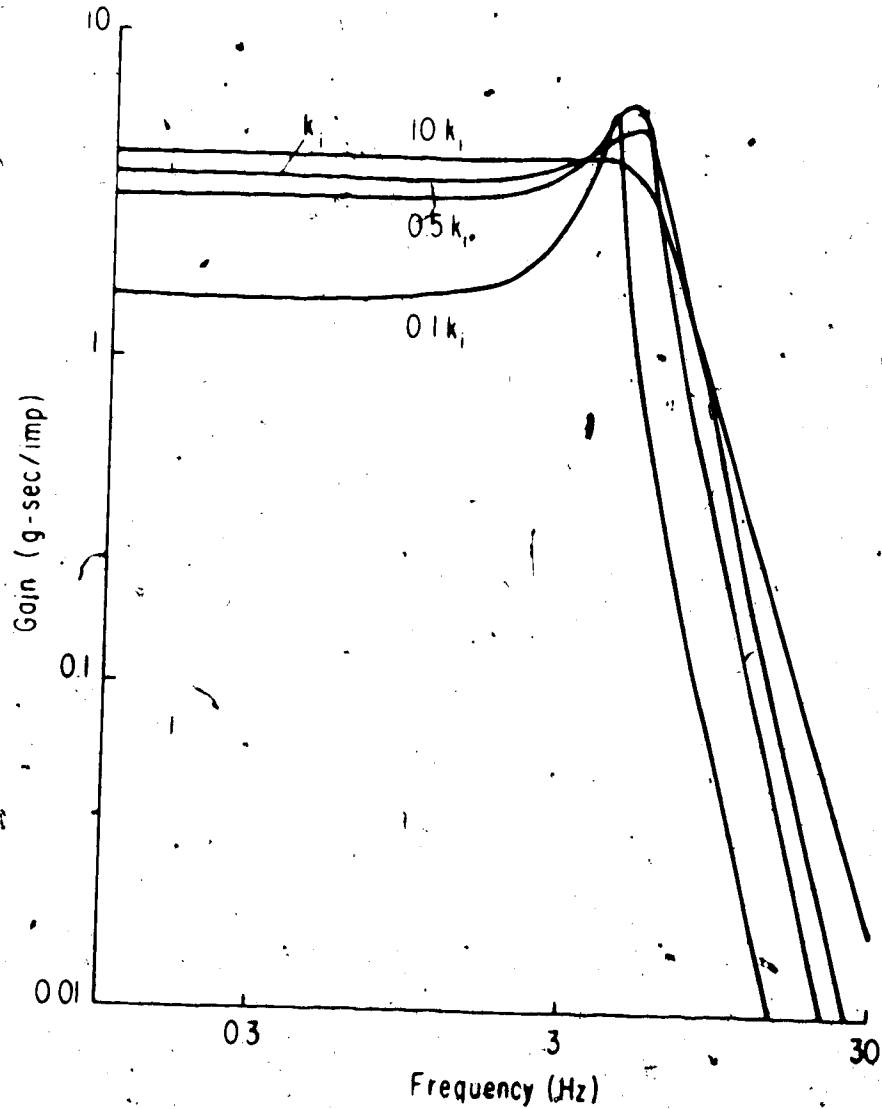


Fig. 4.7. Effect of changing the parameter k_i , keeping other parameters constant, is shown above. The value k_i and other parameters are the same as used in Fig. 4.4, $M = 1500$ g. The variation is expressed as a factor of k_i .

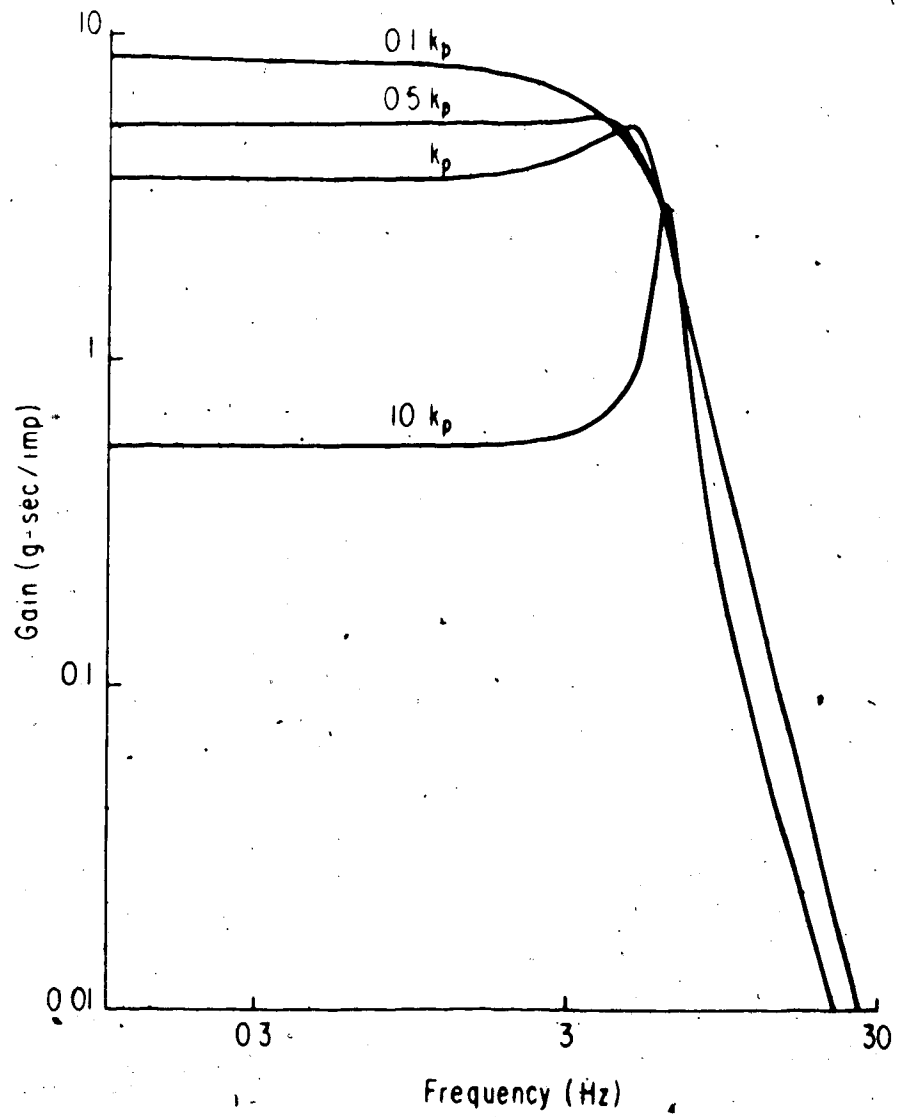


Fig. 4.8. Effect of changing the parameter k_p . The variation is expressed as a factor of k_p where k_p is the experimentally computed value. All other parameters used are the same as in Fig. 4.4,

$M = 1500$ g.

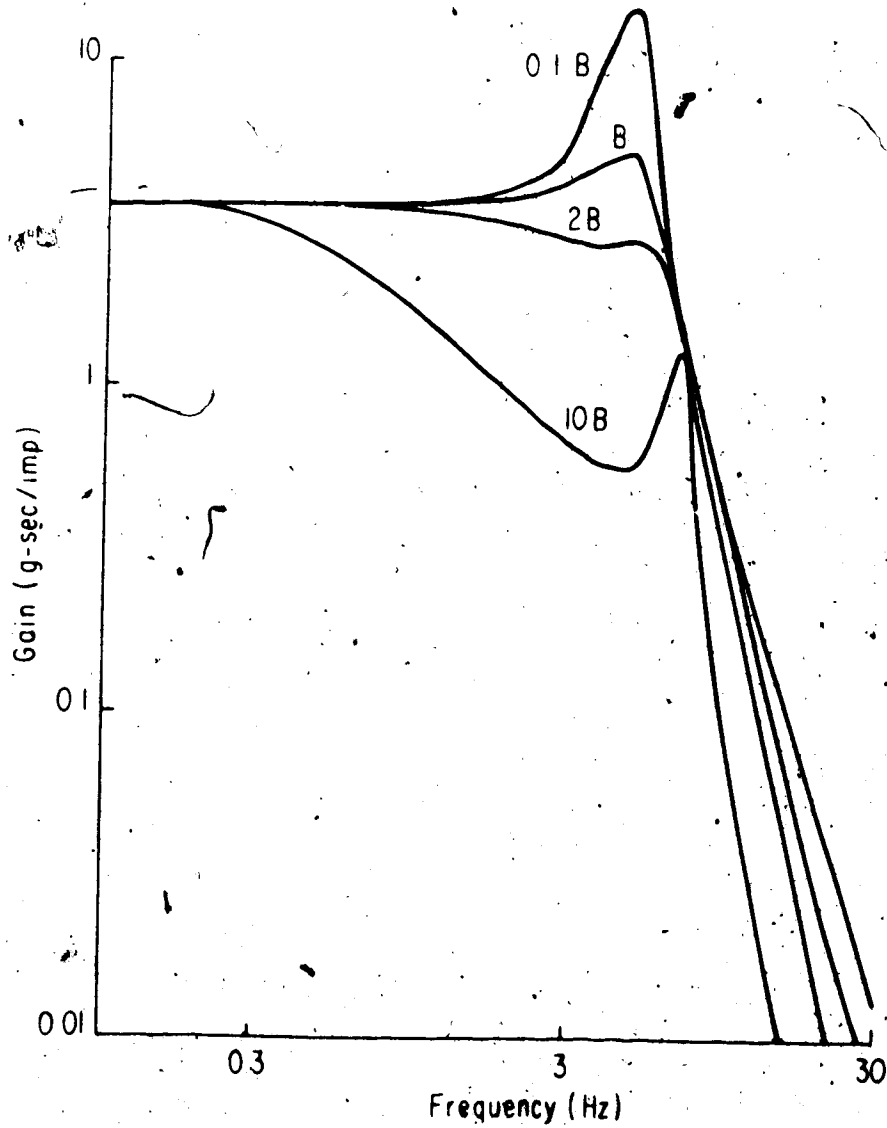


Fig. 4.9. Effect of changing the coefficient of viscosity, keeping other parameters of the model the same as in Fig. 4.4, $M = 1500$ g.

B is the computed experimental value and the variation is expressed as a factor of B .

Effect of β .

The low frequency effect is given by Eq. (4.19). The gain decreases as β increases as shown in Fig. 4.10. The rate constant β determines the falling phase of the twitch, therefore if β increases, the area under the twitch decreases and hence the gain decreases. The frequency of oscillation does not seem to be affected much. The high frequency gain is not affected (Eq. (4.19)) with changing β . Similar effects have been shown for an isometric twitch of frog sartorius muscle by Stein and Wong (1974).

The effects of variation of D are not very important from $0.1 D$ to $10 D$ for Eq. (4.7). In actual systems, i.e., with antagonistic muscle instead of the spring, damping is extremely high as compared to D and hence the oscillations will be heavily damped.

DISCUSSION

The results presented here show the substantial predictive power of a simple, linear model of muscle which in many respects goes back to the model introduced by A.V. Hill in 1938. We have used the model to predict the responses of muscle to random stimulus trains under a variety of elastic and inertial loads. Springs in series with the muscle markedly affect the force output of the muscle, whereas inertial loads, as pointed out by Partridge (1966, 1967) have virtually no effect on the low frequency responses. The responses do fall off sharply at high frequencies and the upper frequency limits are progressively reduced with increasing inertial masses. For example, in Fig. 4.4 the

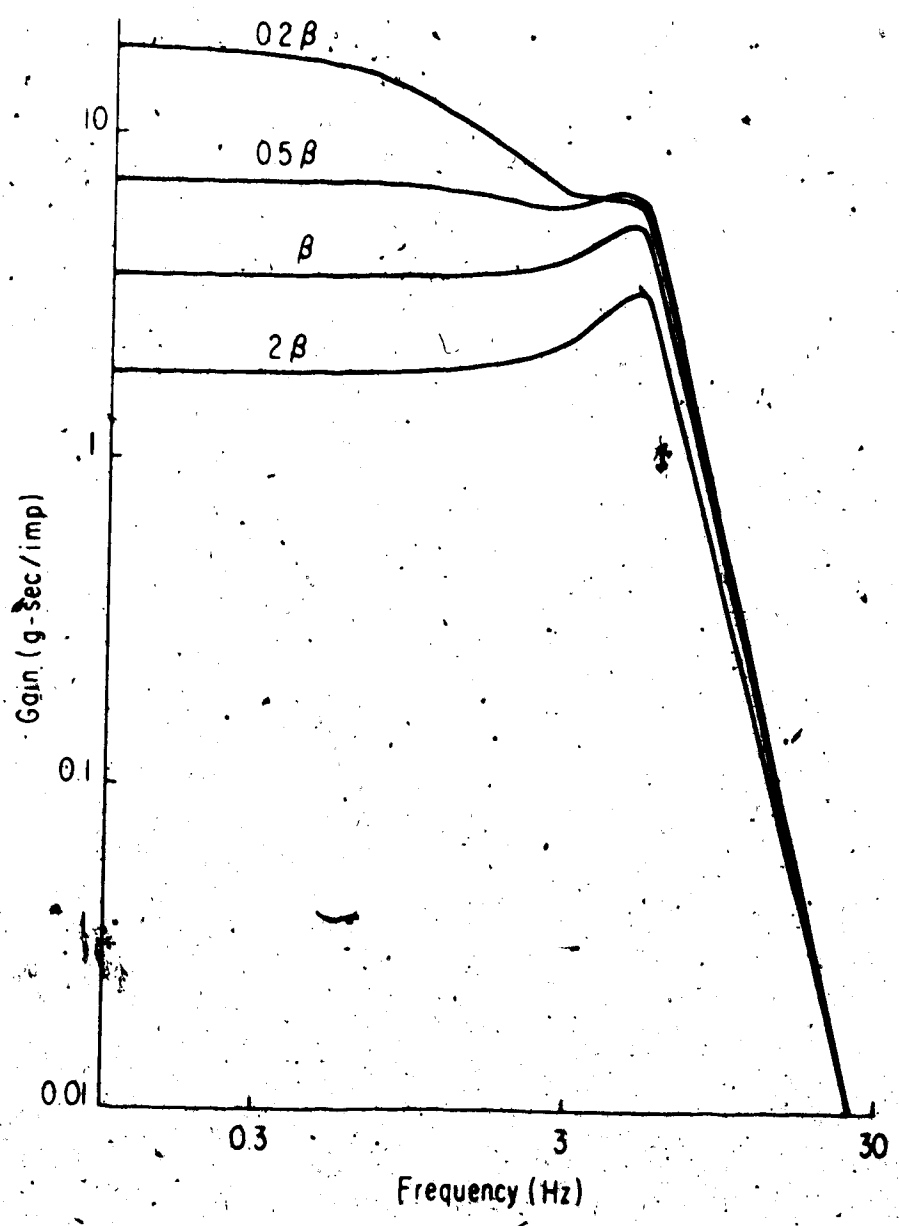


Fig. 4.10. Effect of changing the decay constant β , keeping other parameters the same as in Fig. 4.4 for $M = 1500$ g. The variation is expressed as a factor of the experimentally computed value of β .

response with an inertial mass of 1500 g declined to 0.1 g-sec/impulse at 14 Hz, compared to 30 Hz with an inertial mass of 40 g. However, even with the largest inertial mass used which is probably close to the upper limit normally experienced by the muscle, as calculated from values given by Grillner (1972), the response was still large up to 6 Hz. The range from 0 to 6 Hz includes the major frequency components of most movements. Thus, muscles appear to generate the forces required to produce most normal movements demanded by the nervous system despite wide variations in inertial loads. This ability follows, not from any special internal feedback or other mechanisms for inertial compensation, but rather from a simple model in which the visco-elastic and active state elements limit the response at low frequencies, and inertial masses within physiological limits only affect the response to higher frequencies.

With the intermediate mass of 300 g damped oscillations were observed which were close to the tremor frequency of cat muscles (Lippold, Redfearn & Vučo, 1958). This observation does not imply that physiological tremor is normally caused by muscle properties, but it does highlight the fact that muscle properties must be carefully studied before ascribing other causes to the generation of tremor (see also Oguztoreli & Stein, 1975).

Methods were also developed whereby all the parameters of the model could be evaluated experimentally. We already noted that the values of active state tension produced in response to a stimulus were consistent with the twitch tension, although both were much smaller after 10,000 or more stimuli than would be produced by a fresh muscle. The

effective stiffness of the muscle was measured in two ways which produced consistent values (Table 1).

The overall stiffness of the muscle could be further subdivided into a series and a parallel elastic component and a viscous element. The magnitudes of these components have not been measured for plantaris muscle using conventional methods. Values are available in the literature for soleus muscle (Rack & Westbury, 1969; Joyce, Rack & Westbury, 1969; Grillner, 1972), but the nonlinearities present in this muscle (Chap. 3) prevented a full analysis with linear methods. Nonetheless, certain characteristic differences were noted between the two muscles under isometric conditions. The natural frequency of soleus was only 1 Hz, rather than 5 Hz for plantaris (Chap. 3), while the damping ratio was similar for the two muscles. This suggests that both rate constants were reduced, i.e., the active state decays more slowly in soleus muscle and the visco-elastic rate constant is less. This second rate constant depends on the ratio of the stiffness of the muscle to its viscosity (Eq. (4.11)). Joyce and Rack (1969) measured the series stiffness of soleus muscle using small length changes and obtained values which from their Fig. 9 varied between 250 and 600 g/mm for the tensions studied here (200-500 g). Their values are in good agreement with our results for plantaris muscle (Table 1). This implies that the lower visco-elastic rate constant for soleus may arise from a larger viscosity, although the magnitudes of the viscous components are not well studied for either muscle. To verify this implication would require further experimental work using methods such as those of Joyce et al. (1969) and Joyce and Rack (1969).

CHAPTER 5

PROPERTIES OF HUMAN SOLEUS MUSCLE AND THE ASSOCIATED FEEDBACK LOOP

INTRODUCTION

Soleus muscle of the cat has been extensively studied because of its role in posture and locomotion (Joyce *et al.*, 1969; Joyce & Rack, 1969; Rack & Westbury, 1969; Houk *et al.*, 1970; Grillner, 1972; Nichols & Houk, 1973). The effects of length, stimulus rate and the number of active motor units all contribute to changes in the contractile visco-elastic properties of the muscle which manifest themselves as changes in the twitch tension, the time course of the twitch, the fusion rate, etc. The dynamics of the soleus muscle have also been studied in the frequency domain (Partridge, 1966; Poppele & Terzuolo, 1968; Rosenthal, McKean, Roberts & Terzuolo, 1970; Chap. 3). The soleus muscle of the cat behaves like a low-pass filter, following low frequencies efficiently and attenuating the higher frequencies. In Chapter 3 it was shown that the low pass filter characteristics are of second-order and can thus be described by three parameters: low frequency gain, natural frequency and damping ratio. In the frequency domain changes in length, initial force and stimulus rate produce systematic changes in these three second-order parameters. In Chapter 4 we also showed that these visco-elastic properties of muscle are responsible for the compensation for inertial loads which muscles exhibit at low frequencies (Partridge, 1966).

The problems of load compensation and stability of posture are

much greater in a bipedal animal such as man, but no studies are available to compare human soleus to that of the cat. The reasons are the obvious difficulties of isolating the soleus muscle in a living human being, but the human soleus differs in that a substantial portion of it lies superficially in the leg. This has enabled us to stimulate the human soleus muscle selectively to study its properties in the time and frequency domains and to compare an intact muscle in a normal human subject to a partially isolated cat muscle.

An advantage of studies on humans is that the observations are made under more natural physiological conditions in which the conditions of the muscle or the associated reflex pathways can be altered voluntarily. When a subject relaxes completely, motoneuronal activity ceases, and even quite large stimuli to motoneurons will not induce further activity. This results from the fact that subsequent activity in Golgi tendon organs will tend to inhibit motoneurons, and the pause in the discharge of muscle spindles will reduce any residual excitation. Thus, the reflex loops are effectively open. However, when voluntary force is exerted, the spindles are more sensitive. (Vallbo, 1973) and the muscle receptors can modulate the ongoing motoneuronal activity. Under these "closed loop" conditions, the twitch and the EMG often show oscillations following stimulation of motoneurons. Comparison of open loop and closed loop conditions shows that the gain of the muscle is high compared to that of the feedback part of the loop. This point will be elaborated in the Discussion.

Various workers (Phillips, 1969; Malyill Jones & Watt, 1971; Everts, 1973; Marsden, Merton & Morton, 1973) have suggested that the

"functional stretch reflex" in primates differs from the usual monosynaptic spinal stretch reflex, and a cortical reflex has come to dominate the spinal reflex in these animals. This hypothesis has been tested here with normal human subjects by analyzing the properties of the feedback part of the loop with twitch tension considered as an input and EMG as an output. The delay for the feedback from tension to EMG shows that the reflex does not have the monosynaptic spinal latency, but rather a latency comparable to the "functional stretch reflex" studied by Melvill Jones and Watt (1971). This suggests that the motor cortex may be involved in the feedback pathway.

METHODS

Sixteen experiments were conducted on five volunteer subjects, both male and female, with ages ranging from 20 to 35 years. The subject lay prone with his left foot on the pedal carrying the strain gauges for force measurement. The foot was as tightly strapped to the pedal as could be done without occluding the blood supply to the foot. Thus, the measurements were nearly isometric. The subject could observe the mean level and the fluctuations of force on an oscilloscope. Surface electrodes measuring EMG were placed on the midline at the back of the leg about 20 cm from the bottom of the foot and about 8 cm (indifferent electrode), as shown schematically in Fig. 5.1 (see also Agarwal & Gottlieb, 1972).

Stimulation

To stimulate the soleus muscle independently of the other left

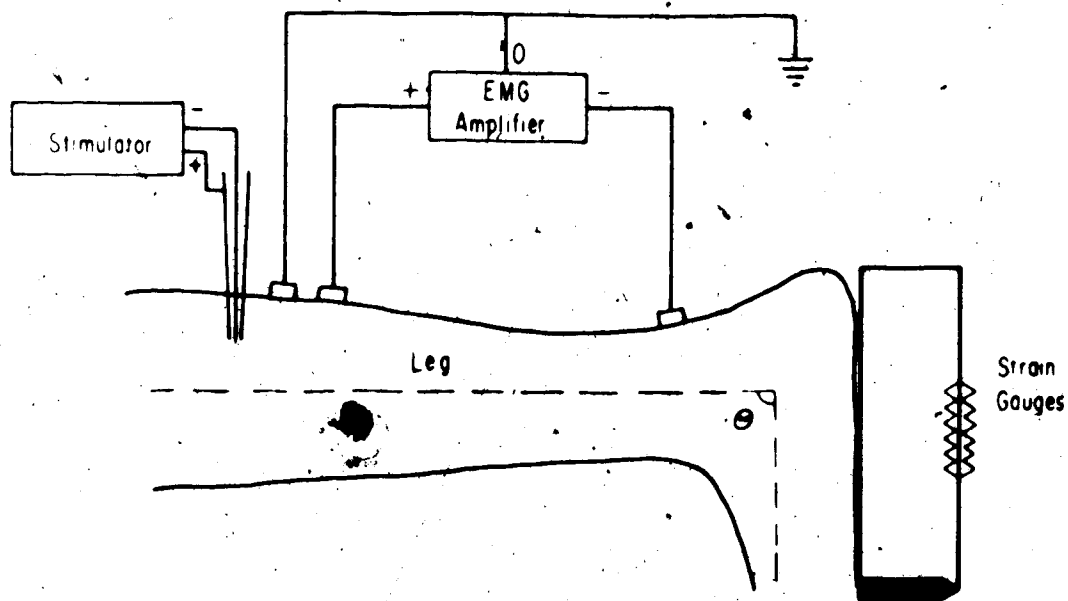


Fig. 5.1. Schematic diagram of the experimental arrangement. A branch of the nerve to the soleus muscle was stimulated with a bipolar needle electrode. The EMG was recorded by surface electrodes, while strain gauges measured the tension output. The angle of the ankle, θ , was measured between the long axes of the leg and that of the foot.

leg muscles a bipolar needle electrode was inserted into the muscle proximal to the motor point. The needle was carefully positioned so as to stimulate a nerve branch supplying a fraction of the muscle maximally with a minimum amount of current. The stimulus was kept brief (0.05-0.2 msec) so as to favour stimulation of nerve rather than muscle fibers. Once positioned the needle generally remained stable for the remainder of the experiment, and subjects reported less pain than with trans-cutaneous stimulation of the whole nerve at the popliteal fossa. Also, with stimulation of a small branch, there was often no H-wave in the EMG (Hoffman, 1918) so the direct effects of stimulating motoneurons could be studied in isolation.

The stimulus pulses were distributed in time according to a gamma distribution of order $p = 4$ (Fisz, 1963), since interspike interval histograms for many nerve cells are well fitted by this distribution (Stein, 1965). The power for such a distribution is high over the range of frequencies studied so that the coherence between input and output is not limited by low power at any frequency in the spectrum. The standard deviation of the interspike intervals for this distribution is half the mean interval. In earlier experiments on cat muscles (Mannard & Stein, 1973), power at low frequencies (up to 0.4 Hz) was low, which resulted in low coherence values at these low frequencies. W.J. Roberts (personal communication) suggested that the low power at low frequencies could change the parameters of the second-order system, so we repeated a few runs under similar physiological conditions in humans, both with the gamma distribution of pulses and the distribution used for the cat experiments. The computed parameters of the second-order system in both

cases were the same to within experimental error.

Single stimulus pulses at 1/sec followed by random stimulation (Mannard & Stein, 1973) for 1 minute were applied through the needle electrode. The mean rate of random stimulation was 5/sec, as for soleus muscle in the cat (Chap. 3), except when the effect of rate was studied.

Force Measurement

The twitch tensions (up to 1.5 kg) indicated that we were stimulating only about 10% of the motor units with the maximal shocks to branches of the nerve to soleus. The force measured by the strain gauges was recorded on an FM tape recorder along with the surface EMG and the stimulus pulses. For the frequency response function between tension as input and EMG as output, 100 stimuli were applied at a rate of 1 every 3 sec. The twitches and the corresponding EMG's were averaged on-line by a Digital Equipment Co. LAB-8 computer (program described by French, 1973b). Force records were obtained at various angles of the ankle (77°-106°) and different voluntary force levels (0-9 kg). The transducer was calibrated at each angle using masses placed 15 cm from the axis of rotation of the foot plate. Since the lever length was constant, values have been given in grams weight for ease of comprehension. These values can be converted into equivalent torque values in gm-cm by multiplying with 15 cm or in Newton-meters by multiplying with $0.15 \times 9.8 \times 10^{-3} = 1.47 \times 10^{-3}$.

EMG

The EMG from the tape recorder was rectified and filtered (Paynter filter; Gottlieb & Agarwal, 1970) before feeding into the

computer. The phase lags introduced by the Raynter filter at various frequencies were measured and the data were corrected for these lags. Since we were interested in the late waves in the EMG and these were small compared to the direct motor, or M-wave, and in some experiments to the H-wave, we had to eliminate the M- and H-waves to see the responses clearly. For this purpose a delay of between 36 to 54 msec was added to the EMG channel before averaging. This delay was also taken into account in calculating the phase changes.

ANALYSIS

Random Stimulation

Details of the spectral analysis using random stimulation have been given in Mannard and Stein (1973) and French (1973). Frequency response functions were calculated for the stimulus pulses as input and the tension as output. The gains and phases obtained were fitted by those expected for a linear, second-order system (Chap. 3). The parameters of the second-order system: low frequency gain, natural frequency and damping ratio, were calculated for each angle of the ankle and each stimulation rate. The transfer function of this second-order system under rest conditions will be denoted by $G(s)$ where s is the Laplace transform variable. When the loop is closed by the addition of voluntary activity, the closed loop transfer function, $C(s)$ is given by

$$C(s) = \frac{G(s)}{1 + G(s)H(s)} \quad (5.1)$$

where $H(s)$ is the feedback transfer function, assuming a block diagram for such a closed loop system as shown in Fig. 5.2 (Ogata, 1970). Under the further assumption that $G(s)$ changes very little with voluntary force, $H(s)$ can be calculated from knowledge of $C(s)$ and $G(s)$. This extra assumption is examined further in the Appendix, but did not prove to be valid.

Twitches

As an alternative method for calculating $H(s)$, separate twitches were averaged. The closed loop transfer function between stimulus as input and twitch tension as output is given by Eq. (5.1). The transfer function for the stimulus pulse as input and EMG as output (after eliminating the direct effects of the stimulus - see EMG above) is given by $F(s)$ where

$$F(s) = \frac{G(s) H(s)}{1 + G(s) H(s)} \quad (5.2).$$

Dividing $F(s)$ by $C(s)$ we obtain $H(s)$. The results obtained for $H(s)$ from the experimental data involve a pure time delay from tension input to EMG output. The transfer function for the primary muscle spindle afferents (Poppele & Bowman, 1970) is given by

$$H_p(s) = \frac{K s(s + .44)(s + 11.3)(s + 44)}{(s + .04)(s + .816)} \quad (5.3).$$

The details of the various factors have been discussed by Poppele (1973). Assuming that no dynamics, other than those of primary afferents, are

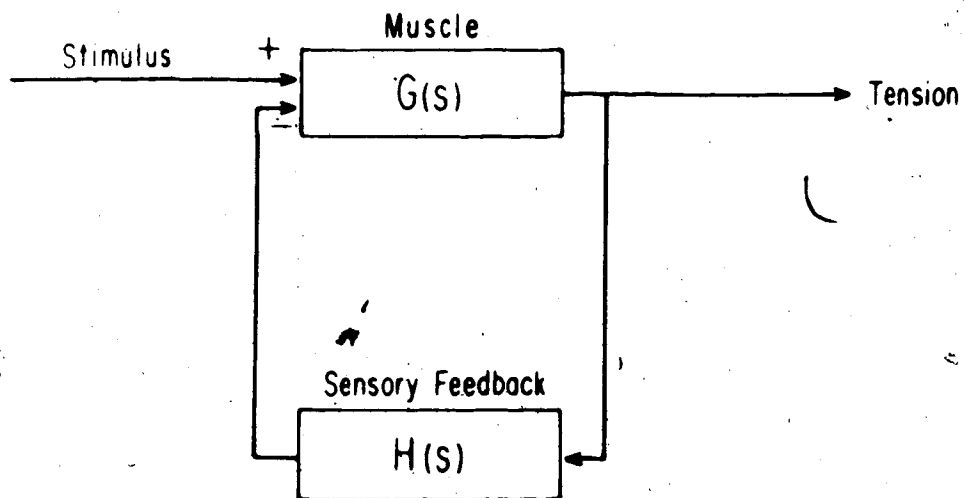


Fig. 5.2. A block diagram for the functional stretch reflex. $G(s)$ is the transfer function between stimulus as input and tension as output. $H(s)$ is the transfer function of the sensory receptors and includes the delay between tension as input and EMG as output.

added to $H(s)$ by the reflex pathway (Poppele & Terzuolo, 1968), the feedback transfer function is given by

$$H(s) = H_p(s) e^{-sT} \quad (5.4),$$

where T is the delay of the feedback pathway. The time delay does not affect the gain, but only introduces a phase lag given by

$$\begin{aligned} \phi &= \angle H(j\omega) - \angle H_p(j\omega) \\ &= -\omega T \end{aligned}$$

where ω is the frequency in radians/sec and $j = \sqrt{-1}$. Plotting ϕ vs. ω , or the frequency $f = \frac{\omega}{2\pi}$, the delay T was calculated.

RESULTS

Properties of Human Soleus Muscle Under Rest Conditions.

When a subject is completely at rest, the synaptic inputs to motoneurons are not sufficient to cause them to discharge. Even during random stimulation, such as we applied, no EMG activity was observed except that directly evoked by the stimulus. By adjusting the stimulus to be maximal for the nerve branch stimulated, the evoked activity was constant (to within 5%) for each pulse in a train. Under such conditions the stretch reflex loop is effectively opened at the level of the motoneurons (see INTRODUCTION). By recording the tension fluctuation in response to random stimulation, the dynamic properties of the muscle

could be determined (see METHODS and Chap. 3). The muscle properties were studied (1) at various lengths of the muscle by changing the angle of the ankle, and (2) at various mean rates of stimulation by playing back pre-recorded stimulus tapes at different speeds. Fig. 5.3 shows an experimentally measured frequency response curve from random stimulation of human soleus muscle. The gain measures the change in tension (in g) resulting from modulating of the stimulus rate (in impulses/sec) at a given frequency, and thus has the units g-sec/impulse. The phase measures the difference between the modulation in the response and that of the stimulus. In general, the muscle shows a phase lag which increases with frequency. The entire frequency response curve can be efficiently measured from a single period of random stimulation by spectral analysis, because the random signal contains a wide range of stimulus frequencies (Mannard & Stein, 1973).

The continuous thick lines in Fig. 5.3 show the predictions for the best-fitting linear, second-order system. These fitted curves are specified by the parameters: low frequency gain, natural frequency, damping ratio and delay, as described previously (Mannard & Stein, 1973). In addition, the coherence function was measured (Bendat & Piersol, 1971). The values of this function are normalized between 0 and 1 and give information about the linearity of the system. The coherence values for the data of Fig. 5.3 were generally around 0.8 or 0.9, and always above 0.5 up to 16 Hz. The good fit of the continuous curves and the high coherence values imply that a linear, second-order model accounts quite well for the data over this frequency range. The thin lines show the 95% confidence intervals for the data points.

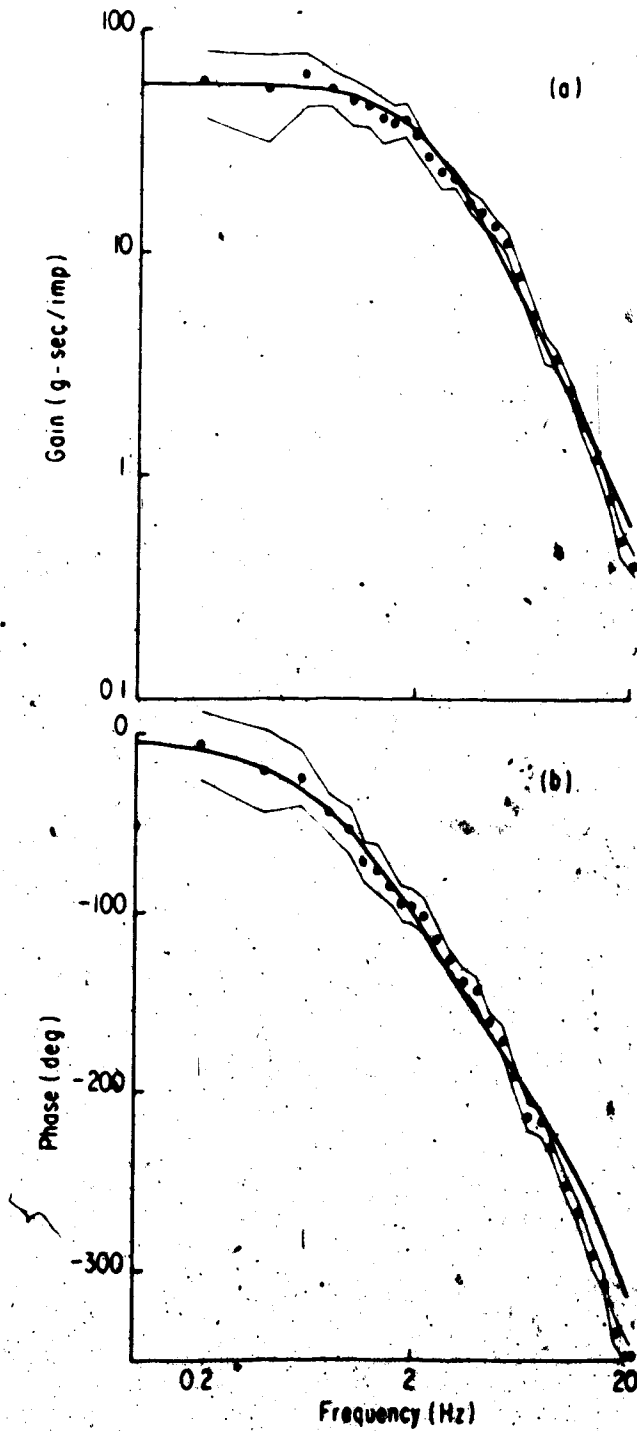


Fig. 5.3. Values for the gain and phase of the responses for human soleus muscle to random stimulation at rest with the ankle fixed at an angle of 88° . The thick continuous lines are fitted second-order curves as described in the text. The thin lines are 95% confidence intervals for data points. The scales for gain and frequency are logarithmic.

Fig. 5.4 shows the absolute values of gains at angles of 83°, 88° and 95°. As the angle at the ankle increases, which is equivalent to decreasing the length of the muscle, the gain decreases. Fig. 5.5 shows the variation of low frequency gain, natural frequency and damping ratio with change in ankle angle. Data have been pooled from two subjects. The low frequency gain increases, the natural frequency decreases and the damping ratio stays unchanged or increases somewhat with increases in muscle length (decreases in angle). Similar trends were shown for plantaris muscle (Mannard & Stein, 1973) and for soleus muscle (Bawa & Stein, unpublished observations) in the cat. However, the values of the damping ratio are mostly less than 1, typically between 0.7 and 1.0, whereas for the isometric cat muscles these values were mostly greater than 1. The values of natural frequency are around 2 Hz, which are similar, though slightly higher than those for soleus in the cat. The computed time delays which gave the best fit to the phase data were typically 15-20 msec independently of the angle.

To test the effect of stimulus rate, random stimulation at mean rates of 5, 10 and 20/sec were applied in a few subjects. For most subjects the gain decreased continually with increase in rate, although in one subject it increased from 5/sec to 10/sec. The natural frequency often decreased with increase in rate and the damping ratio often increased, as for the cat. The responses were largely fused at 20/sec, although moments of relaxation were observed (and subjectively felt) whenever intervals in the pulse train were much longer than average. At 10/sec, the fluctuations in tension could be felt much more than that at 20/sec, while with 5/sec, periods of complete relaxation occurred

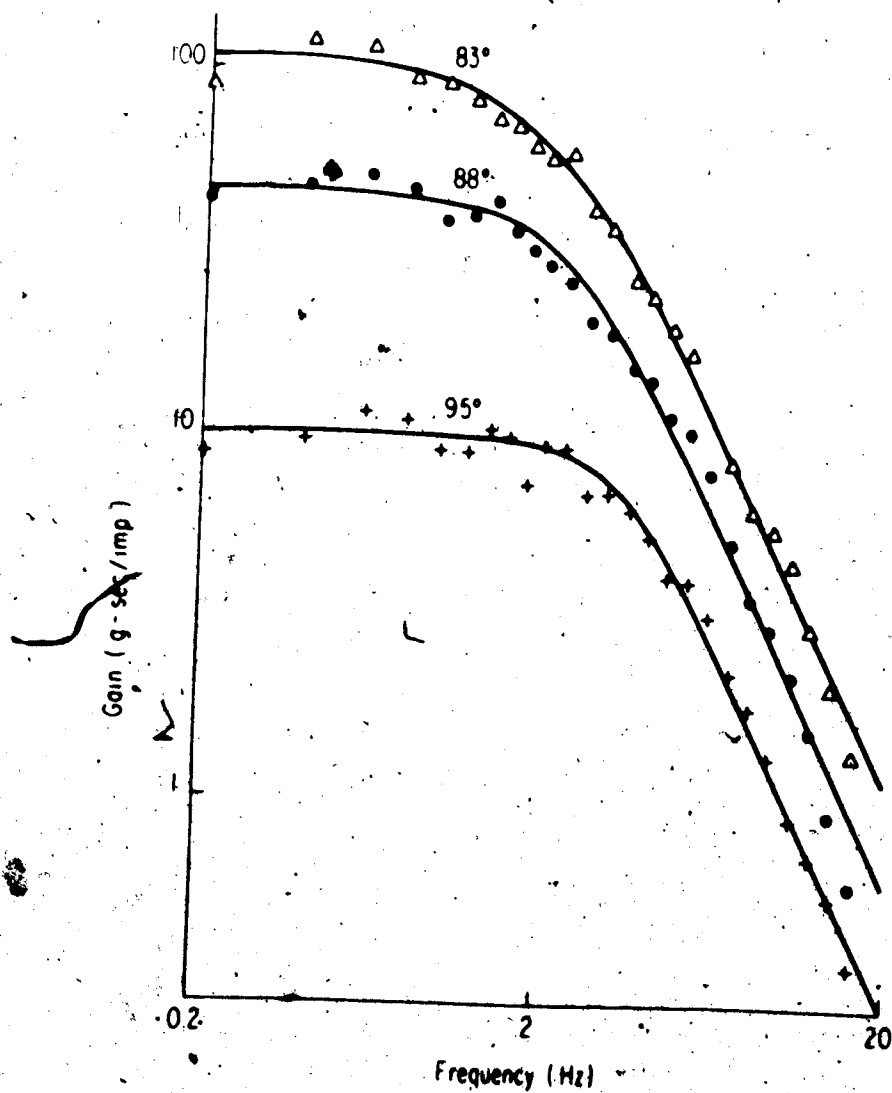


Fig. 5.4. Gain of human soleus muscle at rest for angles of 83° (Δ), 88° (\cdot) and 95° ($+$) are shown above on a log-log plot. As the angle at the ankle increases, the gain decreases, and the natural frequency increases.

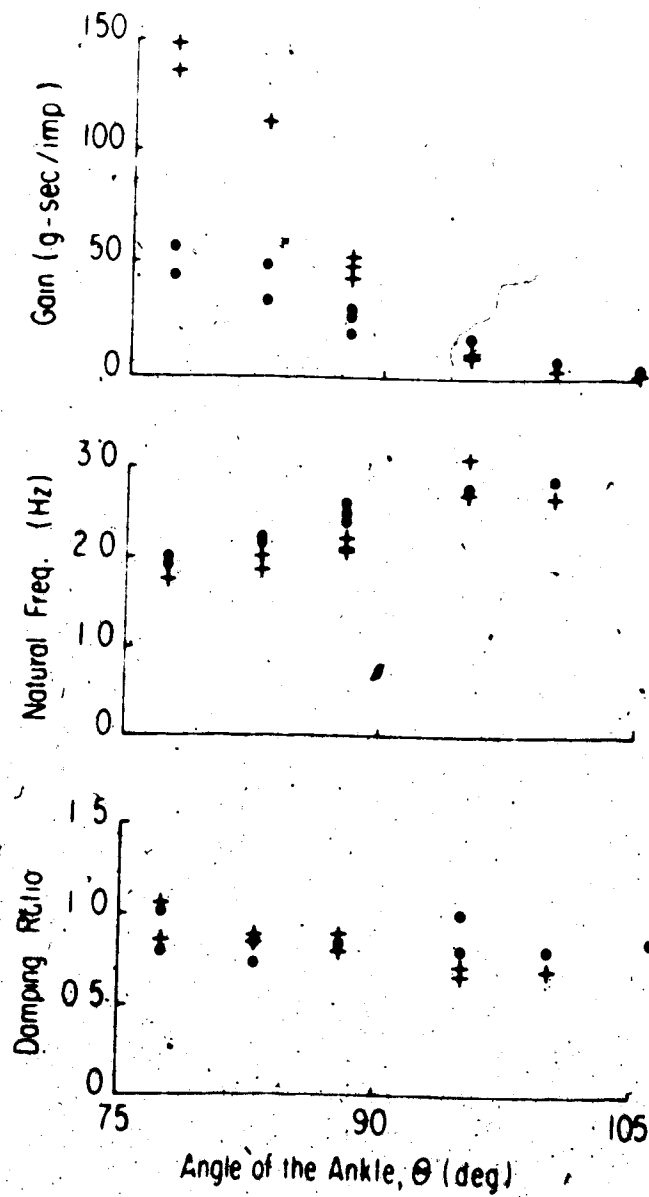


Fig. 5.5. Variation of low frequency gain, natural frequency and damping ratio with angle of the ankle on a linear scale. Data have been shown for two subjects (+ and •). All values are for rest conditions.

between periods of partially-fused contractions. The increasingly fused nature of the contraction with increase in rate explains the decrease in low frequency gain under these conditions.

Twitch Contractions at Rest.

To conclude the results under rest conditions, Fig. 5.6A shows three superimposed twitches at three different angles for the first 400 msec after the stimulus pulse was applied. These twitches will be compared to the twitches under voluntary force conditions. These twitches are non-oscillatory although the damping ratios from the frequency domain data are less than 1. The implications of these results will be considered in the DISCUSSION. Figs. 5.6B and 5.6C show the changes in the contraction times and half-relaxation times of the twitches with changes in length of the muscle.

Effects of Voluntary Contractions.

Fig. 5.7 shows gains and phases for the closed loop transfer function $C(s)$ at 88° when the subject exerted a voluntary force of 3 kg. The lines show 95% confidence intervals for the data points. The peak around 6 Hz in the data for gain corresponds to the frequency of oscillation of single twitches under the same conditions. Peaks were present in the data for the voluntary force conditions, although the peak shown in Fig. 5.7 is more prominent than in other observations. As the voluntary force was increased, the twitch was faster and the twitch tension decreased.

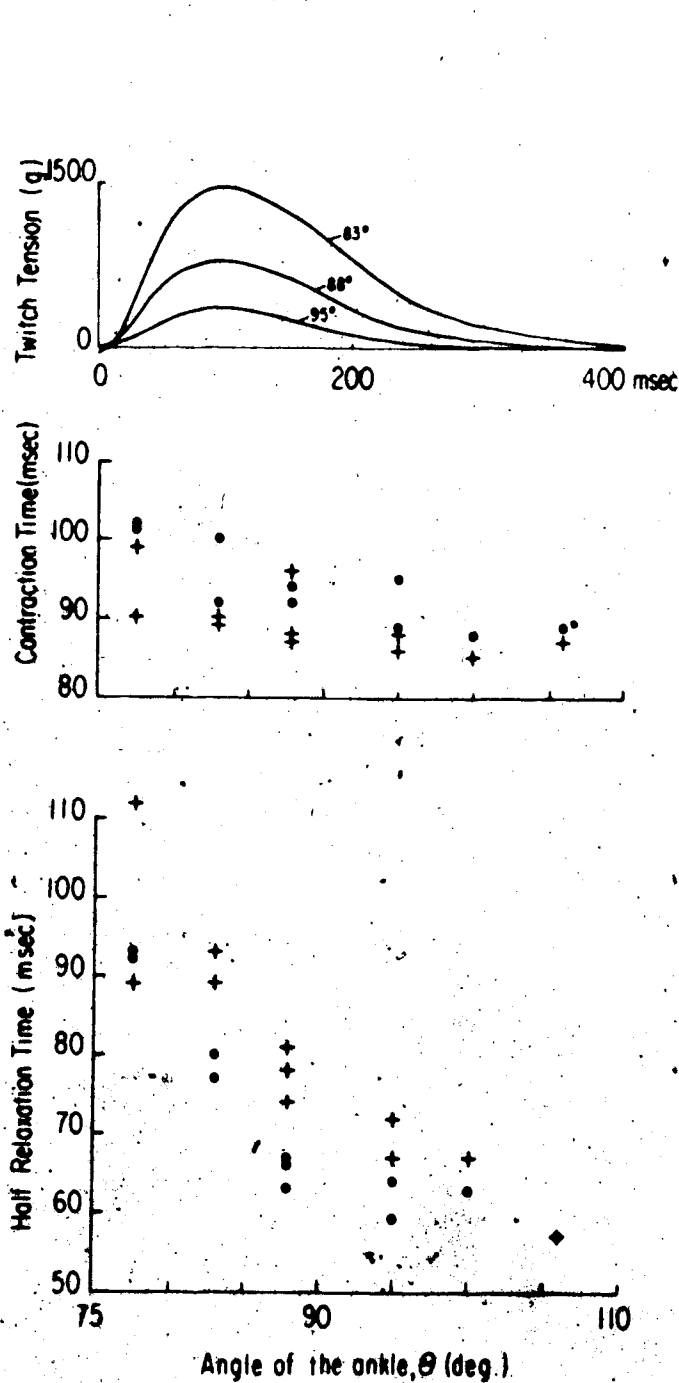


Fig. 5.6. Response of human soleus muscle to single stimuli at rest. A) Time course of twitches at 83°, 88° and 95°. As the muscle length increases (angle decreases) the twitches become slower and the twitch tension increases. B) There is a slight decrease in contraction/time with decrease in length. (•) are twitches before and (+) are twitches after a period of random stimulation. C) There is a large decrease in half-relaxation time with decrease in length of the muscle.

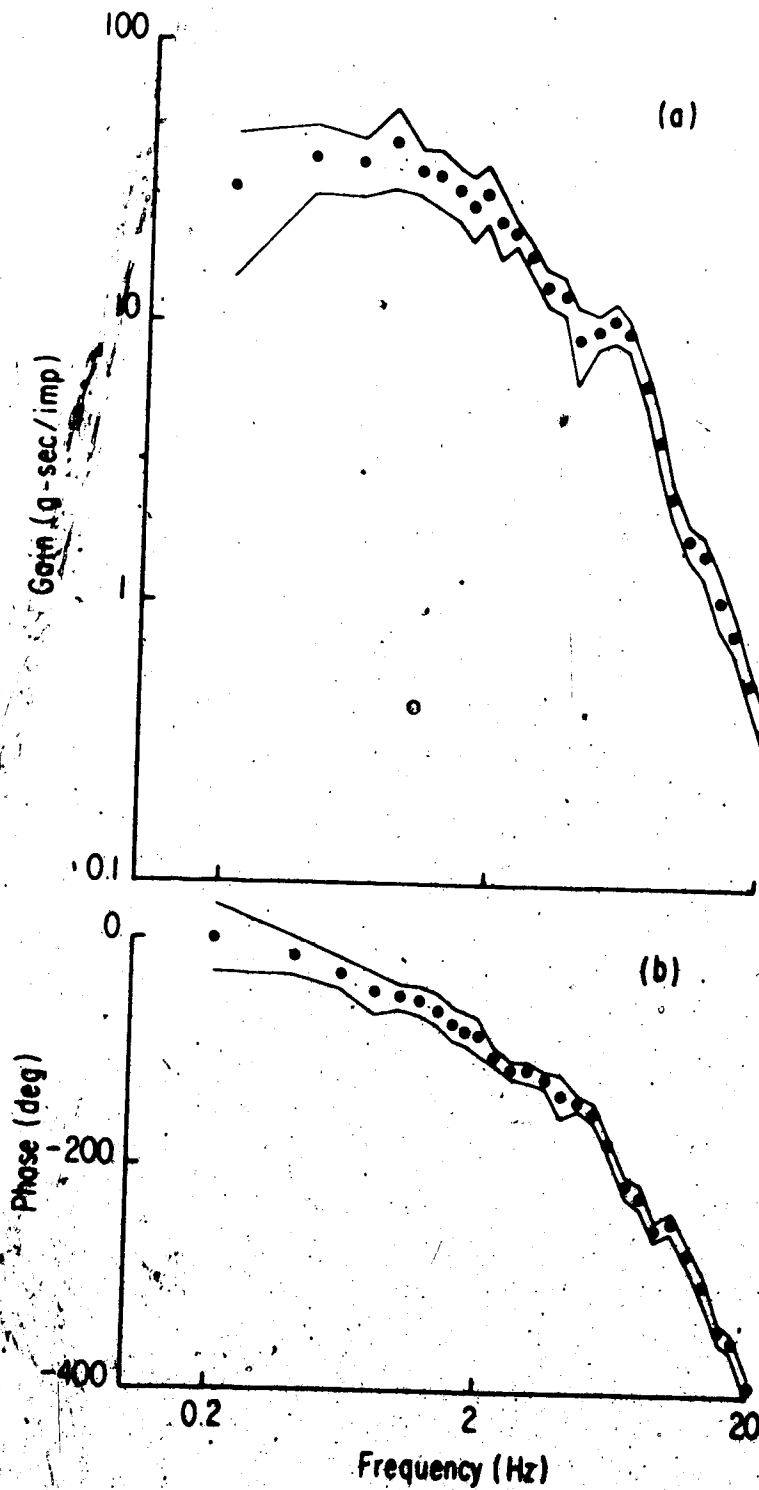


Fig. 5.7. Frequency response curve during a period of random stimulation while the subject maintained a voluntary contraction of about 3 kg. The angle of the ankle was 88°. Note the peak in the gain curve near 6 Hz... The lines are 95% confidence intervals for the data points.

Feedback Transfer Function.

For the reasons to be given in the DISCUSSION and the APPENDIX, we could not use the random stimulation data to determine the transfer function for the effects of sensory feedback during maintained voluntary contractions. Instead, we applied stimulus pulses at the rate of 1 every 3 sec and averaged 100 twitches and the corresponding surface EMG's. Under voluntary force conditions the twitches were oscillatory with corresponding oscillatory bursts in EMG activity. The M- and H-waves in the EMG, which are produced by stimulation of the α -motor axons and large Ia sensory fibers (via the monosynaptic stretch reflex) were often much larger in amplitude than the later oscillatory bursts. A delay of between 36 and 54 msec was added in the EMG channel during averaging to eliminate the M- and H-waves in order to amplify the later waves sufficiently for clear observation. Fig. 5.8 shows the oscillatory twitch at an 88° angle of the ankle with 6 kg voluntary force. Also shown is the rectified EMG trace for 1.5 sec. The second half of the EMG trace shows the sustained level of voluntary activity. During the first 100 msec after the H-wave there was less activity, which corresponds to the silent period shown by other workers (Merton, 1951; Agarwal & Gottlieb, 1972). This silent period could be due, for example, to unloading of the spindle afferents, to inhibitory feedback from Golgi tendon organs and to Renshaw inhibition. Corresponding to the silent period in EMG activity, the tension falls below rest level. This was clear for the subjects with briefer twitches and for all subjects at shorter lengths of the muscle where the twitches are briefer. For the subjects with longer twitches, the fall in tension during the silent

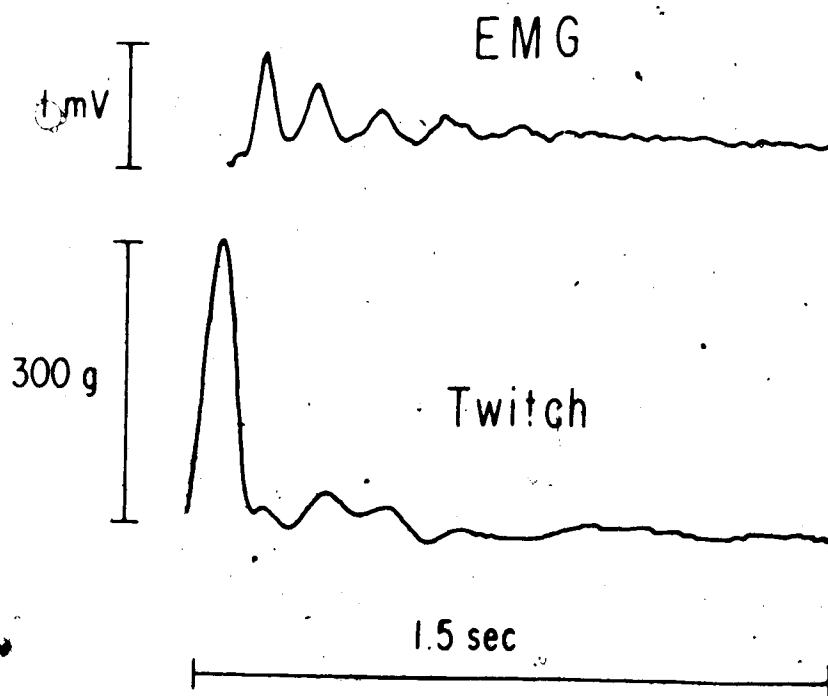


Fig. 5.8. The top trace shows the average rectified EMG after eliminating the M- and H-waves from the start of the trace. The latter half of the trace shows the sustained EMG activity due to the voluntary force of 6 kg. The beginning of the EMG trace shows a brief silent period followed by oscillations in the EMG activity. The lower trace shows the twitch of the muscle followed by the corresponding oscillations in force.

period did not go below the rest level. The rise in tension after the silent period showed up as a peak on the falling phase of the twitch (Fig. 2.7a). The oscillation frequency for the five subjects ranged between 5.5 and 7 Hz.

The transfer function $H(s)$ between the tension fluctuations as input and the average, rectified EMG as output was calculated (see methods) after eliminating the M- and H-waves, as in Fig. 5.8, because these waves resulted directly from the stimulus, rather than the tension fluctuations. Fig. 5.9 shows the data points for the gain and phase of the feedback pathway. The continuous lines are the gain and phase curves of the transfer function for primary muscle spindle afferents $H_p(s)$ given by Eq. (5.3). The gain curves for the secondary muscle spindle afferents (Poppele & Bowman, 1970) were also tried, but never gave as good a fit. Since the gain curve fitted well, the phase data were compared. The theoretical phase values of $H_p(s)$ show a phase advance of 156° at 20 Hz, while the experimental data showed phase lags of almost 600° at 20 Hz.

The theoretical curves are for the transfer function between length and spindle activity while we used tension as the input in our experiments. Assuming that the maximum internal shortening (minimum length) occurs at maximum contractile force, the experimental phase values were shifted by 180° so as to correspond to a transfer function between length as input and EMG as output.

The large discrepancy in phases at high frequencies is due at least in part to the time delay in the feedback pathway. A pure time delay should produce a phase lag which increases linearly with frequency, so the phase differences between $H(s)$ and $H_p(s)$ were plotted against

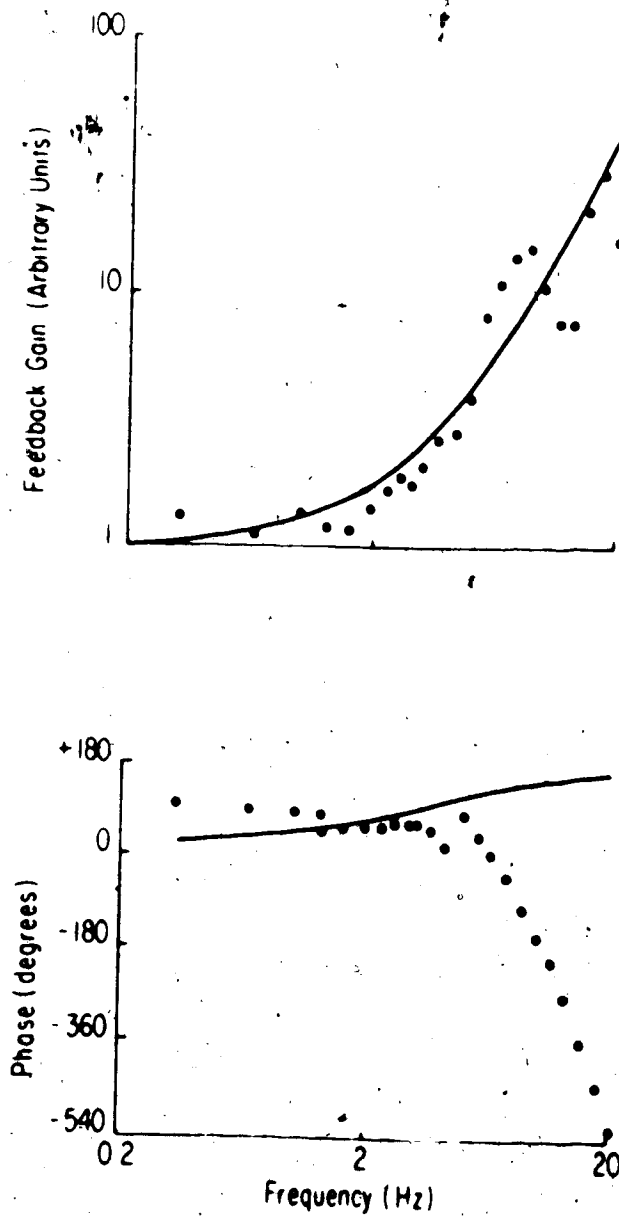


Fig. 5.9. The gain and phase of the feedback transfer function $H(s)$ measured from the average responses to single shocks during a voluntary contraction. The continuous lines are the theoretical values expected for primary muscle spindle afferents (Poppele & Bowman, 1970). Note the good fit of the gain data, but the discrepancies in phase.

frequency up to 20 Hz (Fig. 5.10). A straight line was fitted through the points which minimized the mean square error. The corresponding linear correlation coefficient was usually better than 0.98 and never below 0.95. The range of delays thus calculated ranged between 87 and 120 msec. These long delays do not agree with values for the monosynaptic spinal reflex (35 msec; Eccles & Mitchell, 1970). There is enough time to involve higher centers including fast pathways to and from the motor cortex (Evarts, 1973; Marsden *et al.*, 1973).

The fitted straight line for the phase differences vs. frequency did not pass through the origin which indicates that there is a further, but as yet unknown, mechanism producing a phase advance of nearly 90° in Fig. 5.10. In ten observations the measured values of the extra phase advance were 78 ± 7 (mean \pm S.E.).

DISCUSSION

Muscle Properties

These experiments show that in the absence of voluntary contraction the human soleus muscle behaves like a low-pass filter of second-order. Similar results have been shown for partially isolated cat muscles (Mannard & Stein, 1973; Chap. 3). Under isometric conditions the best-fitting second-order system for the cat generally had two real time constants, one of which was determined by the visco-elastic properties and the other by the decay of the active state. However, the values of the damping ratio in these human experiments were mostly less than 1 (Fig. 5.5). Such systems should show damped oscillations

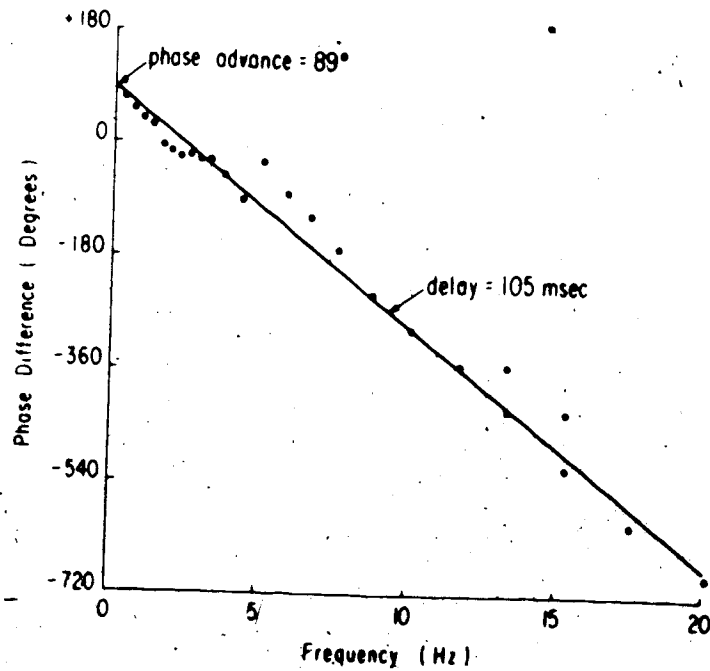


Fig. 5.10. Phase differences between the observed responses due to sensory feedback and those expected for the primary muscle spindle afferents. Same data as in Fig. 5.9, except that the differences have been calculated and plotted against frequency on a linear scale. The slope of the fitted straight line gives the value of the time delay that would account for these differences.

and not possess two real time constants, but the twitches under rest conditions were not oscillatory (Fig. 5.6A).

The apparent conflict between the low damping ratios and non-oscillatory twitches suggests that the soleus muscle is not simply a second-order system. Several explanations can be offered. Firstly, in the intact leg there will inevitably be an effect due to the mass of the foot and the attachment of the muscle to the transducer. We showed earlier (Chap. 4) that the addition of inertial masses converts the second-order system of the muscle to a fourth-order system, although the differences would only be detectable at high frequencies under nearly isometric conditions. The result of these differences will be to reduce the effective damping, so that under certain conditions the twitches become frankly oscillatory (Chap. 4). In the frequency domain analysis (Fig. 5.3) deviations of data points from second-order fitted curves are seen at higher frequencies, particularly above 20 Hz. However, we cannot give much weight to these data points due to low coherence values above 20 Hz.

Secondly, nonlinearities were observed for soleus muscle in the cat using elastic loads (Chap. 3) which produced low values of the damping ratio in the absence of oscillatory twitches. Furthermore, the best-fitting parameters of the second-order system vary with the rate of stimulation. This would not occur in a purely linear system, and the variation means that results from random stimulation at 5/sec cannot be applied immediately to twitches generated once every few seconds. Thus, the discrepancy between the observed twitches and the partially fused responses is not too surprising. This discrepancy does serve to point out

that, although a linear, second-order model may be useful for a number of purposes, it is obviously a simplification of the complex nature of mammalian muscles.

Typical values of the natural frequency of the human soleus muscle were around 2 Hz, which was somewhat higher than the average value for the cat (Chap. 3), although in the same range. The contraction times and the half-relaxation times of the twitches for human soleus (60-100 msec) were also similar. In fitting the phase data to a second-order system, time delays which were typically between 15 and 20 msec were calculated. These again were in the range measured for the cat, so mechanically human and cat muscles behave similarly, despite the obvious differences in bulk and force output.

Sensory Feedback

The evaluation of the feedback transfer function from Eq. (5.3) was not possible for the reasons given below. The open loop transfer function between stimulus as input and tension as output is denoted by $G(s)$ under rest conditions. With the same stimulus and voluntary force added, this transfer function changes and will be denoted by $G'(s)$. The closed loop transfer function between stimulus input and tension output is then

$$C(s) = \frac{G'(s)C}{1 + G'(s)H(s)}$$

If $G'(s) = G(s)$, then

$$C(s) = \frac{G(s)}{1 + G(s)H(s)}$$

Knowing the open loop transfer function $G(s)$ and the closed loop transfer function $C(s)$, one can calculate $H(s)$. However, the results of an analysis which is described in the Appendix showed that $G'(s)$ is quite different from $G(s)$ and we could not obtain a valid approximation for $H(s)$ by this method. These results bring out the importance of visco-elastic properties of the muscle. Since we were stimulating only about 10% of the muscle fibers, the voluntary force recruited more motor units, changing the visco-elasticity of the muscle considerably. Changes in visco-elastic properties upon generation of voluntary force were larger than the changes due to closing the reflex loop. Grillner and Udo (1971) have suggested that the properties of muscle might account for the properties of the whole reflex loop which implies that the contribution of the feedback transfer function is small. However, the oscillatory responses we measured during voluntary contractions indicate that the effect of feedback is significant, at least at the frequency of oscillation.

The feedback transfer function was determined after averaging twitches and the corresponding EMG's. The time delay calculated for this feedback pathway was in the range 87 to 120 msec, which is much too long for a monosynaptic spinal reflex. Melvill Jones and Watt (1971) showed that the latency from stretch of human gastrocnemius to the appearance of EMG in that muscle was 120 msec. They named it the "functional stretch reflex" because it adds much more to the muscle tension than the spinal monosynaptic reflex. Marsden et al. (1973) have also found evidence of these long latency reflexes for the jaw, hand and toe muscles.

The latencies, ranging from 13 msec for the jaw to 75 msec for the toe, are twice as long as those for the corresponding spinal reflexes.

Evarts (1973) found similar results in monkeys and showed that pyramidal tract cells were activated at the right latency to participate in this reflex. Thus, our work adds to the growing body of data which supports the suggestion of Phillips (1969) that "... this segmental circuit, which has its most obvious importance in postural reactions, has been overlaid in the course of evolution by a transcortical circuit".

The frequency response we calculated for this pathway is consistent with the primary muscle spindle afferents being the sensory receptor responsible. Poppele and Kennedy (1974) have recently shown that human muscle spindles have an identical frequency response to cat spindles. Secondary muscle spindle afferents have a somewhat different dynamic response (Poppele & Bowman, 1970) which did not fit our data as well. However, Anderson (1974) has recently measured the dynamics of Golgi tendon organs which are similar to those of the primary muscle spindle afferents, so tendon organs may also be involved. Finally, our data indicate that in addition to the time delays due to this longer pathway, there is an extra phase advance of nearly 90° . This result can be described formally by modifying Eq. (5.4) to

$$H(j\omega) = H_p(j) e^{-j(\omega T - \psi)} \quad (5.5)$$

which would add a phase advance ψ at all frequencies. However, the mechanisms which could produce such a phase advance in the reflex pathway are unclear, and will require further study.

APPENDIX

If the parameters of the muscle do not change when the loop is closed, the closed loop transfer function between stimulus as input and tension as output is given by

$$C(s) = \frac{G(s)}{1 + G(s) H(s)} \quad (1)$$

where $G(s)$ is the transfer function of the muscle under rest conditions. However, under voluntary force conditions $G(s)$ changes to $G'(s)$ because the muscle becomes more visco-elastic. The closed loop transfer function, then, is given by

$$C'(s) = \frac{G'(s)}{1 + G'(s) H(s)} \quad (11).$$

The transfer function around the feedback loop $G'(s) H(s)$ is given by

$$G'(s) H(s) = \frac{G'(s)}{C'(s)} - 1 \quad (111).$$

When we calculated the loop transfer function, we assumed that $G'(s) = G(s)$, and substituted $G(s)$ instead of $G'(s)$ (which was not known) on the right-hand side of Eq. (111).

The *estimated* loop transfer function was then, from Eqs. (11) and (111)

$$\begin{aligned}
 G_e(s) H_e(s) &= \frac{G(s)}{G'(s)} - 1 \\
 &= \frac{G(s) - G'(s)}{G'(s)} + G(s) H(s) \quad (\text{iv}).
 \end{aligned}$$

If $G(s) \approx G'(s)$, then the first term on the right-hand side of Eq. (iv) is negligible and we should get a good approximation of $G(s) H(s)$.

Similarly, we estimated the feedback transfer function by

$$\begin{aligned}
 H_e(s) &= \frac{1}{G(s)} \left[\frac{G(s) - G'(s)}{G'(s)} + G(s) H(s) \right] \\
 &= \frac{1}{G(s)} \cdot \frac{G(s) - G'(s)}{G'(s)} + H(s) \quad (\text{v}).
 \end{aligned}$$

Again, if $G(s) \approx G'(s)$, $H_e(s) \approx H(s)$.

Both the estimated loop transfer function and the estimated feedback transfer function gave unexpected results. The value of the transfer function for the loop should show 180° phase lag at about the frequency of oscillation. The phases observed in computing Eq. (iv) deviated only slightly from 0° , as would be expected if the first term were dominant (Rosenthal *et al.*, 1970). Similarly, the phases computed from Eq. (v) were more like those expected for the first term (the phases were approximately those of $G(s)^{-1}$) rather than of $H(s)$, as given by Poppele and Bowman (1970). Thus, we were not able to estimate the loop gain of the feedback transfer function $H(s)$ by random stimulation.

CHAPTER 6

DYNAMICS OF THE MUSCLE AFFERENTS AND THE FEEDBACK PATHWAY

INTRODUCTION

Fibres from muscle spindles and Golgi tendon organs form the sensory component of the feedback pathways of the myotatic reflex. It is important to determine the contribution of these afferents to the total dynamics of the feedback pathway. The dynamics of this system are best represented in the frequency domain.

The biggest problem in analyzing the response of these afferents has been their highly nonlinear behaviour. Nonlinear properties, such as phase locking, carrier dependence and nonlinear response to large amplitudes of stretch, all limit the usefulness of a quantitative analysis based only on a linear approximation. The nonlinear properties of spindles (Hasan & Houk, 1975a, b; Matthews, 1972) and tendon organs (Rosenthal *et al.*, 1970; Anderson, 1974; Houk & Simon, 1967; Houk & Henneman, 1967) have been discussed in detail.

The transfer characteristics of spindle afferents (Matthews & Stein, 1969a; Poppele & Terzuolo, 1968; Rosenthal *et al.*, 1970; Poppele & Chen, 1972) and of Golgi tendon organ afferents (Rosenthal *et al.*, 1970; Anderson, 1974), operating in the linear range, have been studied. Empirical expressions of the transfer functions have been given both for the spindles (Matthews & Stein, 1969a; Poppele & Bowman, 1970; Rosenthal *et al.*, 1970) and the tendon organs (Houk & Simon, 1967; Rosenthal *et al.*, 1970; Anderson, 1974) when stretches of small

amplitude were applied to the appropriate muscle. For the tendon organs, in addition to stretches, sinusoidal changes in active tension were also applied. All three afferents have two main components of response, the response to steady length (static component) and the response to changes in length (dynamic component). The result is a vector sum of these two responses. In the frequency domain the static and dynamic components are equal at the corner frequency, which is around 1.7 Hz for all three afferents (Matthews, 1972). The value of the corner frequency varies with the state of the preparation used (Matthews, 1972). Secondary afferents show linear behaviour over a much wider range of amplitudes than do the primaries (Matthews & Stein, 1969a). Golgi tendon organs are also more linear in their response (Houk & Simon, 1967).

Fusimotor activity affects the dynamics of different afferents in different ways (Matthews, 1972; Goodwin & Matthews, 1971; Chen & Poppele, 1973). The stimulation of dynamic gamma fibers does not seem to have much effect on the static or dynamic sensitivities¹ of the spindles. The stimulation of static gamma fibers has complex effects. When static gamma fibers are stimulated at high rates (75/sec or above), the static and dynamic sensitivities of the afferents are reduced equally so that the shape of the frequency response curve is not changed, but it is shifted downwards. When static gamma fibers are stimulated at low rates, static sensitivity, or sensitivity to low frequencies, is reduced, leaving the dynamic sensitivity unchanged. This lowers the value of the corner frequency. There is no effect on the

¹ Sensitivity of a muscle spindle afferent ending has been defined by Matthews and Stein (1969a) as the amplitude of its response divided by the amplitude of the length change in impulses/sec/mm.

tendon organs.

Reflex studies in decerebrate cats, to determine the dynamics of the feedback pathway, have been done in very few laboratories (Partridge & Glaser, 1960; Jansen & Rack, 1966; Poppele & Terzuolo, 1968; Rosenthal *et al.*, 1970); only the latter two papers have shown the transfer function with muscle length as input and EMG as output. This transfer function for the spinal reflex has the same form as that of the primary spindle afferent. This suggests that the dynamics of the primary muscle spindle endings determine the dynamics of the whole feedback pathway. Jansen and Rack (1966) in their experiments with decerebrate cats, encountered two main types of preparations, one which they called more statically sensitive and the other less statically sensitive. In the less statically sensitive preparations they observed clonus with frequencies of 6-8 Hz. With more statically sensitive preparations there were no oscillations. Also, from their observations, they suggested additional phase advances at the level of the spinal cord to account for phase advances of EMG with respect to muscle length inputs. Their results will be referred to again in the DISCUSSION in relation to our experiments.

For this project the frequency response characteristics for (i) motor spikes as input and tension as output (efferent-muscle), (ii) motor spikes as input and afferent spikes as output (efferent-afferent) and (iii) tension as input and afferent spikes as output (muscle-afferent) have been computed using random stimulation to S1 or L7 ventral root filaments. The fit of the muscle-afferent frequency response data with the empirical transfer functions given by Poppele

and Bowman (1970) has been discussed in the RESULTS section. The afferents compensate for the muscle properties both in gain and phase at low frequencies, as shown by Poppele and Terzuolo (1968). The compensation is poorer as the frequency increases.

The behaviour of the afferents at low frequencies to changes in external load was investigated. The low frequency efferent-muscle gain increases with increase in the stiffness of the spring load (Chap. 3). The low frequency muscle-afferent gain decreases with increase in stiffness. For the efferent-afferent transfer function the low frequency gain changes differently for the spindle and tendon organ afferents.

Further, the transfer function with tension as input and EMG as output was computed (Chap. 5). There were some inconsistencies in the results which limit the usefulness of these data. Since we found that this transfer function was the same as that of the primary afferents in humans, we expected similar results for decerebrate cats except that the delays calculated for this reflex pathway were expected to be short. However, the gain of the transfer function was usually steeper than that of the muscle-primary afferent at higher frequencies. The latencies for feedback pathway calculated varied anywhere from 12 msec to 150 msec. The shorter latencies can be attributed to spinal reflexes but not the very long latencies. Moreover, longer latencies were always associated with additional phase advances, not accounted for by the spindle transfer function; the short latencies did not show these phase advances. Multiple cerebello-spinal pathways are known (Eccles *et al.*, 1975a, b; Allen & Tsukahara, 1974) which could be involved

in these reflexes. The large variation in the latency measurements could be due to changes in the excitability of the pathway and multiple loops in a pathway.

METHODS

Adult cats, both male and female, weighing 2-5 kg, were used. The trachea was cannulated and the carotid arteries were looped while the cat was under fluothane anaesthesia. Next the femoral and the obturator nerves were cut. Decerebration by suction was done either at the intercollicular level or more rostral to it after which the anaesthesia was stopped. A laminectomy was performed, exposing L5-S1 roots. The sural, common peroneal, nerves to plantaris, lateral gastrocnemius and medial gastrocnemius muscles, nerves to hamstrings, tenuissimus, hip and tail muscles were cut. The branch of the sciatic going to soleus and its blood supply were kept intact. Before cutting the calcaneum, the maximum physiological length was measured. The details of the muscle preparation and loading conditions were the same as those described in Chap. 3 (METHODS).

The skin and fascia around the exposed part of the spinal cord were used to form a pool for paraffin oil. Small ventral root filaments were prepared for bipolar stimulation. To record from single afferents, small dorsal root filaments were carefully isolated, lifted into the oil and placed on bipolar electrodes for recording. The afferent impulses were fed to a preamplifier and then to the tape recorder for recording. To test whether the unit was a secondary,

primary or Golgi tendon organ, whole nerve to the soleus (or plantaris), was stimulated. The response to a single twitch and the conduction velocity gave a clear indication of the type of afferent. Some Golgi tendon organs, which increased their firing rate on the rising phase of the twitch, behaved like a primary afferent on ventral root filament stimulation. The tendon organs with this behaviour were presumably not in series with the motor units being stimulated. Therefore, when other parallel motor units were stimulated, these tendon organs were unloaded and stopped firing on the rising phase of the twitch. The tendon organs which were not in series with the motor units we were stimulating were not studied.

To record EMG teflon coated Ag wires bared by 1 cm at the end were inserted into the belly of the soleus muscle. These two wires were connected to the preamplifier, the output of which was fed to the tape recorder. The cut-off frequencies of the preamplifier for EMG recording were 10 Hz and 3,000 Hz and for afferent recording 30 Hz and 3,000 Hz. The stimulus pulses, tension, EMG and afferent activity were simultaneously monitored on an oscilloscope.

EMPIRICAL RELATIONS

Poppele and Bowman (1970) have given transfer functions both for the muscle spindle primary and secondary afferents. Anderson (1974) has shown that the transfer function for the Golgi tendon organ is the same as that for the primary afferent. We compared our data with the empirical expression given by the former authors.

For the primary afferent at 37°C, the transfer function for length as input and afferent activity as output, is given by

$$H_p(s) = K_p \frac{s(s + 0.44)(s + 11.3)(s + 44)}{(s + 0.04)(s + 0.816)} \quad (6.1)$$

where K_p is a normalized constant with appropriate units and s is the complex Laplace variable. The term $(s + 44)$ is temperature-dependent term, in which the value 44 at 37°C changes to 12.56 at 26°C. This can also be considered as the expression for the acceleration response.

The term $\frac{s}{(s + 0.04)}$ accounts for a very slow time constant decay. Hasan and Houk (1975) have studied the spindle characteristics at very low frequencies which we have not considered. The term $(s + 11.3)$ can be considered as the velocity response giving a corner frequency of 1.7 Hz.

The empirical expression for the secondary ending is given by

$$H_s(s) = K_s \frac{(s + 0.44)(s + 11.3)}{(s + 0.816)} \quad (6.2)$$

Eq. (6.2) does not have the terms for slow decay, acceleration and temperature dependence. Poppele (1973) has discussed the phase locking and carrier-dependent expressions which we have not considered; the reasons will be given in the DISCUSSION.

RESULTS

Afferent transfer functions.

The frequency response characteristics of the muscle afferents

shown in this chapter have been computed from random stimulation data with tension as input and afferent activity as output. Sometimes, to compare averaging and spectral analysis results, both techniques were used for the same unit, one kind of stimulation following the other. The results agreed to within experimental error except at frequencies where the coherence values for random stimulation were less than 0.2.

Fig. 6.1 shows the data points for the frequency response gain of a primary muscle afferent for soleus muscle in decerebrate cat. A small filament of S1 ventral root was stimulated randomly at a mean rate of 5/sec. The mean firing rate of this afferent was ~27/sec. The spring against which the muscle contracted had a stiffness of 97 g/mm which resulted in a shortening of the muscle by ~0.1 mm during a single twitch. This amplitude is beyond the linear range of primary afferent response according to other workers. A single twitch resulted in a mean pause of ~60-70 msec in the firing of the afferent which showed up as a trough in the gain curve at ~15 Hz (Chap. 2). The fine lines show 95% confidence intervals of the data points and the thick continuous line shows the empirical curve computed from Eq. (6.1). The response curve agrees well up to 10 Hz with the linear empirical curve. The deviation of the curve from the data points is probably due to the various nonlinearities of the spindle afferent, e.g. a pause of ~60 msec, giving a trough at ~15 Hz, scatter due to variability in the firing rate of Ia afferent, etc. The phases of this afferent increased from +15° at low frequencies to +65° at 7 Hz and then started to get less positive until it was negative at 15 Hz. The phase data also showed a minimum around 15 Hz. In the post-stimulus time histogram

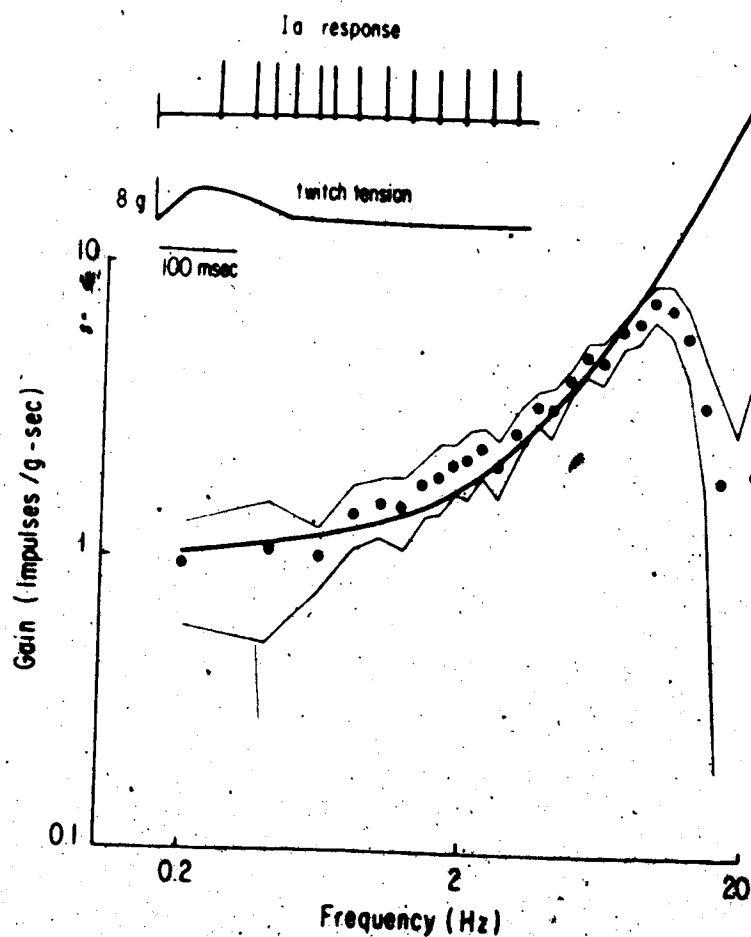


Fig. 6.1. The data points show the gain of muscle-primary afferent transfer function in a decerebrate preparation. The soleus muscle contracted against a spring of stiffness 97 g/mm resulting in a mean pause -60 msec. The thick curve is the empirical gain computed from Eq. (6.1). The fine lines show 95% confidence intervals of the data points. The upper left hand corner shows response of the afferent fibre to a single twitch in time domain.

(PSTH) (Fig. 6.6a) where 80 twitches were averaged, the firing rate was highest at ~100 msec, i.e. approximately at half-relaxation time. This effect was extremely pronounced in some primary afferents, spindles of which were probably innervated by dynamic gamma fibers. The general response of primary afferents was an increase in firing during the falling phase of the twitch and a longer interval at the completion of the twitch. The left-hand corner of the figure shows the response to a single twitch in the time domain.

Fig. 6.2 shows the gain data for a secondary ending from soleus muscle in a decerebrate cat. The muscle contracted against a spring of stiffness 155 g/mm which caused a shortening of ~0.2 mm. A single shock to a S1 ventral root filament resulted in a pause of ~50 msec in the firing of the afferent. This pause showed up as a trough at ~20 Hz in the frequency domain gain curve. The mean firing rate of .30/sec showed up as a peak in the gain curve at 30 Hz (not shown). The fine lines show 95% confidence intervals of the data points. Fit to the empirical curve (Eq. (6.2)) is very good except at the lowest frequencies. All frequency response curves with good coherence values showed this low frequency trend for this particular afferent. This kind of effect has been discussed by Goodwin and Matthews (1971) and Chen and Poppele (1973).

The phase data showed a continuous increase from -15° at low frequencies up to 86° at 12 Hz and then it started to fall to a minimum (21°) at 21 Hz.

Fig. 6.4c shows the response of another secondary from plantaris muscle in an anaesthetized cat. Coherences, except for the

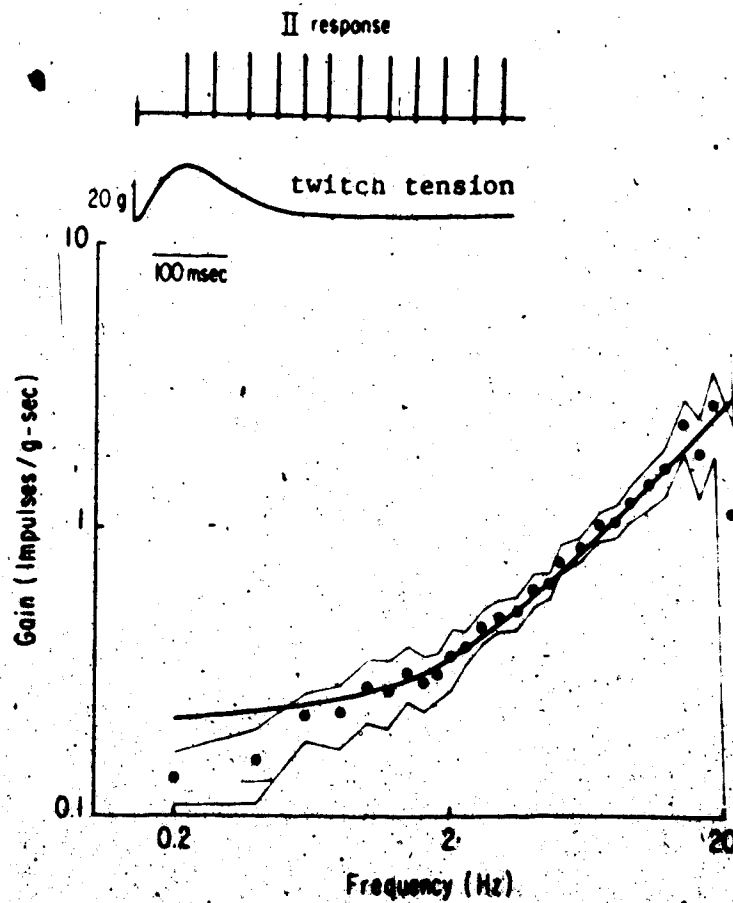


Fig. 6.2. Gain of the transfer function for a secondary ending in a decerebrate cat is shown above. The soleus muscle contracted against a spring of 155 g/ml. The thick line is the empirical curve from Eq. (6.2). The fine lines show 95% confidence intervals of the data points. On the top left is shown a typical response of this afferent to a single twitch in time domain.

first point, are above 0.8 up to 8 Hz, fall off to 0.6 by 16 Hz and 0.4 by 21 Hz. In general, for all muscle afferents, the coherences were very high for anaesthetized preparations of the plantaris muscle. The reason could be that there was less variability in an anaesthetized preparation or that the more linear plantaris muscle (Chap. 3) governed the linearity of the afferent endings. The fact that the coherence values do fall off more sharply with increase in frequency for soleus muscle than for the plantaris muscle supports the latter possibility. The phases increased from $+25^\circ$ at lower frequencies at $+47^\circ$ at 8 Hz and then started to decrease coming down to -12° at 21 Hz.

For Golgi tendon organs we found two typical types of responses when coherences were high and therefore the results were reproducible. When a Golgi tendon organ had a very high threshold for firing, i.e. there was no spontaneous firing even at large stretches, a single twitch resulted in 4-5 impulses on the rising phase of the twitch and the afferent was silent again. In such a case the frequency response curve was flat at all frequencies except showing a peak at the effective firing rate. If each twitch results in four impulses, then 10/sec rate of stimulation will result in 40 impulses/sec and in the analysis, this is treated as the mean firing rate, although it is not the carrier rate of the afferent. These types of tendon organs were found both in anaesthetized (plantaris) as well as in decerebrate preparations (soleus). The phases for this afferent were also flat, varying between -10° and $+20^\circ$, except at the effective firing rate.

For a Golgi tendon organ afferent firing spontaneously, the firing rate increased on the rising phase of the twitch and decreased

during the falling phase. Sometimes there was a short pause during the falling phase of the twitch. Fig. 6.5c shows the frequency response gain data of a tendon organ afferent from soleus muscle in a decerebrate cat. Fig. 6.6b shows PSTH for the same tendon organ where 80 responses have been averaged. Coherence values for frequency response results were above 0.8 up to 4 Hz, down to 0.5 by 9 Hz and 0.01 by 16 Hz. The sharp fall in coherence values with frequency could be because of the soleus muscle. Coherences were high up to much higher frequencies for Golgi tendon organs from plantaris muscle as mentioned for the secondary ending above. The firing rate of this Golgi tendon organ was 30/sec which showed up as a peak in the gain curve (not shown). The phases were $+14^\circ$ at low frequencies, increased to 67° at 6 Hz and then decreased smoothly to -40° at 18 Hz.

None of our Golgi tendon organ curves fitted Eq. (6.1) for the primary transfer characteristics, but most of them fitted Eq. (6.2) well for the transfer function of the secondary.

Compensation of muscle properties by afferents

Fig. 6.3a is the gain curve for the efferent-muscle transfer function for soleus muscle in a decerebrate cat, Fig. 6.3c is the muscle-afferent gain and Fig. 6.3b is the efferent-afferent gain for the same primary as shown in Fig. 6.1. For Fig. 6.3b coherence values are above 0.6 until 8 Hz and then fall to 0.2 at 12 Hz. The primary afferents seem to compensate well for the muscle properties at least up to 8 Hz. Poppale and Terzuolo have shown this result up to 6 Hz.

Curve 6.4a shows the gain of the efferent-muscle transfer

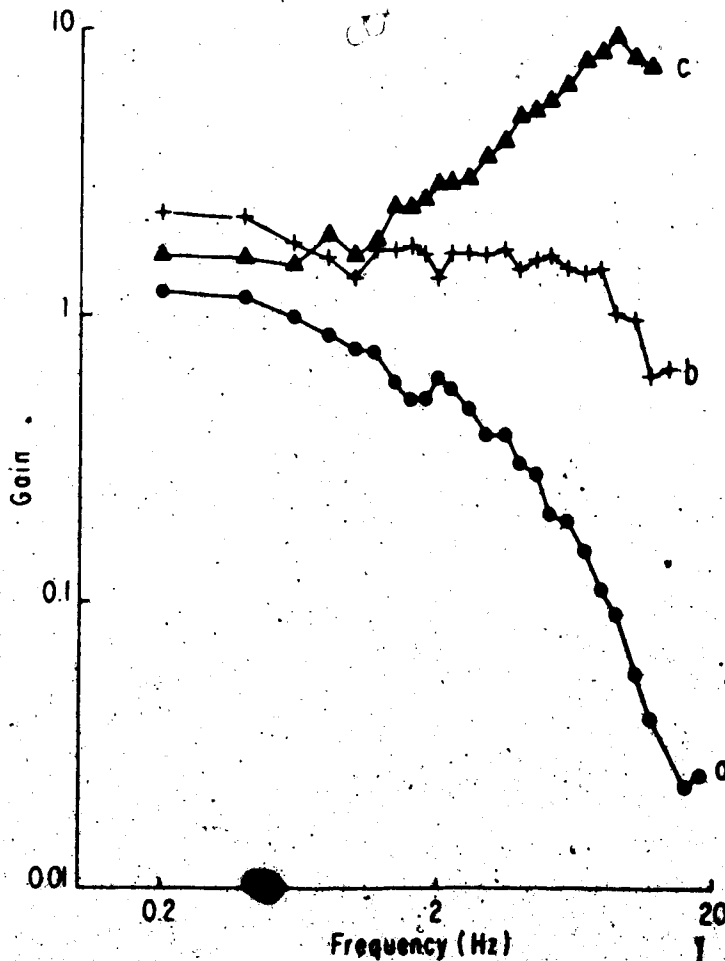


Fig. 6.3. Absolute values of gains for (a) efferent-muscle in gm-sec/imp, (b) efferent-afferent, and (c) muscle-afferent in impulses/(gm-sec). frequency response functions are shown for a primary afferent in a decerebrate cat. The soleus muscle contracted against a spring of stiffness 97 g/mm.

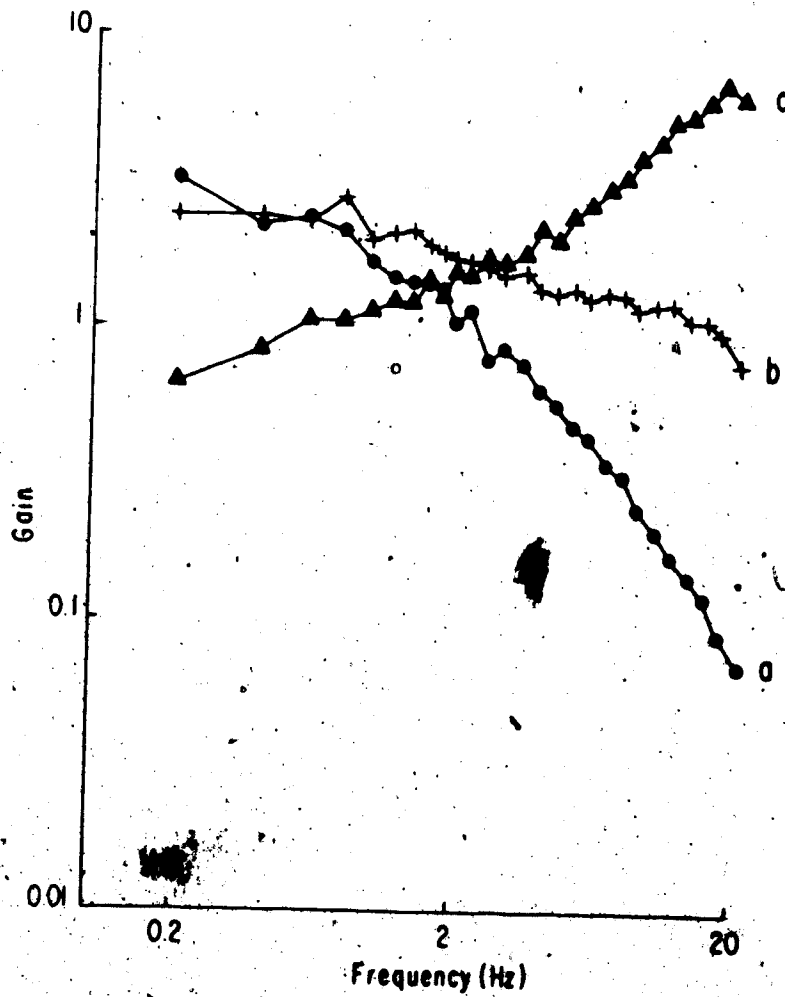


Fig. 6.4. Gain curves of secondary afferent are shown in absolute units for plantaris muscle of an unanaesthetized cat, (a) motor nerve spike train input and tension output in (gm-sec)/imp, (b) motor nerve spike train input and secondary afferent firing output, (c) tension input and secondary afferent as output in impulses/(gm-sec). See text for details.

function for plantaris muscle in an anaesthetized preparation. The natural frequency was 3.5 Hz with damping $\zeta = 1.8$. Curve 6.3b shows the gain of the efferent transfer function of a secondary ending. The coherence was above 0.8 up to 18 Hz except at the first point. The plantaris muscle with a high value of natural frequency shows a reduction of gain by the secondary afferent for the decrease in gain in the muscle is quite good.

Figure 6.3b shows the gain curve for efferent-muscle transfer function for soleus muscle. The natural frequency is 1.7 Hz and damping ratio is 1.8. Damping ratio was always greater than one for soleus in decerebrate preparations as opposed to anaesthetized preparations (Chapter 5). Figure 6.4b shows the gain curve for efferent-Ib afferent transfer function. It clearly shows that the afferent does compensate to a small extent for the declining gain of the muscle with frequency. The compensation is not as good as that in the plantaris muscle (observations on plantaris muscle). The phases decreased steadily from -15° at low frequency to -160° at 18 Hz which included the phase lags due to the dynamics and phase lags due to pure time delays.

Low frequency behaviour using various loads.

In Figs. 6.3b, 6.4b and 6.5b we have looked at the compensation by the afferents for the muscle properties as a function of frequency. We were also interested in studying the response of the afferents as compared to that of the muscle with change in load stiffness at low frequencies. Low frequency gain values for muscle-afferent and

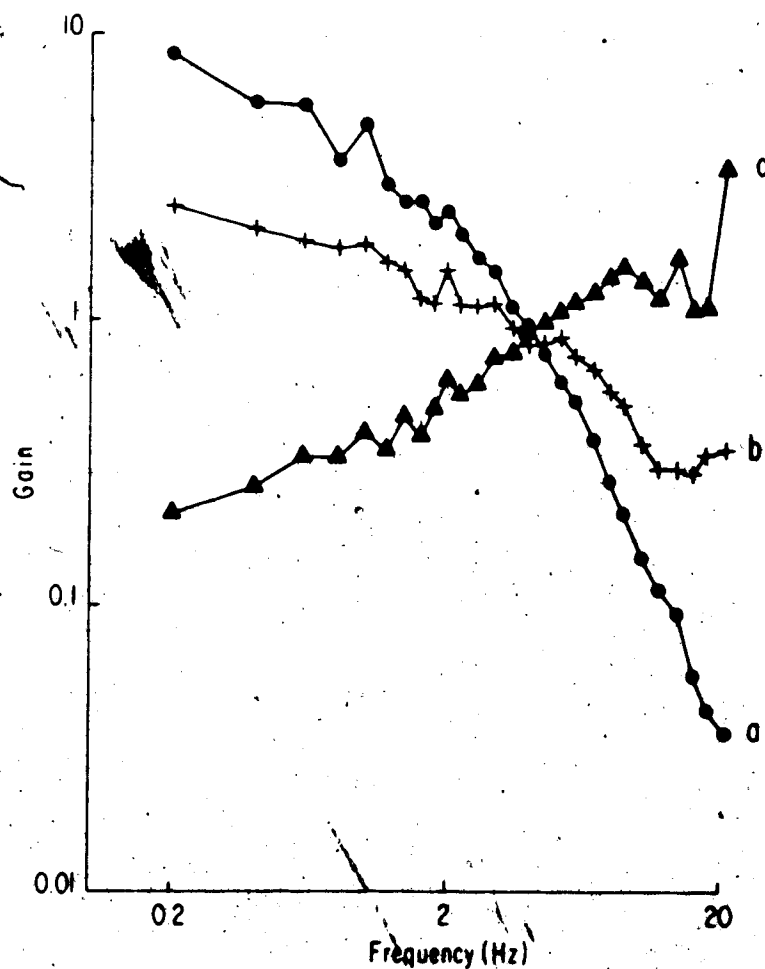


Fig. 6.5. Absolute values of gains are shown for (a) motor nerve spike train input and muscle tension output in (gm-sec)/imp, (b) motor nerve spike train input and Golgi tendon organ output, (c) tension input and Golgi tendon organ output in impulses/(gm-sec) for the soleus muscle in decerebrate cat. See text for details.

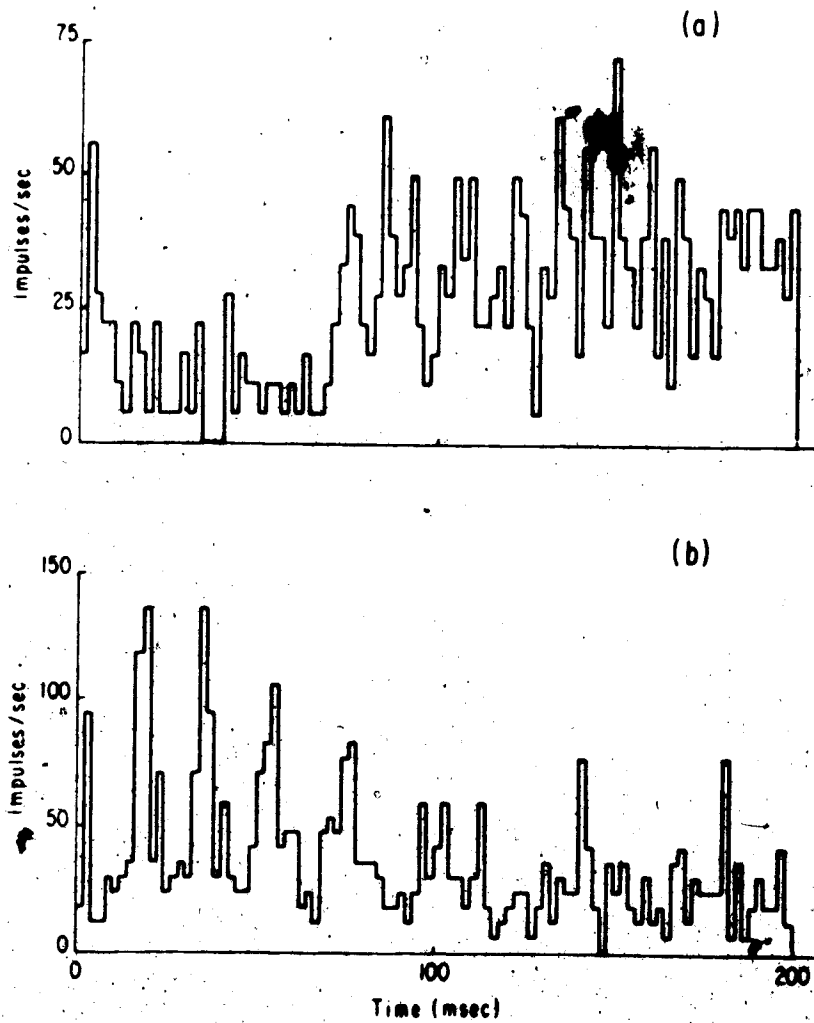


Fig. 6.6. Post-stimulus time histograms are shown for (a) primary afferent, same as in Fig. 6.1 and (b) Golgi tendon organ, same as in Fig. 6.5. Each record is an average of 80 responses.

efferent-afferent frequency response data have been plotted in Fig. 6.7 for various spring loads. Data have been pooled for a few different muscles to show the general trend for spindles as well as tendon organs. From Chap. 3 (Fig. (3.3)) for the frequency response curves of nerve-muscle preparations, we know that the low frequency gain increases as the external stiffness increases. Figs. 6.7c and d show that both for Golgi tendon organs and spindles, the low frequency gain for muscle-afferent frequency response curve decreases as the external stiffness increases. The efferent-afferent low frequency gain (Fig. 6.7a) increases with increase in external stiffness for the tendon organs. For spindles (Fig. 6.7b), the efferent-afferent gain is flat over the range of stiffnesses studied, except at the isometric value. There seems to be a saturation in response to muscle contraction at lower stiffnesses. Similar results were observed in decerebrate cats (soleus muscle) when the preparations were stable.

The efferent-afferent data shown in Fig. 6.7 were computed from random stimulation. Similar results were obtained by applying regular stimulus pulses once every second to the ventral root filament and recording afferent responses. Post stimulus time histogram (Matthews & Stein, 1960a) was computed for a sweep time of 500 msec. The sweep time was divided into 125 equal bins, each bin being 4 msec in duration. The lowest frequency (2 Hz) sine wave fitted to PSTH gave the level of modulation at this frequency. The level of modulation for different springs at 2 Hz was found to be almost the same.

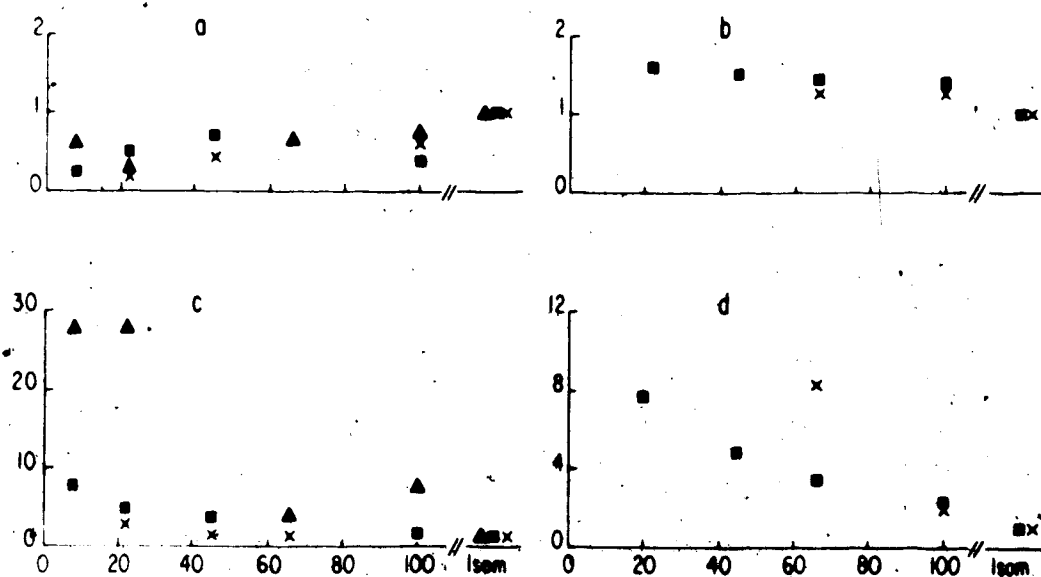


Fig. 6.7. Low frequency gains are shown for Golgi tendon organ afferents (a) and (c) and spindle afferents (b) and (d) plotted against the stiffness of the external spring. Figures (a) and (b) are for efferent-afferent frequency response functions and (c) and (d) for muscle tension-afferent frequency response functions. Different symbols represent different preparations. All values have been scaled for different experiments so that the isometric value corresponds to one. Isometric values have been displaced for clarity.

Reflex studies.

To study the dynamics of the feedback pathway, an averaging technique was used (Chap. 2). The state of each decerebrate preparation was different from the other. Some had good tone and were walking vigorously, some had a feeble tone which could be increased by contralateral stimulation and some had hardly any reflexes. The frequency domain analysis showed up a variety of different results which made quantitative assessment very difficult.

When a cat was walking, the low frequency gains for tension as input and EMG as output were high with a peak at the walking rate (around 2 Hz). Most of the time single motor unit rates showed up in EMG which appeared as peaks in the frequency response data around 7-10 Hz. When there was a complete silent period in EMG caused by a twitch it appeared as a saturation nonlinearity (Chap. 2) in the analysis.

There were a few records where the frequency response gain data fitted the empirical curve of the primary afferent (Eq. (6.1)). As explained in Chap. 5, from the phase data of these records the time delays in the feedback pathway were computed. These values varied from 12 msec to 150 msec. The shorter latencies were attributed to spinal reflexes. The longer latency pathways could involve the cerebellum and the brainstem. Moreover, the longer latencies were always accompanied by constant phase advances. The longer the latency, the greater was the value of the phase advance. The long latencies were associated with low frequency (6-9 Hz) damped oscillations in the time domain EMG and tension records. One such record is shown in

Fig. 6.8. The muscle contracted against a spring of stiffness 8 g/mm. EMG was rectified and filtered and the M-wave was eliminated from the analysis. The gain and phase values for the transfer function with tension as input and EMG as output were computed. The gain data fitted the gain curve of Eq. (6.1) up to 10 Hz. The deviation of the phase data from phases of Eq. (6.1) were plotted against frequency (Fig. 6.9) on a linear scale. The time delay computed from the fitted straight line was 75 ± 5 (mean \pm S.E.) msec with a constant phase advance of 58° at all frequencies.

Because of the inconsistency in the results, the observations on reflexes are too diverse for generalization.

DISCUSSION

Frequency response data for the muscle afferents have been computed and shown to agree well with the transfer functions given by other workers for primary and secondary endings (Matthews & Stein, 1969a; Poppele & Bowman, 1970; Rosenthal *et al.*, 1970) but not for the tendon organs (Rosenthal *et al.*, 1970; Anderson, 1974). Our tendon organ data fitted with the transfer characteristics of the secondaries and not primaries. The deviations of our data from other studies, when observed, are probably due to the difference in the methodology of our work. The authors quoted above applied sinusoidal stretches to the muscle to study the modulation of the afferent discharge at each frequency separately. In the present work random stimulation was applied to ventral root filaments of the appropriate muscle. With this

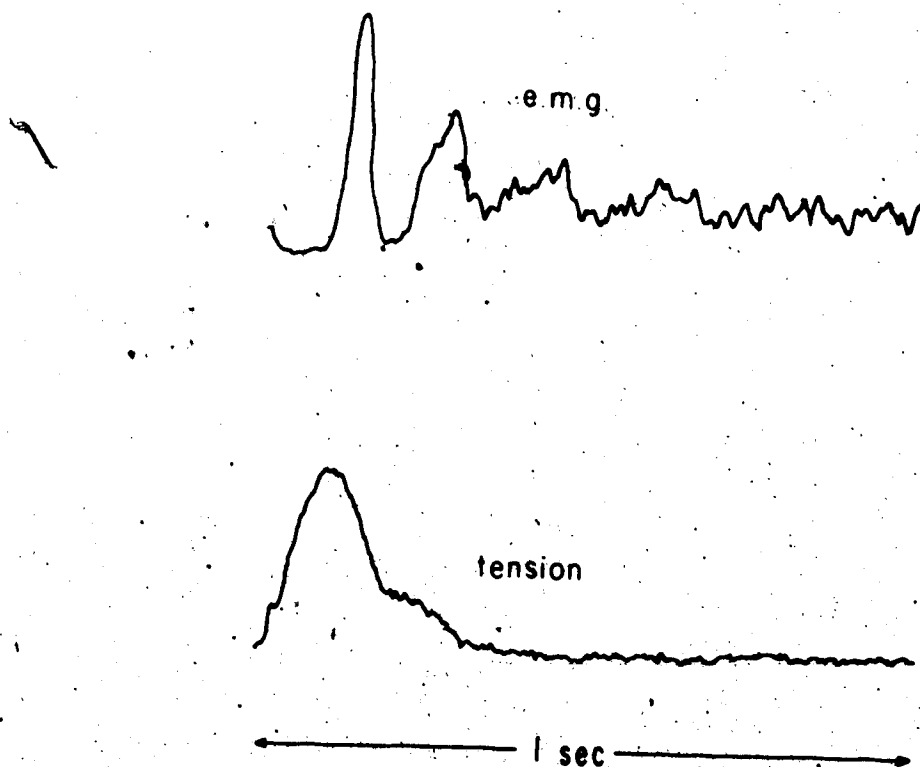


Fig. 6.8. This figure shows rectified and filtered EMG above and corresponding tension record below. The M-wave has been eliminated from the EMG record. The muscle contracted against a spring of stiffness 8 g/mm.

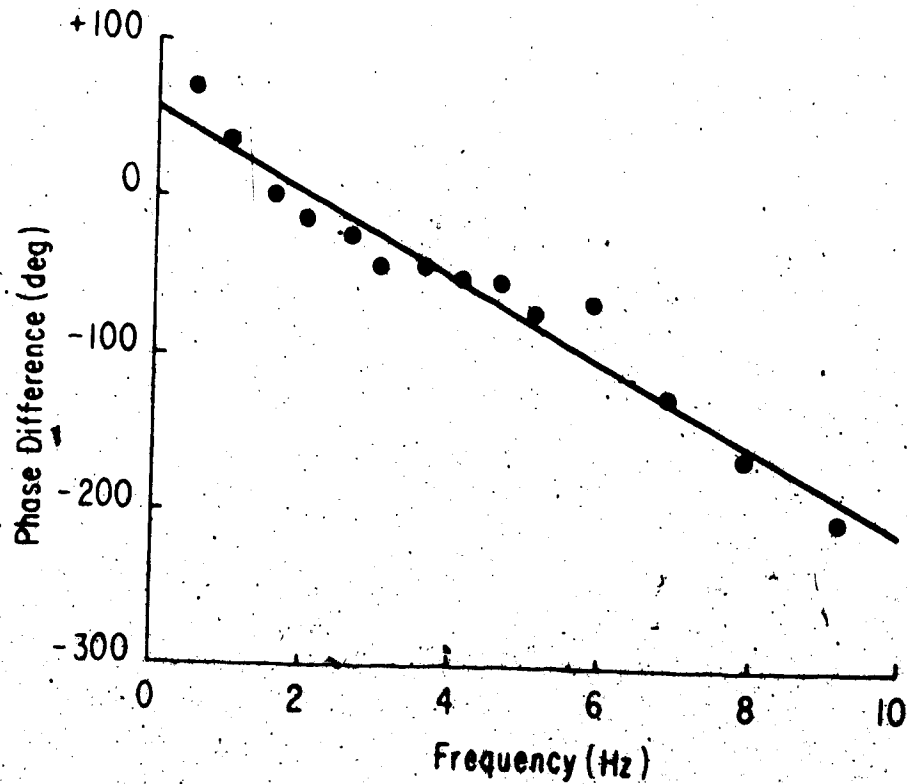


Fig. 6.9. Phase deviations of data points from the primary transfer function are plotted against frequency on a linear scale. The delay calculated from the fitted straight line is 75 ± 6 msec (mean \pm S.E.). Mean phase advance at all frequencies is 58° .

method the stimulus to the afferent endings was active contractions applied in a random manner. All frequencies of modulation desired to be studied were included in one run. For a perfectly linear system random stimulation and separate sinusoids should give the same results. Since the afferents are known to be highly nonlinear, the two methods cannot be expected to give exactly the same results. When sinusoidal length changes are applied to the muscle the nonlinearities of the nerve-muscle preparation (Chap. 3) are by-passed. In our method the properties of the muscle did affect the response of the afferents. The coherence values fell more sharply with frequency for soleus muscle and soleus muscle afferents than for the plantaris muscle and its afferents (Chap. 3 and Chap. 6, RESULTS).

The random stimulation we used for plantaris muscle preparations had low power up to ~ 0.6 Hz which resulted in low coherence values of the first two or three points of the frequency response curves. This has been discussed for the results shown in Fig. 6.4.

Out of the three muscle afferents, the tendon organs had the highest coherence values, secondary afferents were next and then the primaries. For one type of muscle the coherence values fell more sharply with frequency for primaries than for the secondary or Golgi tendon organs. These observations indicate that with the range of amplitudes of contraction we used, primary endings were more nonlinear than the secondary endings or the tendon organs. Since the coherence values fell more sharply for the primaries than for the secondaries, the data deviated from the empirical transfer functions of Poppele and Lowman (1970) at lower frequencies for primaries than for the secondaries.

(Figs. 6.1 and 6.2).

The secondary and tendon organ afferents showed carrier dependence, i.e. peaks in gain and phase data at the frequency corresponding to the steady firing rate of the afferent. This effect has been discussed by Poppele (1973) for secondaries and Anderson (1974) for the tendon organs. They have argued that carrier dependence is different from phase locking, a property exhibited by the primary endings only. According to these authors, carrier dependence and phase locking are attributed to differences in the nerve endings of the afferents. Since we have observed carrier dependence in afferents, model neurons (Chap. 2) and motoneurons (reflex experiments on cats), it does not seem to be dependent on a particular kind of nerve ending. For the tendon organ (RESULTS) which were not spontaneously firing, peaks were observed at the effective firing rate. Thus the carrier dependence seems to be inherent in the analysis rather than being a property of the secondary or tendon organ nerve endings. The carrier-dependent and phase locking peaks can be abolished by adding noise at the expense of increasing the scatter (Chap. 2; Stein, 1970).

The muscle is a low pass filter of second-order while the afferents show an increase in gain with increase in frequency. The muscle introduces phase lags which increase with increase in frequency, the afferents introduce phase advances which increase with increase in frequency. Thus the muscle afferents compensate to some extent for the decreasing response of the muscle. By introducing phase advances the range of frequencies over which the reflex loop is stable is

increased (Stein, 1974). The primary afferents compensate better than do the secondary or the tendon organ afferents.

We have shown that for the efferent-afferent frequency response of Golgi tendon organs, the low frequency gain increases with increase in stiffness of the load. The lower the stiffness, the lower is the tension generated by the muscle (Chap. 3). This implies that the lower the tension the lower is the efferent-afferent gain of the tendon organs. In other words, lower muscle tension results in less feedback inhibition. This observation suggests that the tendon organs could compensate for fatigue by adding less inhibition.

The low frequency gains for spindles were flat over the range of stiffnesses studied except at the isometric value. There is saturation in the response of afferents to contractions of the muscle by various lengths, both in anaesthetized and decerebrate preparations. This result supports Nichols and Houk's (1973) observation that during release the reflexes do not effectively compensate for muscle properties.

The data on reflex experiments are incomplete. Most of the time no reflex oscillations were observed and the frequency response curves for tension as input and EMG as output were very variable. When the oscillations were very clear and damped, the frequencies of oscillation ranged from 6-9 Hz, the gain curves fitted with those of the primary spindle afferents. The phase data deviated markedly from that of the Ia afferent because of the time delay in the feedback pathway. These delays were long (up to 150 msec) which could not be attributed to spinal reflexes. Pathways, probably with multiple

loops, involving the cerebellum and the brainstem, may be involved. The large variation in the latency values can be due to changes in excitability of the pathways.

The computed long time delays were always associated with constant phase advances. The values of these phase advances increased as the delay increased. Jansen and Rack (1966) have suggested phase advances introduced in the feedback pathway in the preparations which oscillated at 6-8 Hz. They further suggested that Renshaw inhibition could introduce these phase advances.

Jansen and Rack (1966) also observed the variable states of the decerebrate cats which we observed. The phase lags at 2 Hz in their experiments could be due to active walking or the tendency of the animal to walk at that frequency. The large phase lags at 6-8 Hz where they observed clonus could have involved higher centers. Their statically less sensitive preparations could correspond to our preparations where long latency reflex pathways were dominant.

Most of the time, even when the tone of the muscle and ongoing EMG activity were good, no reflex oscillations were observed and the frequency response curves had no consistent shape. The reason could be that when more than one reflex pathway converges on the same motoneuronal pool, the oscillations are damped out.

BIBLIOGRAPHY

- AGARWAL, G.C. & GOTTLIEB, G.L. (1972) The muscle silent period and reciprocal inhibition in man. *J. Neurol. Neurosurg. Psychiat.* 35, 72-76.
- ALLEN, G.I. & TSUKAHARA, N. (1974) Cerebrocerebellar communication systems. *Physiol. Rev.* 54, 957-1006.
- ANDERSON, J.H. (1974) Dynamic characteristics of Golgi tendon organs. *Brain Res.* 67, 531-537.
- ANGEL, A. & LEMON, R.N. (1975) Sensorimotor cortical representation in the rat and the role of the cortex in the production of sensory myoclonic jerks. *J. Physiol.* 248, 465-488.
- ASANUMA, H. (1975) Recent developments in the study of the columnar arrangement of neurons within the motor cortex. *Physiol. Rev.* 55, 143-156.
- ASHLEY, C.C. & MOISESCU, D.G. (1973) The mechanism of free calcium change in single muscle fibres during contraction. *J. Physiol.* 231, 23-24P.
- BAWA, P., MANNARD, A. & STEIN, R.B. (1975) Effects of elastic loads on contractions of cat muscles. Submitted for publication.
- BAWA, P., MANNARD, A. & STEIN, R.B. (1975) Predictions and experimental tests of a visco-elastic muscle model using elastic and inertial loads. Submitted for publication.
- BAWA, P. & STEIN, R.B. (1975) Properties of human soleus muscle and the associated feedback loop. Submitted for publication.
- BENDAT, J.S. & PIERSOL, A.G. (1971) *Measurement and Analysis of Random Data.* New York, John Wiley & Sons, Inc.
- BINKHORST, R.A. (1969) The effect of training on some isometric contraction characteristics of a fast muscle. *Pflügers Arch. ges. Physiol.* 309, 193-202.
- BRODAL, A. & WALBERG, F. (1952) Ascending fibers in the pyramidal tract of cat. *Arch. Neurol. Psychiat.* 68, 755-775.
- BROOKS, V.B. & STONEY, S.D. (1971) Motor mechanisms: The role of the pyramidal system in motor control. *Ann. Rev. Physiol.* 33, 337-392.
- BUNKE, R.E., RUDMIN, P. & ZAJAC, F.E. (1970) Catch properties of single mammalian motor units. *Science, N.Y.* 168, 122-124.

- BURKE, R.E., RYMER, W.Z. & WALSH, J.V. (1973) Functional specialization in the motor unit population of cat medial gastrocnemius muscle. In "Control of Posture and Locomotion". eds. R.B. Stein, K.G. Pearson, R.S. Smith & J.B. Redford, pp. 29-44. New York, Plenum Press.
- CHEN, W.J. & POPPELE, R.E. (1973) Static fusimotor effect on the sensitivity of mammalian muscle spindle. *Brain Res.* 57, 244-247.
- CLOSE, R.L. (1972) Dynamic properties of mammalian skeletal muscles. *Physiol. Rev.* 52, 129-197.
- CONNOLLY, R., GOUGH, W. & WINEGRAD, S. (1971) Characteristics of the isometric twitch of skeletal muscle immediately after a tetanus. *J. gen. Physiol.* 57, 697-709.
- ECCLES, J.C., NICOLL, R.A., SCHWARZ, D.W.F., TÁBOŘIKOVÁ, H. & WILLEY, T.J. (1975a) Reticulospinal neurons with and without monosynaptic inputs from cerebellar nuclei. *J. Neurophysiol.* 38, 513-530.
- ECCLES, J.C., SCHEID, P. & TÁBOŘIKOVÁ, H. (1975b) Responses of red nucleus neurons to antidromic and synaptic activation. *J. Neurophysiol.* 38, 947-964.
- EVARTS, E.V. (1973) Motor cortex reflexes associated with learned movement. *Science, N.Y.* 179, 501-503.
- HELMAN, A.G. & ORLOVSKY, G.N. (1972) The influence of different descending systems on the tonic stretch reflex in the cat. *Exp. Neurol.* 37, 481-494.
- FISZ, M. (1963) *Probability Theory and Mathematical Statistics.* New York (3rd edition), John Wiley & Sons, Inc.
- FRENCH, A.S. (1973a) Automated spectral analysis of neurophysiological data using intermediate magnetic tape storage. *Comput. Progr. Biomed.* 3, 45-47.
- FRENCH, A.S. (1973b) Averaging of neurophysiological data prior to frequency domain analysis. *Comput. Progr. Biomed.* 3, 113-122.
- FRENCH, A.S. & BUTZ, E.G. (1973) Measuring the Wiener kernels of a non-linear system using the fast Fourier transform algorithm. *Int. J. Control* 17, 529-539.
- FRENCH, A.S. & HOLDEN, A.V. (1971a) Alias-free sampling of neuronal spike trains. *Kybernetik* 8, 165-171.
- FRENCH, A.S. & HOLDEN, A.V. (1971b) Semi-on-line implementation of an alias-free sampling system for neuronal signals. *Comput. Progr. Biomed.* 2, 1-7.

- FRENCH, A.S. & HOLDEN, A.V. (1971c) Frequency domain analysis of neuro-physiological data. *Comput. Progr. Biomed.* 1, 219-234.
- FRENCH, A.S. & STEIN, R.B. (1970) A flexible neural analog using integrated circuits. *IEEE Trans. Biomed. Engin.* BME-17, 248-253.
- FUCHS, F. (1974) Striated muscle. *Ann. Rev. Physiol.* 36, 461-502.
- GOODWIN, G.M. & MATTHEWS, P.B.C. (1971) Effects of fusimotor stimulation on the sensitivity of muscle spindle endings to small amplitude sinusoidal stretching. *J. Physiol. (Lond.)* 218, 56-58P.
- GORDON, A.M., HUXLEY, A.F. & JULIAN, F.J. (1966) The variation in isometric tension with sarcomere length in vertebrate muscle fibres. *J. Physiol.* 184, 170-192.
- GOTTLIEB, G.L. & AGARWAL, G.C. (1970) Filtering of electromyographic signals. *Amer. J. Phys. Med.* 49, 142-146.
- GOTTLIEB, G.L. & AGARWAL, G.C. (1971) Effects of initial conditions on the Hoffman reflex. *J. Neurol. Neurosurg. Psychiat.* 34, 226-230.
- GRANIT, R. & KAADA, B.R. (1952) Influence of stimulation of central nervous system on muscle spindles in cat. *Acta physiol. scand.* 27, 130-160.
- GRILLNER, S. (1972) The role of muscle stiffness in meeting the changing postural and locomotor requirements for force development by the ankle extensors. *Acta physiol. scand.* 86, 92-108.
- GRILLNER, S. & UDO, M. (1971) Motor unit activity and stiffness of the contracting muscle fibres in the tonic stretch reflex. *Acta physiol. scand.* 81, 422-424.
- HANSON, J. & HUXLEY, H.E. (1953) Structural basis of the cross-striations in muscle. *Nature* 172, 530-552.
- HASSAN, Z. & HOUK, J.C. (1975a) Analysis of response properties of de-efferented mammalian spindle receptors based on frequency response. *J. Neurophysiol.* 38, 663-672.
- HASAN, Z. & HOUK, J.C. (1975b) Transition in sensitivity of spindle receptors that occurs when muscle is stretched more than a fraction of a millimeter. *J. Neurophysiol.* 38, 673-689.
- HENNEMAN, E. (1974) Peripheral mechanisms involved in the control of muscle. In "Medical Physiology", Vol. 1. ed. V.B. Mountcastle, pp. 617-635. St. Louis, Mosby.
- HENNEMAN, E. & OLSON, C.B. (1965) Relations between structure and function in the design of skeletal muscles. *J. Neurophysiol.* 28, 581-598.

- HILL, A.V. (1938) The heat of shortening and the dynamic constants of muscle. *Proc. Roy. Soc. B* 126, 136-195.
- HILL, A.V. (1951) The effect of series compliance on the tension developed in the muscle twitch. *Proc. Roy. Soc. B* 138, 325-329.
- HILL, A.V. (1964) The effect of load on the heat of shortening of muscle. *Proc. Roy. Soc. B* 159, 297-318.
- HOFFMAN, P. (1918) Über die Beziehungen der Sehnen-reflexe zur willkürlichen Bewegung und zur Tonus. *Z. Biol.* 68, 351-370.
- HOUK, J.C., CORNEW, R.W. & STARK, L. (1966) A model of adaptation in amphibian spindle receptors. *J. theor. Biol.* 12, 196-215.
- HOUK, J.C., HARRIS, D.A. & HASAN, Z. (1973) Non-linear behaviour of spindle receptors. In "Control of Posture and Locomotion". eds. R.B. Stein, K.G. Pearson, R.S. Smith and J.B. Redford, pp. 147-163. New York, Plenum Press.
- HOUK, J.C. & HENNEMAN, E. (1967) Responses of Golgi tendon organs to active contractions of soleus muscle of cat. *J. Neurophysiol.* 30, 466-481.
- HOUK, J.C. & HENNEMAN, E. (1974) Feedback control of muscle: Introductory concepts. In "Medical Physiology", Vol. II. ed. V.B. Mountcastle, pp. 608-616. St. Louis, Mosby.
- HOUK, J.C. & SIMON, W. (1967) Responses of Golgi tendon organs to forces applied to muscle tendon. *J. Neurophysiol.* 30, 1466-1481.
- HOUK, J.C., SINGER, J.J. & GOLDMAN, M.R. (1970) An evaluation of length and force feedback to soleus muscles of decerebrate cats. *J. Neurophysiol.* 33, 784-811.
- HUXLEY, A.F. (1957) Muscle structure and theories of contraction. *Prog. Biophys. biophys. chem.* 7, 255-318.
- HUXLEY, A.F. (1971) The activation of striated muscle and its mechanical response. *Proc. Roy. Soc. B* 178, 1-27.
- HUXLEY, A.F. (1973) A note suggesting that the cross-bridge attachment during muscle contraction may take place in two steps. *Proc. Roy. Soc. B* 183, 83-86.
- HUXLEY, A.F. (1974) Muscular contractions. *J. Physiol. (Lond.)* 243, 1-143.
- HUXLEY, A.F. & NIEDERGERKE, R. (1954) Structural changes in muscle during contraction. *Nature* 173, 971-973.

- HUXLEY, A.F. & SIMMONS, R.M. (1971) Proposed mechanism of force generation in striated muscle. *Nature* 233, 533-538.
- HUXLEY, A.F. & SIMMONS, R.M. (1971) Mechanical properties of the cross-bridges of frog striated muscle. *J. Physiol.* 218, 59-60P.
- HUXLEY, H.E. (1969) The mechanism of muscular contraction. *Science* 164, 1356-1366.
- HUXLEY, H.E. (1971) The structural basis of muscular contraction. *Proc. Roy. Soc. B* 178, 131-149.
- HUXLEY, H.E. & HANSON, J. (1954) Changes in the cross-striations of muscle during contraction and stretch and their structural interpretation. *Nature* 173, 973-976.
- JANSEN, J.K.S. & RACK, P.M.H. (1966) The reflex response to sinusoidal stretching of soleus in the decerebrate cat. *J. Physiol.* 183, 15-36.
- JEWELL, B.R. & WILKIE, D.R. (1960) The mechanical properties of relaxing muscle. *J. Physiol.* 152, 30-47.
- JOYCE, G.C. & RACK, P.M.H. (1969) Isotonic lengthening and shortening movements of cat soleus muscle. *J. Physiol.* 204, 475-491.
- JOYCE, G.C., RACK, P.M.H. & WESTBURY, D.R. (1969) The mechanical properties of cat soleus muscle during controlled lengthening and shortening movements. *J. Physiol.* 204, 461-474.
- JULIAN, F.J. (1969) Activation in a skeletal muscle contraction model with a modification for insect fibrillar muscle. *Biophys. J.* 9, 547-570.
- KIRKWOOD, P.A. & SEARS, T.A. (1975) Monosynaptic excitation of motoneurons from muscle spindle secondary endings of intercostal and triceps surae muscles in the cat. *J. Physiol.* 245, 64P.
- LANDGREN, S., PHILLIPS, C.G. & PORTER, R. (1962) Minimal synaptic actions of pyramidal impulses on some alpha motoneurons of the baboon's hand and forearm. *J. Physiol.* 161, 91-111.
- LAPORTE, Y. & EMONET-DÉNAND, F. (1973) Evidence for common innervation of bag and chain muscle fibres in cat spindles. In "Control of Posture and Locomotion". eds. R.B. Stein, K.G. Pearson, R.S. Smith and J.B. Redford, pp. 119-126. New York, Plenum Press.
- LENNAN, J.A.R. & RITCHIE, A.E. (1970) *Clinical Electromyography*. Bath, Pitman Medical.

- LIDDELL, E.G.T. & SHERRINGTON, C. (1924) Reflexes in response to stretch (myotatic reflexes). *Proc. Roy. Soc. B* 96, 212-242.
- LIPPOLD, O.C.J., REDFEARN, J.W.T. & VUČO, J. (1958) The effect of sinusoidal stretching on the activity of stretch receptors in voluntary muscle and their reflex responses. *J. Physiol.* 144, 373-386.
- MANNARD, A. & STEIN, R.B. (1973) Determination of the frequency response of isometric soleus muscle in the cat using random nerve stimulation. *J. Physiol.* 229, 275-296.
- MARMARELIS, P.Z. & NAKA, K. (1972) White noise analysis of a neuron chain: an application of the Wiener theory. *Science, N.Y.* 175, 1276-1278.
- MARSDEN, C.D., MERTON, P.A. & MORTON, H.B. (1973) Latency measurements compatible with a cortical pathway for the stretch reflex in man. *J. Physiol.* 230, 58-59P.
- MATTHEWS, P.B.C. (1972) Mammalian muscle receptors and their central action. Edward Arnold Ltd., London.
- MATTHEWS, P.B.C. (1973) A critique of the hypothesis that the spindle secondary endings contribute excitation to the stretch reflex. In "Control of Posture and Locomotion". eds. R.B. Stein, K.G. Pearson, R.S. Smith and J.B. Redford, pp. 227-244. New York, Plenum Press.
- MATTHEWS, P.B.C. & STEIN, R.B. (1969a) The sensitivity of muscle spindle afferents to small sinusoidal changes in length. *J. Physiol.* 200, 723-743.
- MATTHEWS, P.B.C. & STEIN, R.B. (1969b) The regularity of primary and secondary muscle spindle afferent discharges. *J. Physiol.* 202, 59-82.
- MELVILL JONES, G. & WATT, D.G.D. (1971) Observations on the control of stepping and hopping movements in man. *J. Physiol.* 219, 709-727.
- MERTON, P.A. (1951) The silent period in a muscle of the human hand. *J. Physiol.* 114, 183-198.
- MILNER-BROWN, H.S., STEIN, R.B. & YEMM, R. (1973a) The orderly recruitment of human motor units during voluntary isometric contractions. *J. Physiol. (Lond.)* 230, 359-370.
- MILNER-BROWN, H.S., STEIN, R.B. & YEMM, R. (1973b) Changes in firing rate of human motor units during voluntary isometric contractions. *J. Physiol. (Lond.)* 230, 371-390.

- MILNER-BROWN, H.S., STEIN, R.B. & LEE, R.G. (1975) Synchronization of human motor units: possible roles of exercise and supraspinal reflexes. *Electroenceph. clin. Neurophysiol.* 38, 245-254.
- MILSUM, H.H. (1966) *Biological Control Systems Analysis*. New York, McGraw-Hill.
- MURPHY, J.T., WONG, Y.C. & KWAN, H.C. (1974) Distributed feedback systems for muscle control. *Brain Res.* 71, 495-505.
- MURPHY, J.T., WONG, Y.C. & KWAN, H.C. (1975) Afferent-efferent linkages in motor cortex for single forelimb muscles. *J. Neurophysiol.* 38, 990-1014.
- MURRAY, J.M. & WEBER, A. (1974) The cooperative action of muscle proteins. *Sci. Amer.* 230, 58-71.
- NICHOLS, T.R. (1974) Soleus muscle stiffness and its reflex control. Ph.D. Thesis, Harvard University, Cambridge.
- NICHOLS, T.R. & HOUK, J.C. (1973) Reflex compensation for variations in the mechanical properties of a muscle. *Science, N.Y.* 181, 182-184.
- OGATA, K. (1970) *Modern Control Engineering*. New Jersey, Prentice-Hall.
- OGUZTÖRELI, M.N. & STEIN, R.B. (1975) Tremor and other oscillations in neuro-muscular systems. Submitted for publication.
- OSCARSSON, O. (1965) Functional organisation of the spino- and cuneocerebellar tracts. *Physiol. Rev.* 45, 495-522.
- OSCARSSON, O. & UDDENBERG, N. (1964) Identification of a spinocerebellar tract activated from forelimb afferents in the cat. *Acta physiol. scand.* 62, 125-136.
- PARTRIDGE, L.D. (1966) Signal-handling characteristics of load-moving skeletal muscle. *Amer. J. Physiol.* 210, 1178-1191.
- PARTRIDGE, L.D. (1967) Intrinsic feedback factors producing inertial compensation in muscle. *Biophys. J.* 7, 853-863.
- PARTRIDGE, L.G. & GLASER, G.H. (1960) Adaptation in regulation of movement and posture. A study of stretch responses in spastic animals. *J. Neurophysiol.* 23, 257-269.
- PHILLIPS, C.G. (1969) Motor apparatus of the baboon's hand. *Proc. Roy. Soc. B* 173, 141-174.

- PHILLIPS, C.G. (1973) Cortical localization and 'sensorimotor processes' at the 'middle level' in primates. Proc. Roy. Soc. Med. 66, 987-1002.
- PODOLSKY, R.J., NOLAN, A.C. & ZAVELER, S.A. (1969) Cross-bridge properties derived from muscle isotonic velocity transients. Proc. Nat. Acad. Sci., U.S.A. 64, 504-511.
- POPPELE, R.E. (1973) Systems approach to the study of muscle spindles. In "Control of Posture and Locomotion". eds. R.B. Stein, K.G. Pearson, R.S. Smith and J.B. Redford, pp. 127-146. New York, Plenum Press.
- POPPELE, R.E. & BOWMAN, R.J. (1970) Quantitative description of linear behavior of mammalian muscle spindles. J. Neurophysiol. 33, 59-72.
- POPPELE, R.E. & CHEN, W.J. (1972) Repetitive firing behavior of mammalian muscle spindle. J. Neurophysiol. 35, 357-365.
- POPPELE, R.E. & KENNEDY, W.R. (1974) Comparison between behavior of human and cat muscle spindles recorded in vitro. Brain Res. 75, 316-319.
- POPPELE, R.E. & TERZUOLO, C.A. (1968) Myotatic reflex: its input-output relation. Science, N.Y. 159, 743-745.
- RACK, P.M.H. & WESTBURY, D.R. (1969) The effects of length and stimulus rate on tension in the isometric cat soleus muscle. J. Physiol. 204, 443-460.
- RACK, P.M.H. & WESTBURY, D.R. (1974) The short range stiffness of active mammalian muscle and its effect on mechanical properties. J. Physiol. (Lond.) 240, 331-350.
- ROSENTHAL, N.P., McKEAN, T.A., ROBERTS, W.J. & TERZUOLO, C.A. (1970) Frequency analysis of stretch reflex and its main sub-systems in triceps surae muscles of the cat. J. Neurophysiol. 33, 713-749.
- RUDJORD, T. (1970a) A second order mechanical model of muscle spindle primary endings. Kybernetik 6, 205-213.
- RUDJORD, T. (1970b) A mechanical model of the secondary endings of mammalian muscle spindles. Kybernetik 7, 122-128.
- RYMER, W.Z. & WALSH, J.V. (1973) Effects of secondary muscle spindle afferent discharge on extensor motoneurons in the decerebrate cat. In "Control of Posture and Locomotion". eds. R.B. Stein, K.G. Pearson, R.S. Smith and J.B. Redford, pp. 411-414. New York, Plenum Press.

- SEVERIN, F.V., ORLOVSKII, G.N. & SHIK, M.L. (1967) Work of the muscle receptors during controlled locomotion. *Biophysics* 12, 575-586.
- STEIN, R.B. (1965) A theoretical analysis of neuronal variability. *Biophys. J.* 5, 173-194.
- STEIN, R.B. (1970) The role of spike trains in transmitting and distorting sensory signals. In "The Neurosciences: Second Study Program". F.O. Schmidt, Editor-in-Chief. New York, The Rockefeller University Press.
- STEIN, R.B. (1974) The peripheral control of movement. *Physiol. Rev.* 54, 215-243.
- STEIN, R.B. & WONG, E.Y-M. (1974) Analysis of models for the activation and contraction of muscle. *J. theor. Biol.* 46, 307-327.
- TATTON, W.G. & LEE, R.G. (1975) Motor responses to sudden upper limb displacements in primates, humans and Parkinsonian patients. *Can. Physiol.* 6, 60.
- VALLBO, Å.B. (1971) Muscle spindle response at the onset of isometric voluntary contractions in man. Time difference between fusimotor and skeletomotor effects. *J. Physiol. (Lond.)* 318, 405-431.
- VALLBO, Å.B. (1973) The significance of intramuscular receptors in load compensation during voluntary contractions in man. In "Control of Posture and Locomotion". eds. R.B. Stein, K.C. Pearson, R.S. Smith and J.B. Redford, pp. 211-226. New York, Plenum Press.
- WEBER, A. & ARAY, J.M. (1973) Molecular control mechanisms in muscle contraction. *Physiol. Rev.* 53, 612-673.
- WESTBURY, D.R. (1972) A study of stretch and vibration reflexes of the cat by intracellular recording from motoneurons. *J. Physiol.* 226, 37-56.
- WONG, E.Y-M. (1972) Theoretical and experimental studies on frog skeletal muscle. M.Sc. Thesis, University of Alberta, Edmonton, Canada.